Title
Genetic analyses of Drosophila homologs of non-canonical BLOC-1 subunits

Author
Sundberg, Christopher David

Publication Date
2015

Peer reviewed|Thesis/dissertation

UNIVERSITY OF CALIFORNIA

Los Angeles

Genetic analyses of *Drosophila* homologs of non-canonical BLOC-1 subunits

A dissertation submitted in partial satisfaction of

the requirements for the degree Doctor of Philosophy

in Human Genetics

by

Christopher David Sundberg

2015

ABSTRACT OF THE DISSERTATION

Genetic analyses of *Drosophila* homologs of non-canonical BLOC-1 subunits

by

Christopher David Sundberg

Doctor of Philosophy in Human Genetics

University of California, Los Angeles, 2015

Professor Esteban C. Dell'Angelica, Chair

BLOC-1 (biogenesis of lysosome-related organelles complex 1) is a eukaryotic protein complex required for the efficient formation of lysosome related organelles (LROs), a class of membrane-bound organelles derived from the endosomal-lysosomal pathway. In metazoans, BLOC-1 is an octameric protein complex consisting of pallidin, muted, dysbindin, cappuccino, snapin, BLOS1, BLOS2 and BLOS3. Mutation of the genes encoding dysbindin, pallidin or BLOS3 causes Hermansky-Pudlak syndrome in humans, and mutation of the genes encoding pallidin, muted, dysbindin, cappuccino or BLOS3 causes a related syndrome in mice. In the budding yeast, *Saccharomyces cerevisiae*, a 'BLOC-1' complex was described; however, this protein complex is hexameric and contains homologs of BLOS1, snapin and cappuccino and three non-canonical BLOC-1 proteins: Vab2p, Kxd1p and Bli1p. Kxd1 was previously shown to interact with BLOS1 in mammals, insects and nematodes. To genetically determine the role of *Drosophila* homologs of non-canonical BLOC-1 proteins in relation to canonical BLOC-1, I deleted one of these genes by P element imprecise excision and another by CRISPR/Cas9 (Clustered Regularly Interspaced Short Palindromic Repeats/ CRISPR-associated protein 9)-mediated genomic editing. At the

same time I deleted *Drosophila Blos3*, also using a CRISPR-based approach. *Blos3* is unique among the eight metazoan BLOC-1 subunit genes as mutation of *Blos3* causes an atypically mild BLOC-1 phenotype in mice. I found that deletion of one of the non-canonical BLOC-1 proteins in *Drosophila* did not affect the biogenesis of eye pigment granules, which are LROs that require BLOC-1 function for normal biogenesis; nor did it modify function of BLOC-2, a protein complex previously shown to act epistatically to BLOC-1. On the other hand, deletion of another non-canonical BLOC-1 protein resulted in higher eye pigment levels than those of wildtype flies. Lastly, I found that deletion of *Blos3* caused attenuated BLOC-1 phenotypes in *Drosophila*. These findings support the interpretation that the non-canonical BLOC-1 proteins do not have roles in canonical BLOC-1 activity, though one of them may negatively regulate BLOC-1 function. Finally *Blos3* appears to function in a unique manner among the recognized BLOC-1 subunits even across distantly related eukaryotic species.

The dissertation of Christopher David Sundberg is approved.

Katrina M. Dipple

Julian A. Martinez-Agosto

Volker Hartenstein

Esteban C. Dell'Angelica, Committee Chair

University of California, Los Angeles

2015

I dedicate this work, in appreciation, to my mother, Rebecca L. Sundberg

and to my brother, Eric L. Sundberg.

TABLE OF CONTENTS

LIST OF TABLES

LIST OF FIGURES

ACKNOWLEDGMENTS

- Esteban C. Dell'Angelica
- Andrew Reynoso

  Amy Moreno
- Katrina M. Dipple

  Julian A. Martinez-Agosto

  Volker Hartenstein
- Ronik Khachatoorian

  Nicole Wheatley

  Jina Yun

  Lok Leung
- Ming Guo

  Utpal Banerjee

  Yibin Wang
- National Science Foundation

  AGEP Fellowship
- National Science Foundation

  Graduate Research Fellowship
- MCDB / ACCESS
- Department of Human Genetics

Christopher Sundberg
Department of Human Genetics
University of California, Los Angeles
Los Angeles, CA 90095

EDUCATION:

2003: M.S., Microbiology and Immunology; Stanford University, Stanford, CA.
Effects of p53 mutation on sustained regression of MYC-induced lymphoma

1994: B.S., Biology; University of New Mexico, Albuquerque, New Mexico
Effects of RAS over-expression on iodine metabolism in the thyroid

REASEARCH FELLOWSHIPS:

2010-2013: National Science Foundation, Graduate Research Fellowship
2009: University of California, NSF AGEP Fellowship
1999-2003: Stanford University, Graduate Research Fellowship
1993-1994: Univ. of New Mexico, Howard Hughes Undergraduate Fellowship
1990-1991: Univ. of New Mexico, Minority Access to Research Careers Fellowship

PROFESSIONAL EXPERIENCE:

2012-2015: Graduate Student. Human Genetics Ph.D. Program, University of California, Los Angeles. Esteban C. Dell'Angelica, Ph.D. Dissertation Advisor. *Genetic Analyses of Drosophila Homologs of Non-canonical BLOC-1 Subunits.*

2009-2012: Graduate Student. Molecular, Cell and Dev. Biol. Ph.D. Program, University of California, Los Angeles. Volker Hartenstein, Ph.D. Dissertation Advisor. Ming Guo, M.D./Ph.D., Research Advisor. *Mitochondrial Dynamics and Quality Control.*

2007-2009: Research Associate II. Luc Jasmin, M.D./Ph.D., Supervisor. Gene Therapeutics Research Institute and Neurosurgical Institute, Cedars-Sinai Medical Center. *Effects of ion channel and neurotransmitter modulation on sensory behavior.*

2004-2006: Staff Research Associate II. Tracy McKnight, Ph.D., Supervisor. Center for Mol. and Funct. Imaging, Dept. of Radiology, UCSF. *HR-MAS NMR spectroscopy to correlate changes in metabolism with gene expression (AKT and HIF1alpha).*

1999-2003: Graduate Research Assistant: Master's Thesis. Dean Felsher, M.D./Ph.D., Thesis Advisor. Dept. of Microbiology and Immunology, Stanford University. *Role of p53, $p21^{WAF-1}$ and $p19^{ARF}$ on tumor regression following MYC inactivation.*

1994-1998: Research Assistant. Walt Ream, Ph.D., Supervisor. Dept. of Microbiology, Oregon State University. *Role of VirE1 as a molecular chaperone of VirE2 during the pathogenic transformation of plants by Agrobacterium tumefaciens.*

1992-1994: Undergraduate Researcher. Paul Kerkof, Ph.D., Advisor. Dept. of Biology, University of New Mexico. *Effects of RAS over-expression on iodine metabolism.*

PUBLICATIONS/BIBLIOGRAPHY:

1. Khachatoorian R, Hoveida H, **Sundberg C**, Wheatley N, Jung CL, Ruchala P, Ganapathy E, Gestwicki J, Arumugaswami V, Dasgupta A, French SW. Allosteric Heat Shock Protein Inhibitors Block Hepatitis C Virus Assembly. **IJAA**. *Submitted*. June 28, 2015.

2. Khachatoorian R, Ruchala P, Waring A, Jung CL, Ganapathy E, Wheatley N, **Sundberg C**, Arumugaswami V, Dasgupta A, French SW. Structural characterization of the HSP70 interaction domain of the hepatitis C viral protein NS5A. **Virology**. Jan 15;475:46-55, 2015.

3. Khachatoorian R, Ganapathy E, Ahmadieh Y, Wheatley N, **Sundberg C**, Jung CL, Arumugaswami V, Raychaudhuri S, Dasgupta A, French SW. The NS5A-binding heat shock proteins HSC70 and HSP70 play distinct roles in the hepatitis C viral life cycle. **Virology**. Apr; 454-455:118-27, 2014.

4. Wheatley NM, **Sundberg CD**, Gidaniyan SD, Cascio D, Yeates TO. Structure and identification of a pterin dehydratase-like protein as a ribulose-bisphosphate carboxylase/oxygenase (RuBisCO) assembly factor in the α-carboxysome. **J Biol Chem.** Mar 14;289(11):7973-81, 2014.

5. Ohara PT, Vit JP, Bhargava A, Romero M, **Sundberg C**, Charles AC, and Jasmin L. Gliopathic pain: When Satellite Glial Cells go bad. **The Neuroscientist**. Oct;15(5):450-63, 2009.

6. Vit JP, Ohara PT, **Sundberg C**, Rubi B, Maechler P, Liu C, Puntel M, Lowenstein P, Castro M, Jasmin L. Adenovector GAD65 gene delivery into the rat trigeminal ganglion produces orofacial analgesia. **Mol. Pain.** 5(42), 2009.

7. Jain M, Arvanitis C, Chu K, Dewey W, Leonhardt E, Trinh M, **Sundberg CD**, Bishop JM and Felsher DW. Sustained loss of a neoplastic phenotype by brief inactivation of *MYC*. **Science**. 297(5578):102-104, 2002.

9. **Sundberg CD** and Ream W. The *Agrobacterium tumefaciens* chaperone-like protein, VirE1, interacts with VirE2 at domains required for single-stranded DNA binding and cooperative interaction. **J. Bacteriol.** 181(21):6850-6855, 1999.

10. **Sundberg C**, Meek L, Carroll K, Das A and Ream W. VirE1 protein mediates export of the single-stranded DNA-binding protein VirE2 from *Agrobacterium tumefaciens* into plant cells. **J. Bacteriol.** 178(4):1207-1212, 1996.

11. **Sundberg C**, Meek L, Carroll K, Das A and Ream W. VirE1 protein mediates export of the single-stranded DNA-binding protein VirE2 from *Agrobacterium tumefaciens* into plant cells. **Crown Gall**. APS Press, 126-145; W. Ream (ed.). 1996.

CHAPTER 1

Introduction

BLOC-1

BLOC-1 (biogenesis of lysosome-related organelles complex 1) is a protein complex of approximately 200 kDa that was originally isolated from mammalian tissues and cells in the course of biochemical characterization of pallidin [1]. Pallidin is the protein defective in the 'pallid' line of mice that was characterized as having a role in the biogenesis of lysosome-related organelles [2]. BLOC-1 was subsequently found to be composed of eight protein subunits: pallidin and muted [1, 3], cappuccino [4], dysbindin [5], and snapin, BLOS1, BLOS2 and BLOS3 [6]. With the exception of BLOS3, which displays an intriguing, although functionally undefined GEAxExD motif [7], these proteins are small coiled-coil domain polypeptides that have no homology to other known proteins or identifiable functional domains [6, 8, 9].

Structurally, BLOC-1 has been characterized as an elongated linear assembly of eight globular domains with a marked degree of flexibility along the length of the protein complex [8]. This structure is thought to facilitate the interactions of BLOC-1 with its known interactors, such as the adaptor protein 3 complex (AP-3) and the target-soluble NSF (*N*-ethylmaleimide-sensitive factor) attachment protein receptors (t-SNAREs), syntaxin-13, synaptosomal-associated protein 25 (SNAP-25), and their close relatives [2, 10-12]. The globular domains of the BLOC-1 assembly are not thought to correspond to the individual protein subunits of BLOC-1, but are thought to be a consequence of secondary structure driven by heterotrimeric protein-protein interactions between the coiled-coil regions of the respective subunits [8]. Furthermore, two BLOC-1 sub-complexes have been defined: pallidin, cappuccino and BLOS1, and dysbindin, snapin and BLOS2. Muted and BLOS3 are more peripherally associated with BLOC-1 and are the first subunits to be shed when the complex is perturbed [8]. Notably, mutation of single BLOC-1 subunit genes leads to the reduced accumulation of all of the BLOC-1 subunit proteins, highlighting the tight structural organization of the BLOC-1 protein complex [1, 3, 6].

Lysosome-related organelles

Lysosome-related organelles (LROs) are a class of cellular organelles that, like conventional lysosomes, are biosynthetically derived from the endosomal-lysosomal pathway [13]. LROs exhibit many of the physical characteristics of conventional lysosomes, such as H(+)-ATPase-dependent luminal acidification and the presence of extensively glycosylated integral-membrane proteins including the LAMP (lysosome associated membrane protein) family of proteins [14]. The specialized function of LROs is largely determined by the specific assortment of membrane proteins that are delivered to the developing LRO [13-17]. LROs are also frequently the sites of synthesis of the specific factors that they accumulate, such as when the biosynthetic precursors or products require sequestration from the rest of the cell, or when an acidic luminal pH is required for the synthesis of the sequestered products [15-19].

In some cell types, such as cytotoxic T lymphocytes (CTLs) and osteoclasts, all lysosomes appear to be secretory LROs, whereas in other cell types, such as mast cells, melanocytes and endothelial cells, LROs exist side-by-side with conventional degragative lysosomes [13, 14]. Other examples of LROs include MHC (major histocompatibility complex) class II granules, basophil granules, azurophil granules, lamellar bodies of type II lung epithelial cells, the lytic granules of natural killer cells and synaptic vesicles of some neurons [7, 13, 14, 20]. Melanosomes and platelet dense granules are LROs that were recognized as being coordinately compromised in the pallid and muted lines of spontaneous BLOC-1 mutant mice due to the prolonged bleeding and compromised pigmentation phenotypes that accompanied elevated kidney lysosomal enzymes in these animals [2, 21].

The pigment granules of the *Drosophila* compound eye were subsequently found to be LROs [17]. Among the genes that affect eye color in *Drosophila*, a subset of these function to deliver proteins to lysosomes and pigment granules [17]. Homologs of BLOC-1 subunit genes were identified among this group [22]. In a similar manner, BLOC-1 homologs were identified as

some of the proteins responsible for the proper intracellular sorting of proteins targeted to the *C. elegans* intestinal gut granules, a type of LRO distinct from conventional lysosomes that may be involved in photoprotection and defense against bacterial pathogens [7, 19, 23].

Spontaneous mouse mutants of BLOC-1 subunits – reduced pigmentation

A total of 16 non-allelic mouse hypopigmentation lines have been identified as being associated with the biogenesis of LROs [5, 24]. In addition to the lines of mice with mutations causing the pallid and muted phenotypes (caused by mutation of *Bloc1s6* and *Bloc1s5*, respectively) [2, 21], three more lines of mice, cappuccino, sandy, and 'reduced pigmentation', were found to harbor mutations in genes encoding BLOC-1 subunits – *Bloc1s4* (cappuccino), *Dtnbp1* (dysbindin) and *Bloc1s3* (BLOS3), respectively [4-6, 9]. The four BLOC-1 mouse models, pallid, muted, cappuccino and sandy, exhibit similar prolonged bleeding defects as well as the most severe coat color deficiencies among the spontaneous mouse models of defective LRO biogenesis [25]. In contrast, 'reduced pigmentation' mice, although exhibiting prolonged bleeding caused by compromised formation of platelet dense granules, show a significantly attenuated loss of pigmentation relative the other lines of mice harboring BLOC-1 gene mutations [6, 9].

Hermansky-Pudlak Syndrome

Mutations in a subset of the BLOC-1 genes have been found to cause Hermansky-Pudlak Syndrome (HPS) in humans. HPS is a genetic disorder associated with hypopigmentation of the skin, hair and eyes due to the abnormal formation of melanocytes, and prolonged bleeding caused by defects in the biogenesis of platelet dense granules [25, 26]. HPS-7 is caused by mutations in the gene encoding dysbindin [5]. While HPS-8 is caused by mutation of the gene encoding BLOS3 [27, 28]. HPS-9 is caused by mutation of the gene encoding pallidin [29, 30]. The HPS

subtypes caused by mutation of BLOC-1 subunit genes in humans are so far limited to these three subtypes, but the specific phenotypes of each HPS subtype are heterologous among affected individuals. For example, whereas *Bloc1s3* causes an attenuated HPS-like syndrome in mice [6, 9], in some human patients, mutation of *BLOC1S3* causes HPS pheontypes indistinguishable from HPS caused by mutation of other BLOC-1 genes [5, 27, 28].

BLOC-1 genes

The BLOC-1 subunit genes were first cloned in mice with homologs being readily recognized in humans [2, 6, 4, 21, 31]. Although initially thought to be limited to mammals [21], homologs of the full complement of BLOC-1 subunit encoding genes were identified in *Drosophila* [22] and a subset of BLOC-1 genes were identified in *C. elegans* [7, 23]. However, homologs of BLOC-1 remained elusive in *Saccharomyces cerevisiae* [7, 25] until Hayes *et al*. identified a hexameric protein complex in yeast that contains three proteins exhibiting structural homology to metazoan BLOC-1 proteins (Fig. 1.1): Bls1p, Snn1p and Cnl1p that show homology to metazoan BLOS1, snapin and DUF2365 proteins, respectively – DUF2365 being a protein with some structural similarity to cappuccino [32].

The three other proteins in yeast "BLOC-1" are Kxd1p, Vab2p and Bli1p, and are not homologous to canonical metazoan BLOC-1 subunits. However, one of these proteins, Kxd1p, was recognized as the homolog of a protein shown to interact with Blos1 in *Drosophila* and with both DUF2365 and cno, the suggested nematode cappuccino homolog [32], in *C. elegans* [32-34]. *Kxd1* was subsequently found to elicit melanosome and platelet dense granule phenotypes when knocked-out in mice [35]. In our laboratory, Esteban Dell'Angelica recognized that Vab2p is the yeast homolog of the *Drosophila* protein encoded by *CG11802*, and this protein (hereafter Vab2) was shown to interact with the Blos2·dysbindin·snapin subcomplex of BLOC-1 [36] (Fig. 1.2). Because metazoan homologs of two of the three non-canonical yeast BLOC-1 subunits have been

found in association with canonical BLOC-1 subunits, this raised the question of what role, if any, these non-canonical yeast BLOC-1 proteins had in affecting the function of BLOC-1.

Generation of a Drosophila Vab2 mutant

To test the hypothesis that Vab2 affects the function of canonical BLOC-1 in metazoans, I deleted the *Vab2* gene in *Drosophila melanogaster* using the approach of P element imprecise excision. This work is described in Chapter 2. Briefly, I isolated and identified two independent deletions of *Vab2*: $Vab2^{114}$ and $Vab2^{115}$. $Vab2^{114}$ is a promoter deletion of *Vab2*, while $Vab2^{115}$ is a deletion of the *Vab2* open reading frame (ORF). Because $Vab2^{114}$ was a promoter deletion that left the entire *Vab2* ORF intact, I characterized Vab2 mRNA expression from both of these lines.

Deletion of Kxd1 and Blos3 by CRISPR-mediated genomic editing

To test the hypothesis that Kxd1 affects the function of canonical BLOC-1 in metazoans, and that deletion of *Kxd1* in *Drosophila* would therefore elicit BLOC-1 phenotypes similar to those reported for deletion of *Kxd1* in mice [35], I deleted *Kxd1* in *Drosophila melanogaster* using a CRISPR/Cas9 (Clustered Regularly Interspaced Short Palindromic Repeats/ CRISPR-associated protein 9)-mediated approach. Given the efficiency of CRISPR gene deletion that I observed, I also targeted the *Drosophila Blos3* gene for deletion using a CRISPR/Cas9 approach. I hypothesized that loss of *Blos3* in a phylogenetically distant species (*Drosophila*) could elucidate whether or not the atypical BLOC-1 phenotypes observed of 'reduced-pigmentation' mice were caused by a species-specific effect for the loss of BLOS3 or if the attenuated BLOC-1 phenotypes of *Blosc1s3* mutant mice were an intrinsic characteristic of BLOS3 relative to BLOC-1 function. This work is described in Chapter 3.

Phenotypic characterization of Vab2, Kxd1 and Blos3 mutant flies

In Chapter 4, I describe the phenotypic characterization of the *Vab2*, *Kxd1* and *Blos3* mutant flies. Briefly, in each case I compared the accumulation of two distinct eye pigments in these flies relative to the accumulation of the same eye pigments in wildtype and *blos1* mutant flies. Loss of *blos1*, a canonical subunit of metazoan BLOC-1, causes a profound reduction of red and brown pigments in the compound eyes of *Drosophila* due to defects in the biogenesis of eye pigment granules [22], a type of LRO where red drosopterins and brown ommochromes are synthesized and stored [17, 18]. If *Vab2* or *Kxd1* affected BLOC-1 function, I hypothesized that loss of these gene would phenocopy or partially phenocopy loss of *blos1*. Similarly, I hypothesized that loss of *Blos3* in *Drosophila* would phenocopy *blos1*, in either an attenuated manner (if Blos3 behaved as a non-canonical member of BLOC-1), or in a manner nearly identical to *blos1* (if the mild BLOC-1 phenotypes of the 'reduced pigmentation' mouse are due to a species-specific effect). Finally, I describe the characterization of *Vab2* deletions in combination with loss of *blos1* (a gene encoding a subunit of BLOC-1) and *pink* (a gene encoding a subunit of BLOC-2).

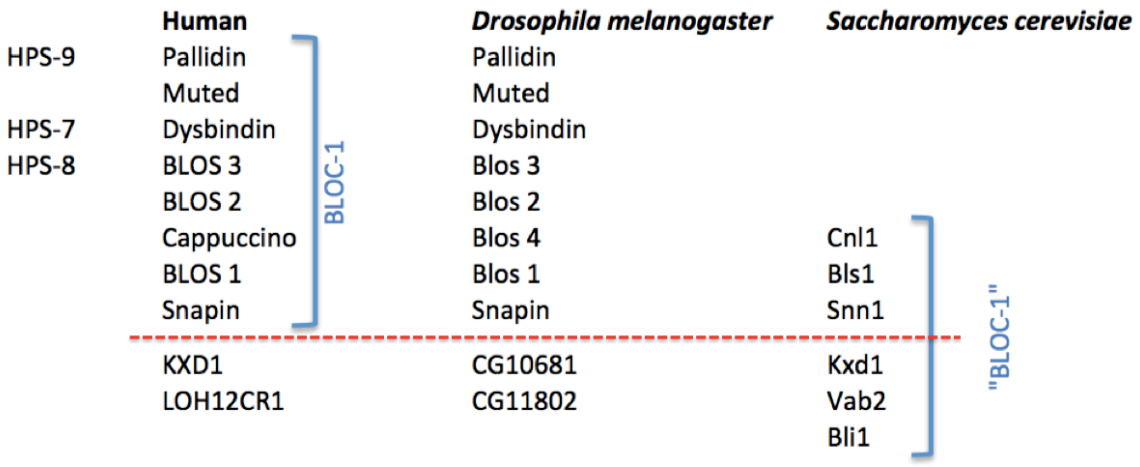

Figure 1.1. Comparison between the known subunits of human, *Drosophila* and yeast BLOC-1. The eight metazoan BLOC-1 subunits are listed above the dotted red line for humans and *Drosophila melanogaster*. The six yeast 'BLOC-1' subunits [35] are listed divided by the dotted red line: those with homology to metazoan BLOC-1 subunits are above, and those with no homology to metazoan BLOC-1 subunits are below. Homologs of two of the yeast-specific 'BLOC-1' subunits were identified in metazoans: KXD1/CG10681 and LOH12CR1/CG11802, in humans and *Drosophila*, respectively (below dashed red line). The subtypes of Hermansky-Pudlak syndrome associated with mutation of BLOC-1 subunits in humans are shown on the left (HPS-9, HPS-7 and HPS-8).

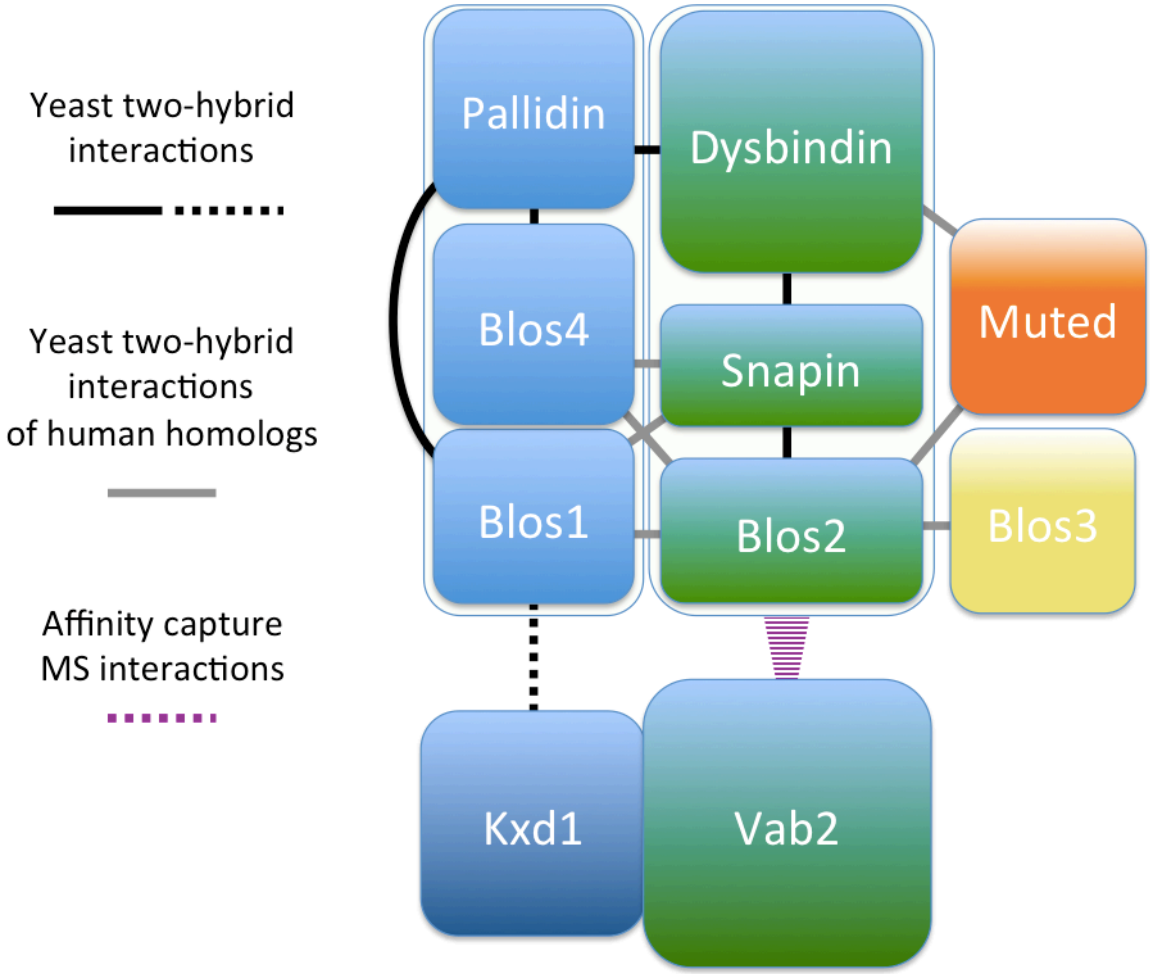

Figure 1.2. Model of *Drosophila* BLOC-1 organization with Vab2 and Kxd1. A cartoon model of *Drosophila* BLOC-1 is shown. The relative size of each subunit is shown by the area of the rectangle representing each protein. The BLOC-1 subassemblies are outlined: Pallidin·Blos4·Blos1 and Dysbindin·Snapin·Blos2. Solid black lines show yeast two-hybrid interactions between *Drosophila* BLOC-1 subunits [22]. The dashed black line shows yeast two-hybrid interaction between *Drosophila* Blos1 and Kxd1 [33]. Solid gray lines show additional yeast two-hybrid interactions observed between the human homologs of the *Drosophila* BLOC-1 proteins [22]. The dashed purple wedge shows the interaction between *Drosophila* Vab2 and the Blos2·Snapin·Dysbindin subassembly of BLOC-1, as determined by affinity capture and mass spectroscopy [36]. The yeast homologs of Kxd1 and Vab2 (Kxd1p and Vab2p) were associated by both yeast two-hybrid and MS affinity capture [32], and hence, the *Drosophila* homologs of these proteins are shown adjacent to each other – however this interaction has not been directly shown for the *Drosophila* proteins.

REFERENCES

1 Falcón-Pérez JM, Starcevic M, Gautam R, Dell'Angelica EC. BLOC-1, a novel complex containing the pallidin and muted proteins involved in the biogenesis of melanosomes and platelet-dense granules. J Biol Chem. 2002 Aug 2;277(31):28191-9.

2 Huang L, Kuo YM, Gitschier J. The pallid gene encodes a novel, syntaxin 13-interacting protein involved in platelet storage pool deficiency. Nat Genet. 1999 Nov;23(3):329-32.

3 Moriyama K, Bonifacino JS. Pallidin is a component of a multi-protein complex involved in the biogenesis of lysosome-related organelles. Traffic. 2002 Sep;3(9):666-77.

4 Ciciotte SL, Gwynn B, Moriyama K, Huizing M, Gahl WA, Bonifacino JS, Peters LL. Cappuccino, a mouse model of Hermansky-Pudlak syndrome, encodes a novel protein that is part of the pallidin-muted complex (BLOC-1). Blood. 2003 Jun 1;101(11):4402-7.

5 Li W, Zhang Q, Oiso N, Novak EK, Gautam R, O'Brien EP, Tinsley CL, Blake DJ, Spritz RA, Copeland NG, Jenkins NA, Amato D, Roe BA, Starcevic M, Dell'Angelica EC, Elliott RW, Mishra V, Kingsmore SF, Paylor RE, Swank RT. Hermansky-Pudlak syndrome type 7 (HPS-7) results from mutant dysbindin, a member of the biogenesis of lysosome-related organelles complex 1 (BLOC-1). Nat Genet. 2003 Sep;35(1):84-9.

6 Starcevic M, Dell'Angelica EC. Identification of snapin and three novel proteins (BLOS1, BLOS2, and BLOS3/reduced pigmentation) as subunits of biogenesis of lysosome-related organelles complex-1 (BLOC-1). J Biol Chem. 2004 Jul 2;279(27):28393-401.

7 Cheli VT, Dell'Angelica EC. Early origin of genes encoding subunits of biogenesis of lysosome-related organelles complex-1, -2 and -3. Traffic. 2010 May;11(5):579-86.

8 Lee HH, Nemecek D, Schindler C, Smith WJ, Ghirlando R, Steven AC, Bonifacino JS, Hurley JH. Assembly and architecture of biogenesis of lysosome-related organelles complex-1 (BLOC-1). J Biol Chem. 2012 Feb 17;287(8):5882-90.

9 Gwynn B, Martina JA, Bonifacino JS, Sviderskaya EV, Lamoreux ML, Bennett DC, Moriyama K, Huizing M, Helip-Wooley A, Gahl WA, Webb LS, Lambert AJ, Peters LL. Reduced pigmentation (rp), a mouse model of Hermansky-Pudlak syndrome, encodes a novel component of the BLOC-1 complex. Blood. 2004 Nov 15;104(10):3181-9.

10 Salazar G, Craige B, Styers ML, Newell-Litwa KA, Doucette MM, Wainer BH, Falcon-Perez JM, Dell'Angelica EC, Peden AA, Werner E, Faundez V. BLOC-1 complex deficiency alters the targeting of adaptor protein complex-3 cargoes. Mol Biol Cell. 2006 Sep;17(9):4014-26.

11 Di Pietro SM, Falcón-Pérez JM, Tenza D, Setty SR, Marks MS, Raposo G, Dell'Angelica EC. BLOC-1 interacts with BLOC-2 and the AP-3 complex to facilitate protein trafficking on endosomes. Mol Biol Cell. 2006 Sep;17(9):4027-38.

12 Ghiani CA, Starcevic M, Rodriguez-Fernandez IA, Nazarian R, Cheli VT, Chan LN, Malvar JS, de Vellis J, Sabatti C, Dell'Angelica EC. The dysbindin-containing complex (BLOC-1) in brain: developmental regulation, interaction with SNARE proteins and role in neurite outgrowth. Mol Psychiatry. 2010 Feb;15(2):115, 204-15.

13 Luzio JP, Hackmann Y, Dieckmann NM, Griffiths GM. The biogenesis of lysosomes and lysosome-related organelles. Cold Spring Harb Perspect Biol. 2014 Sep 2;6(9):a016840.

14 Dell'Angelica EC, Mullins C, Caplan S, Bonifacino JS. Lysosome-related organelles. FASEB J. 2000 Jul;14(10):1265-78.

15 Sitaram A, Marks MS. Mechanisms of protein delivery to melanosomes in pigment cells. Physiology (Bethesda). 2012 Apr;27(2):85-99.

16 Blott EJ, Griffiths GM. Secretory lysosomes. Nat Rev Mol Cell Biol. 2002 Feb;3(2):122-31.

17 Lloyd V, Ramaswami M, Krämer H. Not just pretty eyes: Drosophila eye-colour mutations and lysosomal delivery. Trends Cell Biol. 1998 Jul;8(7):257-9.

18 Kim H, Kim K, Yim J. Biosynthesis of drosopterins, the red eye pigments of Drosophila melanogaster. IUBMB Life. 2013 Apr;65(4):334-40.

19 Coburn C, Gems D. The mysterious case of the C. elegans gut granule: death fluorescence, anthranilic acid and the kynurenine pathway. Front Genet. 2013 Aug 7;4:151.

20 Ryder PV, Faundez V. Schizophrenia: the "BLOC" may be in the endosomes. Sci Signal. 2009 Oct 20;2(93)

21 Zhang Q, Li W, Novak EK, Karim A, Mishra VS, Kingsmore SF, Roe BA, Suzuki T, Swank RT. The gene for the muted (mu) mouse, a model for Hermansky-Pudlak syndrome, defines a novel protein which regulates vesicle trafficking. Hum Mol Genet. 2002 Mar 15;11(6):697-706.

22 Cheli VT, Daniels RW, Godoy R, Hoyle DJ, Kandachar V, Starcevic M, Martinez-Agosto JA, Poole S, DiAntonio A, Lloyd VK, Chang HC, Krantz DE, Dell'Angelica EC. Genetic modifiers of abnormal organelle biogenesis in a Drosophila model of BLOC-1 deficiency. Hum Mol Genet. 2010 Mar 1;19(5):861-78.

23 Hermann GJ, Scavarda E, Weis AM, Saxton DS, Thomas LL, Salesky R, Somhegyi H, Curtin TP, Barrett A, Foster OK, Vine A, Erlich K, Kwan E, Rabbitts BM, Warren K. C. elegans BLOC-1 functions in trafficking to lysosome-related gut granules. PLoS One. 2012;7(8):e43043.

24 Swank RT, Novak EK, McGarry MP, Rusiniak ME, Feng L. Mouse models of HermanskyPudlak syndrome: a review. Pigment Cell Res. 1998 Apr;11(2):60-80.

25 Dell'Angelica EC. The building BLOC(k)s of lysosomes and related organelles. Curr Opin Cell Biol. 2004 Aug;16(4):458-64.

26 Huizing M, Anikster Y, Gahl WA. Hermansky-Pudlak syndrome and related disorders of organelle formation. Traffic. 2000 Nov;1(11):823-35.

27 Morgan NV, Pasha S, Johnson CA, Ainsworth JR, Eady RA, Dawood B, McKeown C, Trembath RC, Wilde J, Watson SP, Maher ER. A germline mutation in BLOC1S3/reduced pigmentation causes a novel variant of Hermansky-Pudlak syndrome (HPS8). Am J Hum Genet. 2006 Jan;78(1):160-6.

28 Cullinane AR, Curry JA, Golas G, Pan J, Carmona-Rivera C, Hess RA, White JG, Huizing M, Gahl WA. A BLOC-1 mutation screen reveals a novel BLOC1S3 mutation in Hermansky-Pudlak Syndrome type 8. Pigment Cell Melanoma Res. 2012 Sep;25(5):584-91.

29 Cullinane AR, Curry JA, Carmona-Rivera C, Summers CG, Ciccone C, Cardillo ND, Dorward H, Hess RA, White JG, Adams D, Huizing M, Gahl WA. A BLOC-1 mutation screen reveals that PLDN is mutated in Hermansky-Pudlak Syndrome type 9. Am J Hum Genet. 2011 Jun 10;88(6):778-87.

30 Badolato R, Prandini A, Caracciolo S, Colombo F, Tabellini G, Giacomelli M, Cantarini ME, Pession A, Bell CJ, Dinwiddie DL, Miller NA, Hateley SL, Saunders CJ, Zhang L, Schroth GP, Plebani A, Parolini S, Kingsmore SF. Exome sequencing reveals a pallidin mutation in a Hermansky-Pudlak-like primary immunodeficiency syndrome. Blood. 2012 Mar 29;119(13):3185-7.

31 Benson MA, Newey SE, Martin-Rendon E, Hawkes R, Blake DJ. Dysbindin, a novel coiled-coil-containing protein that interacts with the dystrobrevins in muscle and brain. J Biol Chem. 2001 Jun 29;276(26):24232-41.

32 Hayes MJ, Bryon K, Satkurunathan J, Levine TP. Yeast homologues of three BLOC-1 subunits highlight KxDL proteins as conserved interactors of BLOC-1. Traffic. 2011 Mar;12(3):260-8.

33 Giot L, Bader JS, Brouwer C, Chaudhuri A, Kuang B, Li Y, Hao YL, Ooi CE, Godwin B, Vitols E, Vijayadamodar G, Pochart P, Machineni H, Welsh M, Kong Y, Zerhusen B, Malcolm R, Varrone Z, Collis A, Minto M, Burgess S, McDaniel L, Stimpson E, Spriggs F, Williams J, Neurath K, Ioime N, Agee M, Voss E, Furtak K, Renzulli R, Aanensen N, Carrolla S, Bickelhaupt E, Lazovatsky Y, DaSilva A, Zhong J, Stanyon CA, Finley RL Jr, White KP, Braverman M, Jarvie T, Gold S, Leach M, Knight J, Shimkets RA, McKenna MP, Chant J, Rothberg JM. A protein interaction map of Drosophila melanogaster. Science. 2003 Dec 5;302(5651):1727-36.

34 Simonis N, Rual JF, Carvunis AR, Tasan M, Lemmens I, Hirozane-Kishikawa T, Hao T, Sahalie JM, Venkatesan K, Gebreab F, Cevik S, Klitgord N, Fan C, Braun P, Li N, Ayivi-Guedehoussou N, Dann E, Bertin N, Szeto D, Dricot A, Yildirim MA, Lin C, de Smet AS, Kao HL, Simon C, Smolyar A, Ahn JS, Tewari M, Boxem M, Milstein S, Yu H, Dreze M, Vandenhaute J, Gunsalus KC, Cusick ME, Hill DE, Tavernier J, Roth FP, Vidal M. Empirically controlled mapping of the Caenorhabditis elegans protein-protein interactome network. Nat Methods. 2009 Jan;6(1):47-54.

35 Yang Q, He X, Yang L, Zhou Z, Cullinane AR, Wei A, Zhang Z, Hao Z, Zhang A, He M, Feng Y, Gao X, Gahl WA, Huizing M, Li W. The BLOS1-interacting protein KXD1 is involved in the biogenesis of lysosome-related organelles. Traffic. 2012 Aug;13(8):1160-9.

36 Guruharsha KG, Rual JF, Zhai B, Mintseris J, Vaidya P, Vaidya N, Beekman C, Wong C, Rhee DY, Cenaj O, McKillip E, Shah S, Stapleton M, Wan KH, Yu C, Parsa B, Carlson JW, Chen X, Kapadia B, VijayRaghavan K, Gygi SP, Celniker SE, Obar RA, Artavanis-Tsakonas S. A protein complex network of Drosophila melanogaster. Cell. 2011 Oct 28;147(3):690-703.

CHAPTER 2

Deletion of *Vab2* in *Drosophila melanogaster* by P element imprecise excision

ABSTRACT

The *Saccharomyces cerevisiae VAB2* gene was predicted and shown to encode one of the subunits of the heterohexameric yeast BLOC-1 complex. On the other hand, no Vab2-like protein has been reported to be a constituent of metazoan BLOC-1. Our laboratory identified *CG11802* as the *Drosophila* homolog of the *Saccharomyces cerevisiae VAB2* gene using a PSI-BLAST (Position-Specific Iterated - Basic Local Alignment Search Tool) sequence homology search. To determine the function of *Vab2* in metazoans, I targeted *Vab2* for deletion in *Drosophila melanogaster* by P element imprecise excision. I obtained Bloomingtom Stock Center line 21873 which harbors a P element insertion in the 5' untranslated region (UTR) of *Vab2* (p{EPg}CG11802^{HP10420}). After mobilizing P{EPg}CG11802^{HP10420} I identified and isolated two deletion alleles of *Drosophila Vab2*. The first of these alleles, *Vab2^{114}* is a short 121 b.p. deletion that removes the upstream and downstream promoter elements of *Vab2*. The second is a large deletion that removes most *Vab2* sequences including the majority of the 5' UTR, the entire open reading frame (ORF), and the 3' UTR, as well as the 3' intergenic space downstream of *Vab2* and a short portion of the 3' UTR of the adjacent gene, *CG1847*, which approaches the *Vab2* locus from the opposite direction. The sequences deleted in the *Vab2^{114}* and *Vab2^{115}* alleles are those that were upstream and downstream, respectively, of the original insertion site of P{EPg}CG11802^{HP10420} and are the products of directional imprecise excision events. Neither *Vab2^{114}* nor *Vab2^{115}* exhibited obvious phenotypes as I isogenized the lines carrying these deletion with Canton S. *Vab2^{115}* expressed no Vab2 mRNA nor did it amplify *Vab2* sequences from genomic DNA, indicating that *Vab2^{115}* was a true genetic null. In contrast, *Vab2^{114}* expressed Vab2 mRNA, although at reduced levels in comparison to wildtype Canton S flies, indicating that *Vab2^{114}* was likely a hypomorphic allele of *Vab2*.

INTRODUCTION

Saccharomyces cerevisiae was recently reported to encode and express a six-subunit protein complex that contains three proteins with limited structural homology to three of the proteins found in metazoan BLOC-1 – yeast Bls1p showing homology to metazoan BLOS1, Snn1p showing homology to snapin, and Cnl1p showing homology to DUF2365, a protein that has cappuccino-like structural features [1]. Based on the homology of these three proteins to this subset of metazoan BLOC-1 proteins, this six-subunit yeast protein complex was named BLOC-1. However, yeast BLOC-1 lacks homologs of the other five metazoan BLOC-1 protein subunits, and it instead contains three additional proteins that are apparently not homologous to metazoan BLOC-1 proteins. The three yeast BLOC-1 proteins that have not been found in the canonical metazoan BLOC-1 are Vab2p, Kxd1p and Bli1p.

By performing PSI-BLAST iterative homology searches, Esteban Dell'Angelica determined that *CG11802* was the *Drosophila melanogaster* homolog of *Saccharomyces cerevisiae VAB2*. Given that the canonical metazoan BLOC-1 differs so significantly in composition from yeast BLOC-1, this raised the question of what *Vab2* might be doing in higher eukaryotes. We hypothesized that, if *Vab2* encodes a component or regulator of BLOC-1 in metazoans, mutations of *Drosophila Vab2* would phenocopy previously described mutations of *Drosophila blos1*, which is a gene encoding a canonical BLOC-1 subunit [2]. To test this hypothesis, I set out to delete *Drosophila Vab2* .

P element imprecise excision is a common strategy of targeted mutagenesis that relies on the endogenous inaccurate repair of chromosomal double-stranded DNA breaks (DSBs) generated during P element transposition to delete genomic DNA sequences flanking the original P element insertion site. P element is a DNA transposon that uses a conservative, non-replicative, cut-and-paste method of transposition to excise itself from one location and reinsert in another [3]. During the process of P element mobilization, the P element recombinase, also known as

'transposase', makes staggered DSBs within the P element terminal inverted repeats (IRs). The DNA ends left on both the excised P element and at the original site of insertion have long single stranded 3' overhangs. On the excised P element these ends are protected by protein factors. The corresponding DSBs at the original site of P element insertion, the donor site, are left unprotected and become substrates for normal DSB repair mechanisms. At a frequency of around 1% substantial DNA resection of the donor site DNA ends occurs during or prior to DSB repair, and DNA sequences adjacent to original site of P element insertion are thus deleted before the donor site is repaired [4]. *Drosophila* geneticists have used such "imprecise excision" deletion events to create mutant alleles of genes proximal to a P element insertion in order to determine gene function. I chose to use an imprecise excision approach to target *Vab2* for deletion in *Drosophila*.

P{EPg} is a genetically engineered P element transposon that contains the artificial Scer\UAS DNA-binding site, for transactivation of adjacent genes by the Scer\Gal4 transcriptional activator, and the w^{+mC} mini-white gene that endows w^{-} fly lines a visibly scorable red eye phenotype. P{EPg} is a non-autonomous transposable element in that it does not encode a transposase gene but can be mobilized *in trans* if transposase is supplied from a different location. Because the P{EPg} encoded w^{+mC} gene marks flies harboring the P element with a visible red eye phenotype, loss of w^{+mC} expression can be used to identify flies with a w^{-} genetic background in which P{EPg} has been mobilized. In these regards, P{EPg} provides a viable starting point for gene deletion of adjacent sequences by P element imprecise excision.

Finally, transposase activity is normally restricted to the *Drosophila* germline by an mRNA splicing event that removes the "2-3" intron between the third and fourth exons of the transposase mRNA. Removal of the 2-3 intron generates an mRNA message that produces the full-length and active transposase. In somatic cells the 2-3 intron is retained in the mRNA and produces a truncated protein that cannot catalyze P element mobilization and instead acts as a repressor of transposition. By removing the 2-3 intron from *transposase* Laski *et al.* created a version of *transposase* known as "Δ2-3" that produces a full-length and active transposase in both

somatic and germline cells [5]. The creation of this construct has been a useful for mobilizing P elements in a variety of situations, and a genetically stable source of Δ2-3 transposase is available in flies that carry the P{ry^+ Δ2-3}99B insertion – a non-mobilizable P element that harbors the artificially constructed Δ2-3 *transposase* gene and is inserted on chromosome 3 at cytological position 99B [6].

MATERIAL AND METHODS

Fly Stocks

FlyBase (flybase.org) was used to identify commonly available fly lines of interest. Canton S, Δ2-3 transposase, TM2/TM6B and line 21873 fly stocks were obtained from Bloomington Stock Center. Line 21873 harbors a P{EPg} P element insertion in the 5' UTR of *Vab2*. FM6 balancer flies were obtained from Ming Guo (Department of Neurology, UCLA). Flies were maintained and bred in a dedicated room maintained at 20-24°C on media prepared by the UCLA Drosophila Media Facility.

PCR screening

DNA was prepared from mobilized-P{EPg}CG11802^{HP10420} w^- lines using either a mechanical extraction and salt precipitation protocol (earlier samples – 10 flies per sample) or using the Macherey-Nagel NucleoSpin Tissue XS spin column kit according to the manufacturer's protocol (later samples – 5 flies per sample), except that columns were eluted with 20 µl of BE (Buffer Elution) per fly used. PCR screening reactions were carried out using the Qiagen Hot Start Master Mix kit according to the manufacturer's protocol (early samples) or using the Bioland Scientific 2 X Taq PCR Premix reagent according to the manufacturer's protocol (later samples). *Rabaptin-5* was screened with primers CDS-004 (GTGCGTGTGTTGTGAAGTCT) and CDS-005 (AACACCGCACCCTACTTCAG) to generate a 760 b.p. band. The *Vab2*-specific primers that were used to amplify across the P{EPg}CG11802HP^{10420} insertion site were CDS-108 (GGTGG CTGGCGTCCGTCGAAGATCTCGTG) and CDS-144 (GCTGACATCAAGCGTGCAGTGGA AACAGCTCGTTATCTGTAC). These primers generate a 371 b.p. band from wildtype *Vab2*. Later *Vab2* screening primers were CDS-109 (CTCTGCTGGAGCATATGCGCCGGCTTGC TG), CDS-110 (CTCCGCTGCTCCTGGCTTAGCTGCAAAATGTGCTG), CDS-111 (CGGC

AGAACGACGACGACGGCCACCAAAACAC), CDS-146 (ACAGCCGCCACAGGCGACTG CTGTTG) and CDS-149 (CTCATCCTCCGCCTCGATTCACATTCAACGGTGTAG).

DNA sequencing

"Purified Template" full service Sanger sequencing services were contracted with Laragen Inc. and consisted of supplying Laragen with purified PCR DNA and primers. In addition to primers CDS-110, CDS-111 and CDS-149 described above, imprecise excision alleles were sequenced with CDS-108 (GGTGGCTGGCGTCCGTCGAAGATCTCGTG).

mRNA detection

mRNA expression was tested by purifying total RNA from 10 flies per sample, using the Machery-Nagel NucleoSpin RNA II kit according to the manufacturer's guidelines. cDNA was subsequently generated from purified total RNA samples using the Clontech RNA to cDNA EcoDry Premix (Double Primed) kit according to the manufacturer's guidelines. Vab2 cDNA was amplified using CDS-146 (ACAGCCGCCACAGGCGACTGCTGTTG) and CDS-147 (CGCCG TGAAACCGAAGCGACCACAGTCCAC). Rabaptin-5 cDNA was amplified using CDS-015b (GCTGGACGAGCTGAAGACACA CCTAATG) and CDS-029b (CTGCTTTTGCAGCAGATC CACCTGTTTC).

RESULTS

The *Drosophila Vab2* gene is located at cytological position 10F2 on the *Drosophila* X chromosome, and Bloomington line 21873 harbors a P{EPg} insertion in the 5' UTR of *Vab2* – P{EPg}CG11802^{HP10420}. This line was obtained as a starting point from which to delete *Vab2* by imprecise excision.

'Pre-Cantonization' of Bloomington line 21873

Bloomington line 21873 was maintained in genetic isolation at the Bloomington Stock Center in order to preserve the integrity of the P{EPg}CG11802^{HP10420} insertion. While bred in isolation, line 28873 may have accumulated secondary mutations, and the original gene hopping events that were used to generate the P{EPg}CG11802^{HP10420} insertion were performed in a w^- line of flies in order to visually follow P{EPg} transposition [7].

One of the most sensitive phenotypes for loss of BLOC-1 in *Drosophila* is a reduction of eye pigment accumulation due to impaired biogenesis of pigment granules, the lysosome related organelles (LROs) in which *Drosophila* eye pigments are synthesized and stored [2], and, in the absence of a functional *w* gene, flies have white eyes due to the lack of the White ABC transporter that is required for the transfer of metabolic intermediates of both red and brown pigments into the pigment granules [8]. Because my aim was to determine if deletion of *Vab2* elicited BLOC-1-like phenotypes, I needed to transfer any *Vab2* deletions that I obtained in line 21873 into a wildtype w^+ background.

I specifically wanted to quantitatively compare *Vab2* eye phenotypes to those that had been determined for loss of *blos1* – a canonical BLOC-1 mutation. The *blos1* mutations had been transferred to a wildtype w^+ background by serially outcrossing the w^- flies in which the *blos1* deletions had been generated to wildtype Canton S flies [2]. I would need to similarly 'Cantonize'

any *Vab2* deletions that I obtained by imprecise excision of P{EPg}CG11802^{HP10420}. In addition to introducing the *w* gene, the purpose of these 'Cantonization' crosses was to bring the three autosomal chromosomes back to wildtype status and to provide recombination opportunities between the X chromosome carrying the P{EPg}CG11802^{HP10420} insertion and a wildtype X chromosome. However, because I was relying on the w^- background of the P{EPg}CG11802^{HP10420}-insertion flies to monitor the mobilization of P{EPg} during the subsequent imprecise excision steps, I did these crosses in two stages. The initial rounds of Cantonization were performed with a w^- line of Canton S flies to address the general goal of isogenizing line 21873 flies with Canton S.

First, before introducing transposase to mobilize P{EPg}CG11802^{HP10420}, I serially crossed the *Vab2*:P{EPg} flies five times to a line of w^- Canton S flies that had previously been generated in the laboratory but were otherwise considered to have a wildtype Canton S background (crosses P1-P5, Fig. 2.1). At each stage, flies that inherited the P{EPg}CG11802^{HP10420} insertion were identified by retention of a red eye phenotype in a w^- chromosomal background. Collectively these crosses were referred to as 'pre-Cantonization' crosses, and they were followed by the imprecise excision of P{EPg}CG11802^{HP10420}. Additional 'Cantonization' crosses, including introduction of a wildtype copy of the w^+ gene were only performed later, after *Vab2* deletions had been generated and identified.

P element mobilization and Imprecise Excision

To generate *Vab2* imprecise excision events in the pre-Cantonized P{EPg}CG11802^{HP10420} line, I introduced the transposase gene, *in trans,* by crossing these flies to a line carrying the P{Δ2-3}99B transposon. P{Δ2-3}99B harbors the Δ2-3 transposase gene on a non-mobilizable P element inserted on the third chromosome. By first crossing the P{Δ2-3}99B line to an FM6 first chromosome balancer line, I was able to create female flies that carried the

FM6 first chromosome balancer and the Δ2-3 gene on the third chromosome. I bred these FM6/*y, w* ; *Sb*, Δ2-3/+ females to pre-Cantonized male flies carrying the P{EPg}CG11802^{HP10420} insertion (cross IE1, Fig. 2.1). A sub-set of the progeny from this cross were flies that carried both the mobilizable P{EPg} insertion in *Vab2* and Δ2-3 *transposase – i.e.* P{EPg}CG11802^{HP10420}/FM6 : *Sb*, Δ2-3/+ flies.

Sb is at cytological position 89B of chromosome 3. Because I was assessing the inheritance of Δ2-3 based on the visible phenotype imparted by the *Sb* marker on the same chromosome, and this chromosome was coming from an unbalanced parent, I estimate that roughly 30% of the flies that I deemed to have inherited the *Sb*, Δ2-3 third chromosome were recombinants that did not inherit Δ2-3 but only the *Sb* marker. Among those that were properly identified to have inherited Δ2-3, it was anticipated that some of these flies would exhibit a mosaic red eye-color, if P{EPg} was efficiently mobilized by Δ2-3 *transposase,* due to the loss of w^{+mC} carried by P{EPg} (and thus loss of pigmentation) in clonal groups of ommatidia derived from progenitor cells in which P{EPg}CG11802^{HP10420} had been mobilized. This, however, was not observed. All of the P{EPg}CG11802^{HP10420}/FM6 : Sb, Δ2-3/+ flies that were observed had uniformly pigmented red eyes characteristic of w^{+mC} expression.

Nevertheless, a number of P{EPg}/FM6 ; *Sb*, Δ2-3/+ flies underwent P{EPg} mobilization in the germline and were able to transmit these mobilization events to their offspring – I crossed individual P{EPg}/FM6 ; *Sb*, Δ2-3/+ female flies to FM6 males (cross IE2, Fig. 2.1) and obtained a mix of w^{+mC} and w^{-} progeny flies. The w^{-} progeny from this cross were deemed to be P{EPg}CG11802^{HP10420} excision flies, some of which potentially harbored imprecise excision deletions of *Vab2*. I individually crossed the w^{-} ; Δ2-3^{-} subset of these to FM6 balancer flies in order to establish putative excision lines for genetic characterization (cross IE3, Fig. 2.1). I elected to only establish lines from the w^{-} flies that were also lacking the *Sb* phenotypic marker, a surrogate marker for the presence Δ2-3, to minimize potential genetic complexities that could arise from a residual P element being mobilized *in trans* in the developing animal.

Screening of putative Vab2 excision lines

Among the 189 w^- founders that were crossed to establish lines, most (171 founders) were successfully bred to the FM6 balancer line and then back-crossed to established homozygous w^- lines (Table 2.1). A minority of the founders did not successfully produce progeny when crossed to the FM6 balancer line, and others were not able to establish homozygous w^- P element-mobilized lines. The latter likely represented large deletions in the vicinity of *Vab2* that included essential genes, but the exact nature of these genotypes was not determined.

To determine the genetic structure of the *Vab2* locus in the P element-mobilized w^- lines that reached a state of homozygosity, I prepared DNA from each of these lines and screened them using 2 separate PCR reactions (Fig. 2.2). I used a *Vab2*-specific pair of primers that amplify across the site of P{EPg}CG11802^{HP10420} insertion to examine the structure of *Vab2* in each line. CDS-108 hybridizes within *Vab2* at the 5' end of the *Vab2* ORF, downstream of the AUG start codon, and 3' of the P element insertion site. CDS-144 hybridizes in the intergenic region upstream of *Vab2* and 5' of the P element insertion site. Together they amplify a 371 b.p. band from wildtype *Vab2*. Imprecise excision deletions in *Vab2* that extended in either direction from the original site of P{EPg} insertion were likely to disrupt amplification of this *Vab2*-specific band if they were of a size significant enough to affected *Vab2* expression. The anticipated readout of the CDS-108/CDS-144 *Vab2* screen for any such deletions was the lack of a *Vab2* PCR product. As a positive control I screened each sample in parallel using a pair of primers that amplified a 760 b.p. *Rabaptin-5* (*Rbpn-5*) band. *Rpbn-5* is an unrelated gene on chromosome 2 that should not have been affected by any of the previous P element mobilization steps. This screen was included to determine the quality of each DNA preparation since I was specifically screening for samples that did not amplify *Vab2* in the CDS-108/CDS-144 PCR reaction.

Vab2 precise excisions

I anticipated observing two general classes of P{EPg} mobilization events among the w^- homozygous lines that were screened: precise excisions and imprecise excisions. I expected the majority of the w^- lines to have arisen from P element precise excision that "restored" the original *Vab2* 5' UTR structure. In reality, truly precise excisions that restore the original sequence structure at the site of insertion are rare. The vast majority of P element precise excision loci include an 8 b.p. duplication of the original P element insertion site and various lengths of the P element inverted repeats (IRs) that are left between the duplicated genomic target site. These residual IR sequences are remnants of the 17 b.p. 3' single-stranded overhangs generated by transposase during P element mobilization. In addition, short insertions (typically 1-15 b.p.) of untemplated bases with low G+C content are frequently found between the residual IR sequences at these sites [3, 9]. Accordingly, in cases of P element precise excision I expected the CDS-108/CDS-144 *Vab2* PCR screen to generate bands of roughly 379 b.p. (and up to ~ 424 b.p.). [371 b.p. wildtype *Vab2* PCR product + 8 b.p. duplicated target site + up to an approximate 30 b.p. derived from the IRs and 15 b.p. untemplated – *c.f.* last lane on right of Fig. 2.2 as an example of a *Vab2* precise excision band of ~ 424 b.p.] Indeed, this is what was observed from the majority of the w^- P element-mobilization lines (123 out of 168 lies screened – Table 2.1).

Type 1 and Type 2 excisions

In addition to recovering a number of precise excision lines I also isolated and established lines from flies harboring several other types of excision events (45 out of 168 – Table 2.1). Most of these anomalous excisions consisted of internally deleted P elements that remained integrated at the original insertion site but had lost, among other sequences, the dominant w^{+mC} marker gene

that imparts a red eye phenotype. These internally deleted P elements fell into two classes, Type 1 and Type 2 excisions, based on the P element sequences that were left behind. Both Type 1 and Type 2 excisions retained the 8 b.p. genomic sequence duplications that flank the original insertion site of P{EPg}, as well as the 5' and 3' P element IR sequences of P{EPg}CG11802HP^{10420}, but they differed from each other based on the internal P element sequences that had been deleted.

The parental P{EPg} transposon has two sets of direct repeats, DR1 and DR2 (Fig 2.3 – upper gene schematic). These exist outside of the terminal IRs but are still situated near the P element ends. These repeats are arranged in tandem and in the same order at both ends of the P element such that, if reading from 5' to 3' along the P{EPg} sequence, they appear in the order:

5' – IR, DR1, DR2… [internal P element sequences]… DR1, DR2, IR – 3'

Sequencing analysis revealed that Type 1 deletions consisted of a residual P element insertion that appeared to have "recombined" between the two DR1 sequences (Fig 2.3 – middle gene schematic). This resulted in the retention of a single DR1 sequence flanked upstream by the 5' IR and downstream by the 3' DR2 and IR sequences. The orientation of this internally deleted P{EPg} remained identical to the orientation of the original P{EPg}CG11802^{HP10420} insertion, and recombination between the two DR1 elements was deemed as the likely etiology of these insertions based on the retention of the large, 255 b.p., spacing between DR1 and DR2 at the 3' end of P{EPg}. The remaining P element sequences in Type 1 excisions can be schematically represented as:

Type 1: [5' – IR, (174 b.p.), DR1, (255 b.p.), DR2, IR – 3']

This structure generated a 1099 b.p. *Vab2* PCR product when screened with the CDS-108/CDS-144 PCR reaction (Fig. 2.2, yellow arrow).

In the case of Type 2 excision events, sequencing analysis showed that recombination had occurred between the two DR2 sequences in a similar manner to that which had occurred between DR1 sequences in Type 1 events (Fig 2.3 – lower gene schematic). Consequently the order of the remaining repeat sequences was identical to that observed in Type 1 excisions (5' – IR, DR1, DR2, IR – 3'), but the spacing between the remaining repeat elements reflected the 2 b.p spacing seen between DR1 and DR2 at the 5' end of P{EPg}. Schematically, Type 2 P{EPg} events can be represented as:

Type 2: [5' – IR, (174 b.p.), DR1, (2 b.p.), DR2, IR – 3']

This structure generated an 884 b.p. *Vab2* PCR product when screened with the CDS-108/CDS-144 PCR reaction (Fig. 2.2, orange arrow).

Together, Type 1 and Type 2 excisions accounted for 40 of the 45 anomalous P element excisions events that were observed and characterized. It must be noted that although I loosely described Type 1 and Type 2 excisions as having apparently resulted from recombination that occurred between the DR1 or DR2 sequences, respectively, the precise mechanism of P element internal deletion in these structures was not demonstrated. However the sequencing data from both of the representative Type 1 and Type 2 excision events that were examined (one of each) revealed that, regardless of the exact site or mechanism of apparent recombination and internal deletion, the nucleotide sequences of the remaining repeat elements and the intervening spacer sequences showed no signs of insertion, deletion or other modification from the parental P{EPg}CG11802^{HP10420} transposon.

Vab2 imprecise excisions

The remaining five homozygous w^- putative P{EPg}-mobilization lines that I screened did not amplify *Vab2* or amplified a mix of *Vab2* bands in the CDS-108/CDS-144 screening reaction (four lines and one line, respectively – Table 2.1) Therefore I deemed these lines to be putative P element imprecise excisions. The line that amplified a mix of *Vab2* bands was not followed up, but each of the lines that failed to amplify a *Vab2* band (but did amplify a *Rbpn-5* control band) were characterized further to determine if any of them harbored a genetic deletion of *Vab2*. Because the CDS-108/CDS-144 screening reaction relies on primer hybridization 5' and 3' proximal to the P{EPg} insertion site, the failure of the reaction to generate a *Vab2*-specific band can indicate that either sequences upstream or sequences downstream of the P{EPg} insertion locus have been deleted – or both. However, other explanations may also account for failure to amplify a *Vab2* band such as the retention of a large fragment of the P element (that has otherwise lost the w^{+mC} dominant marker) that the Taq DNA polymerase cannot extend through – for example, the Type 1 and Type 2 excisions, had the remaining P{EPg} sequences been longer.

To distinguish between the various alternatives and the possibility that portions of *Vab2* had been deleted in these remaining four lines, I ran a series of additional PCR reactions on these samples to specifically identify *Vab2* deletions. The strategy of these additional screens was to move both the upstream and downstream amplification primers further away from the P{EPg} insertion site in a stepwise manner to identify and capture *Vab2* deletions as smaller-than-expected PCR products. Because I anticipated amplifying longer PCR products than were generated in the primary screen of *Vab2*, rather than performing these PCR reactions with Taq DNA polymerase I utilized PrimeSTAR® Max high-fidelity polymerase; a thermo-stable DNA polymerase that is routinely capable of amplifying 6 kb products under standard cycling conditions [10].

To move the 5' *Vab2* primer further upstream of the P{EPg}CG11802^{HP10420} insertion site I designed primers in *CG15739*, gene upstream of *Vab2*. The intergenic sequence between *Vab2* and *CG15739* is A+T rich and is unamenable to PCR primer design. Since *CG15739* is transcribed in the opposite direction from *Vab2* the upstream primers that I designed were located in the first and second exons of *CG15739* (CDS-111 and CDS-110, respectively). Similarly, to move the 3' *Vab2* primer further downstream of the P element insertion site I designed primers at the terminus of the *Vab2* ORF and in the 3' UTR of *CG1847* (CDS-146 and CDS-149, respectively). *CG1847* is the gene immediately downstream of *Vab2* and, like *CG15739*, it is transcribed in the opposite direction from *Vab2*. In this case the 3' UTR of *CG1847* is proximal to the 3' UTR of *Vab2*.

At the same time that this approach was designed to identify *Vab2* deletions of interest, it also allowed me to circumstantially identify deletions that extended into the neighboring genes and were therefore larger than desired for subsequent characterization of *Vab2*. In fact, two of the four putative imprecise excisions, although viable in a heterozygous state, failed to amplify a *Vab2* PCR product even with the most distant combination of primers. This indicated that both of these lines harbored *Vab2* deletions that extended into one or both of the adjacent genes.

Of the two remaining anomalous P{EPg} excision lines, DNA from line ^{3}115 failed to amplify a PCR product with the closer pair of distanced *Vab2* PCR primers (CDS-111/CDS-146) but amplified a smaller-than-expected PCR product with the two most distant *Vab2* PCR primers (CDS-110/CDS-149). This PCR product was approximately 1500 b.p. long and roughly 1670 b.p. smaller than the 3195 b.p. product that was amplified from a wildtype *Vab2* template.

The last of these lines that failed to amplify a *Vab2* PCR product in the initial PCR screen was line ^{3}114. These flies produced long *Vab2* PCR bands that did not appear to be significantly different than those amplified from a wildtype *Vab2* template when screened with the distanced *Vab2* PCR primers (CDS-111/CDS-146 producing a 1853 b.p. band and CDS-110/CDS-149 producing a 3195 b.p. band from wildtype *Vab2*). However, I reasoned that line ^{3}114 failed the

initial *Vab2* screen (the CDS-108/CDS-144) because at least one binding site for one of the initial screening primers was not present in this line. To locate the genetic lesion carried by this line, I screened with several additional combinations of primers pairs, moving the annealing sites closer to the P element insertion site and within the *Vab2* coding region (detailed below). This generated *Vab2* PCR products from line ^{3}114 DNA that were distinguishably smaller than those generated from wildtype templates and revealed that line ^{3}114 harbored a small deletion of roughly 120 b.p. that extended in the opposite orientation of that found in line ^{3}115.

Vab2 deletion alleles

To determine the molecular structure of the *Vab2* allele in line ^{3}115, I submitted the *Vab2* PrimeSTAR® PCR product from this line for bidirectional sequencing. The sequencing results indicated that line ^{3}115 harbored a large, 1670 b.p. deletion of *Vab2* that extended in a 3' direction from the original P{EPg}CG11802^{HP10420} insertion site, and encompassed a portion of the *Vab2* 5' UTR, the entire *Vab2* ORF, the entire *Vab2* 3' UTR, the 130 b.p. intergenic region downstream of *Vab2* and the last 92-95 b.p. of the 3' UTR of the neighboring gene, *CG1847*: a putative aryl hydrocarbon receptor-interacting protein (Fig. 2.4). Although the ^{3}115 deletion extended into the mRNA sequences of both of the annotated transcripts for *CG1847*, only the last 95 b.p. was deleted from the longest of the *CG1847* transcripts (*CG1847*-PB, isoform A) out of a total of 734 b.p. in the 3' UTR of this transcript. Thus, the *Vab2* allele harbored by line ^{3}115, *Vab2*^{115}, represented a *bona fide* molecular null of *Vab2* and. at the same time, was unlikely to have profound effects on the expression of the neighboring genes.

The last remaining *Vab2* allele to be characterized was that harbored by line ^{3}114. Like line ^{3}115, this line failed to amplify a *Vab2* PCR product in the initial CDS-108/ CDS-144 screen. In the subsequent screening reactions, when both of the PCR primers were moved more distal to the original P element insertion site, it was difficult to observe a difference between the band

sizes generated from line ^{3}114 and those generated from wildtype Canton S flies. Nevertheless line ^{3}114 appeared to generate a shorter band in the CDS-111/CDS-146 PCR reaction – PCR primers hybridizing to exon 1 of the upstream *CG15739* gene (CDS-111) and to the 3' end of the *Vab2* ORF (CDS-146). To confirm this observation I moved the downstream primer closer to the original P{EPg} insertion site by designing a 3' primer that hybridized to the middle of the *Vab2* ORF (CDS-109). This primer along with the *CG15739* exon 1 primer (CDS-111) produced a shorter PCR product from both wildtpe and ^{3}114 flies and confirmed that line ^{3}114 carried a deletion of *Vab2* that affected hybridization of at least one of the initial screening primers more proximal to the original P element insertion site.

To determine the molecular structure of the *Vab2* allele carried by line ^{3}114, I submitted both the CDS-111/CDS-146 and the CDS-111/CDS-109 PCR products for bidirectional sequencing. Unlike the ^{3}115 sequencing reactions in which the *Vab2* deletion was approachable from both the 5' and 3' directions, both of the ^{3}114 sequencing reactions that approached from the 5' side were unable to extend through the poly-A tracts of the intergenic region upstream of *Vab2*. However the same two PCR templates yielded high-quality identical sequencing results from the 3' approach. Specifically, line ^{3}114 carried a *Vab2* allele that was missing the 5' UTR upstream of the original P{EPg}CG11802^{HP10420} insertion site and an additional 91 b.p. of the upstream intergenic region. The total size of the ^{3}114 *Vab2* deletion was 121 b.p. Because the original P{EPg} insertion site overlapped with the 6 b.p. downstream promoter element (DPE), the deletion of *Vab2* sequences 5' of the P{EPg} insertion site in *Vab2^{114}* deleted part of the *Vab2* DPE as well as the annotated *Vab2* transcriptional start site (Fig. 2.5).

In addition, the loss of the upstream intergenic region also deletes -20 and -30 consensus TATA promoter elements that may constitute part of the *Vab2* core promoter sequences:

```
          -30       -20                  +1
            |         |                   |
cagctcgttatctgtactttaataccgaaaaacgcactagcgCATTTCAGCTGGCAGCTGGGAAA

       +30
        |
TTTTTAGGTCCTGAAT
        P{EPg}
```

These findings implied that *Vab2*^{114} was missing key regulatory gene expression sequences.

By identifying the precise boundaries of the *Vab2*^{155} and *Vab2*^{114} deletions, I confirmed that each of these alleles was a *bona fide* genomic deletion of *Vab2* (Fig. 2.6). I then used this information to design PCR screens to identify individuals or groups of individuals that carried the respective deletions for the continued Cantonization of these lines. In both cases these screens consisted of one PCR reaction that only amplified a product from the wildtype *Vab2* allele and a second reaction that amplified a deletion-specific PCR product. (Three PCR reactions total: *wt* + *Vab2*^{155}-specific and *wt* + *Vab2*^{114}-specific.)

Cantonization of lines ^{3}*115 and* ^{3}*114*

Vab2^{115} and *Vab2*^{114} were both isolated from *w*$^{-}$ flies harboring p{EPg}CG11802^{HP10420} that had been pre-Cantonized by serial outcrossing to a *w*$^{-}$ line of Canton S prior to P element mobilization. This *w*$^{-}$ background allowed for the loss of the *w*$^{+mC}$ construct carried by P{EPg} to be followed visually and was the basis by which the ^{3}115 and ^{3}114 lines were first selected for further characterization. However, since one of the predominant phenotypes of a *blos1* deletion is a visible reduction in the accumulation of red and brown eye pigments (pteridines and ommochromes, respectively) [2], both of the *Vab2* deletion alleles needed to be introduced into a wildtype, *w*$^{+}$ background in order to determine if loss of *Vab2* acted in a manner phenotypically

similar to loss of *blos1*. To accomplish this I crossed $Vab2^{115}$ and $Vab2^{114}$ male flies to wildtype w^+ Canton S virgin females (cross C1-C5 – Fig. 2.1). All of the F1 females that arose from this mating would carry a *Vab2* deletion allele over a wildtype, w^+, X chromosome. These heterozygous females were then crossed to male Canton S flies to complete one round of Cantonization (cross C1'-C5' – Fig. 2.1). Each round of Cantonization, therefore, consisted of the primary cross (C) and the secondary cross (C'). Although the two-cross Cantonization strategy only provided for chromosomal recombination through the heterozygous female parent of the C' cross, each cross to Canton S allowed the introduction of wildtype somatic chromosomes.

The first round of Cantonization (C1 and C1') had the additional specific goal of obtaining male *Vab2*, w^+ recombinants ($Vab2^{115}$, w^+ or $Vab2^{114}$, w^+ – depending on the starting allele). Although *Vab2* and *w* are both on the X chromosome (*Vab2* at cytological position 10F2 and *w* at cytological position 3B6), the genetic distance between the two genes suggested a recombination rate of approximately 30% between these two genes. Indeed, the first round of Cantonization generated 33.3% w^+, $Vab2^{115}$ recombinants (7 out of 21 w^+ males) and 33.3% w^+, $Vab2^{114}$ recombinants (5 out of 15 w^+ males). Notably none of the w^+ male progeny from cross C1' showed an eye color phenotype even though 33.3% were ultimately determined to have been hemizygous for either $Vab2^{115}$ or $Vab2^{114}$. Rather, to identify the individual w^+ males that were carrying a *Vab2*-deletion allele, all of the w^+ males that arose from cross C1' were screened by PCR (as described above under *Vab2 deletion alleles*) after they had produced progeny in the respective C2 Cantonization crosses. Because these males represented a segregation point for the *Vab2* allele being followed and *Vab2* status was only determined after successful breeding, I established multiple C2-C5 crosses for each round with each replicate cross involving an individual male.

In the rounds subsequent to C1/C1', half of the male progeny that arose from the C' Cantonization crosses were expected to have inherited the *Vab2*-deletion allele that was being Cantonized. In a manner analogous to that used to identify the initial *Vab2*, w^+ recombinant

males, all of the males that arose out of crosses C2'-C5' were screened with the two-reaction PCR screen specific to the *Vab2* allele that they might have inherited. As anticipated, half of the males coming from the C' crosses inherited a *Vab2*-deletion from their heterozygous female mother.

In total, five rounds of two-step serial Cantonization were performed in order to further isogenize the $Vab2^{115}$ and $Vab2^{114}$ lines with Canton S and with their *blos1* counterpart. Not including the isogenization that was accomplished by pre-Cantonization, this should have reduced the genetic content from the $^{3}115$ line or from the $^{3}114$ line, respectively, in the final Cantonized *Vab2* lines to less than 0.001% for the somatic chromosomes and less than 0.05% for the X chromosome. Furthermore, I maintained each Cantonization lineage separately though out the serial Cantonization process, such that in the end I had accumulated 10 independently Cantonized $Vab2^{115}$ lines and 10 independently Cantonized $Vab2^{114}$ lines.

$Vab2^{115}$ and $Vab2^{114}$ Homogenization

The C5' Cantonization step (*c.f.* above) for each of the *Vab2*-deletion alleles generated animals in which the *Vab2* alleles were distributed in a mixed heterozygous population. Half of the males coming out of cross C5' were hemizygous for a *Vab2*-deletion allele and half of the female progeny arising from these crosses were heterozygous for the respective *Vab2*-deletion allele while the other half were homozygous for a wildtype X chromosome. I had already determined that, in a hemizygous state, loss of *Vab2* did not have an obvious eye color deficiency. To determine if deletion of *Vab2* affected eye pigmentation or had other appreciable phenotypes in a homozygous state, I backcrossed the C5' progeny to their peers in a pairwise manner (single male, single female) in order to obtain homozygous *Vab2*-deletion flies. These crosses were called HC crosses (Homozygosity Crosses).

In order to further isogenize the $Vab2^{115}$ and $Vab2^{114}$ lines with Canton S, HC crosses were performed with C5' progeny from parallel Cantonization lineages. Since each Cantonization lineage had been independently generated and maintained through 10 outcrosses to Canton S, other than loci in linkage disequilibrium with *Vab2*, no two lineages were likely to have carried the same residual non-Canton S genetic backgrounds.

Notably, *Vab2* homozygous females were obtained after the HC backcross, but as was seen of the hemizygous males in the earlier Cantonization crosses, none of the *Vab2* homozygous females showed an eye color deficit, and they were indistinguishable from the *Vab2*-heterozygous and homozygous wildtype females that were generated from the same crosses. Because each of the HC crosses was set up with a single male and a single female, and because it was not possible to visually assess the *Vab2* genotype of these animals prior to breeding, only 1 out of 4 of the HC crosses was expected to have included both a *Vab2* hemizygous male and a *Vab2* heterozygous female and, therefore, to be capable of generating *Vab2* homozygous females. The parental genotypes for the HC crosses were determined by recovering the parents after they had successfully produced offspring and determining their genotypes individually by PCR.

In order to obtain stable homozygous *Vab2*-deletion lines, *Vab2* homozygous females needed to be crossed with *Vab2* hemizygous males. This was accomplished by crossing individual F1 males that were obtained from PCR verified *Vab2*-deletion HC crosses to individual F1 females collected from similar *Vab2*-deletion verified HC crosses (*Vab2*-deletion verified HC cross, meaning that both of the parents of a given HC cross were found to harbor one Vab2 mutant chromosome). As with the HC crosses, I did not cross immediate siblings, but crossed individual HC progeny flies to individuals from parallel HC crosses. These crosses were called FC crosses (Final Crosses).

As was the case for HC crosses, the genotype of the single female and single male that were used to set up each FC cross was not determinable ahead of time. Instead I determined the genotype of each FC parental fly by PCR after the pair had successfully bred. From the FC

crosses I identified and established three sublines harboring *Vab2*^{114}: FC14, FC16 and FC17; and three sublines homozygous for *Vab2*^{115}; FC33.2, FC36.2 and FC38.1.

mRNA expression of Vab2-deletion alleles

To determine if either *Vab2*^{115} or *Vab2*^{114} expressed *Vab2* mRNA, I purified total RNA from representative FC sublines lines, using the Macherey-Nagel NucleoSpin® RNA II kit, and reverse-transcribed a portion of each RNA preparation using the Clontech RNA to cDNA EcoDry™ Premix (Double Primed) kit. This approach created cDNA samples that were double-primed using poly-dT and random hexamer primers. The resulting cDNA preparations were used as PCR templates to amplify a 587 b.p. product from the 3' end of the *Vab2* ORF. Amplification of this product from any given sample indicated that a putative full length *Vab2* mRNA was being produced by that fly line. As a positive control for *Vab2* mRNA expression, total RNA was also prepared from Canton S flies. As expected, Canton S cDNAs amplified the 3' *Vab2* ORF in a robust manner, whereas cDNA preparations from the *Vab2*^{115} line (FC38.1) failed to amplify a *Vab2* PCR product (Fig 2.7A). Rather unexpectedly, samples prepared from the *Vab2*^{114} fly lines (FC16 and FC14) also amplified the *Vab2* PCR product.

Failure to amplify the *Vab2* PCR product from any of the cDNA samples could have indicated a lack of *Vab2* mRNA expression in the line being tested or have been due could be due to template quality issues. Although I anticipated that a *Vab2* PCR product would not be amplified from the *Vab2*^{115} line, since this allele lacks the entire *Vab2* ORF, to assess the quality of each of the cDNA preparations I amplified a segment of the *Rbpn-5* gene as a second positive control. This remained an important positive control since limited amplification of *Vab2* was observed from each of the *Vab2*^{114} lines, which could have arisen due to poor RNA or cDNA preparations from both of those lines. However, all of the cDNA samples amplified the *Rbpn-5* PCR product in an equally robust manner indicating that the limited amplification of the 3' *Vab2*

ORF product from the *Vab2*^{114} samples reflected a biological reduction in *Vab2* mRNA in these lines, but not a total lack of *Vab2* expression from the *Vab2*^{114} allele.

One final consideration when interpreting these results was that amplification of the *Vab2* PCR product could have occurred from genomic DNA contamination that was carried over in any of the RNA preparations. Indeed, the Macherey-Nagel RNA kit relies on an on-the-column RNase-free DNase digestion step to remove DNA from a general nucleic acid preparation. The *Rbpn-5* positive control target crossed an exon-exon junction, such that a 637 b.p. PCR product was expected if the *Rbpn-5* band was generated from a cDNA template, whereas a 692 b.p. band was expected if the *Rbpn-5* PCR band arose from contaminating genomic DNA. Unlike *Rbpn-5*, the *Vab2* mRNA is encoded as a single exon. Therefore, to control for genomic DNA contamination, purified RNA that was not reverse-transcribed was tested as a PCR template. Each of the RNA samples tested, except for the RNA purified from *Vab2*^{115}, amplified trace amounts of the *Vab2* 3' ORF PCR product. Nevertheless, the cDNA samples from each of these line amplified significantly stronger *Vab2* PCR products and both of the *Vab2*^{114} lines amplified a less abundant *Vab2* cDNA PCR product than did Canton S.

Lastly, to semi-quantitatively assess the abundance of *Vab2* mRNA in each of the lines, I set up a series of four identical PCR reactions for each of the cDNA samples and utilized a stringent PCR amplification protocol to amplify *Vab2* transcript. I then removed one of the replicate PCR reactions for each cDNA sample after 20, 25, 30 or 40 amplification cycles and resolved the PCR products on an agarose gel (Fig 2.7.B). This revealed that *Vab2* mRNA was, indeed, less abundantly expressed in the *Vab2*^{114} lines than in wildtype Canton S, and therefore suggested that *Vab2*^{114} represented a hypomorphic allele of *Vab2* rather than a true genetic null.

DISCUSSION

Identification of a Drosophila Vab2 homolog

The description of protein complex in yeast that contained three homologs of metazoan BLOC-1 by Hayes *et al.* was a groundbreaking discovery [1]. Prior to this report, no yeast homologs of BLOC-1 protein subunits had been identified [11]. In order to identify these yeast homologs, Hayes *et al.* had to employ structural homology search algorithms in addition to traditional sequence/position based homology searches, but the validity of their findings were bolstered by several previously published reports indicating that the proteins that they had identified as BLOC-1 homologs interacted in a protein complex. In this sense, rather than having identified three independent homologs of BLOC-1 subunits with no known association with each other, *Hayes et al.* had identified a yeast protein complex that roughly paralleled the association of the metazoan BLOC-1 homologs to which they had been linked.

Among the three non-BLOC-1 subunit homologs that were identified as components of yeast BLOC-1, Kxd1p homologs had been previously identified in metazoans and shown to interact with Blos1 in worms and *Drosophila* [1]. Curiously, another of the non-canonical yeast BLOC-1 subunits, Vab2p, was not recognized by Hayes *et al.* to have an identifiable homolog in metazoans. However, by performing PSI-BLAST homology searches, Esteban Dell'Angelica determined that yeast Vab2p is homologous to human LOH12CR1 and *Drosophila CG11802*. This opened up the possibility of directly testing the association of Vab2 with metazoan BLOC-1 by targeting *Vab2* for deletion in *Drosophila*.

Use of P element imprecise excision to delete Drosophila Vab2

A classical approach to determining gene function in *Drosophila* is to use a reverse genetics approach, whereby one targets the specific gene-of-interest for mutation or deletion. In this regard, the P element transposon has proved to be an invaluable tool because of the abundance of gene insertions [7, 12-14] and because of the development of a stable and ubiquitously expressed P element transposase gene [5, 6]. Using these resources I identified a readily available line of flies harboring a P element insertion in the 5' UTR of *Drosophila Vab2*, P{EPg}CG11802^{HP10420} [7]. I efficiently mobilized this P element by introducing Δ2-3 transposase *in trans* [5, 6], and through so doing, I obtained two independent genomic deletions of *Vab2*. The alleles were notable in that both genomic deletions extended unidirectionally from the original site of P element insertion and removed different genetic elements of the *Vab2* gene.

Vab2^{114} – a promoter deletion of Vab2

The *Vab2^{114}* deletion allele removed 121 b.p. 5' of the P{EPg}CG11802^{HP10420} insertion site. The P{EPg}CG11802^{HP10420} insertion sequence in *Vab2* is between positions +30 to +38 of the annotated *Vab2* transcript – *Vab2* nucleotides +30 to +38 are duplicated 5' and 3' of the P{EPg}CG11802^{HP10420} insertion [7]. Although the *Vab2* promoter elements have not been functionally defined, I was able to identify consensus -20 and -30 TATA promoter elements upstream of the annotated transcriptional start site, as well as consensus 6 b.p. DPE (downstream promoter element) sequences in the *Vab2* 5' UTR sequences [15-17]. All of these genetic elements were removed in the *Vab2^{114}* deletion allele as a result of P{EPg}CG11802^{HP10420} imprecise excision.

Although the putative upstream and downstream promoter elements of the *Vab2^{114}* deletion allele had been eliminated, the entirety of the *Vab2* protein coding sequences, including

the translational initiation site, were intact in the *Vab2*^{114} allele. This raised the possibility that *Vab2*^{114} was not entirely transcriptionally silent, and that some amount Vab2 mRNA and protein could still be expressed from this allele. Of particular concern was that the gene upstream of *Vab2*, *CG15739*, did not have recognizable TATA promoter elements or DPE sequences, raising the likelihood that *CG15739* is transcribed from a *Drosophila* bidirectional promoter [18, 19]. If this was the case, *Vab2* coding sequences could have been expressed from the *Vab2*^{114} allele based on transcriptional activity originating from the *CG15739* promoter elements.

Indeed, when I tested for the presence of Vab2 mRNA sequences in lines of flies that were homozygous for *Vab2*^{114}, I found that both 5' and 3' Vab2 mRNA sequences were amplified from reverse-transcribed total RNA preparations from these flies, and, although the same PCR products could be generated from the non-reverse transcribed total RNA preparations, indicating the presence of non-digested genomic DNA in the RNA samples, this amplification was dramatically less efficient meaning that Vab2 mRNA sequences were present in these lines. While these findings did not point to the transcriptional origin of the Vab2 mRNAs, they did define *Vab2*^{114} as a hypomorphic allele of *Vab2* rather than a true genetic null.

Vab2^{115} *– an open reading frame deletion of Vab2*

The second deletion of *Vab2* that I identified and isolated was *Vab2*^{115}. In contrast to *Vab2*^{114}, the genetic deletion in this allele proceeded in a 3' direction from the original P{EPg}CG11802^{HP10420} insertion site and extended from the 5' UTR of *Vab2* through to the 3' UTR of the downstream gene, *CG1847*. This meant that the whole of the *Vab2* coding sequence was deleted from this allele making it a *de facto* genetic null. Unlike *Vab2*^{114}, no *Vab2* coding sequences could be amplified from either genomic DNA preparations, total RNA preparations or reverse-transcribed cDNA samples generated from homozygous *Vab2*^{115} lines of flies.

The imprecise excision event responsible for creating the *Vab2*^{115} allele also removed DNA sequences encoding the tail ends of the 3' UTRs of the *CG1847* mRNA transcripts. *CG1847* is annotated to produce two mRNA transcripts. The longer transcript was missing the last 95 nt of the 3' UTR while the shorter *CG1847* transcript was missing the last 92 nt of the 3' UTR. However, both of the *CG1847* transcripts are rather long, 735 and 732 nt, respectively, and although 3' UTRs are know to be important for mRNA stability and sub-cellular localization, many RNAs that are localized through sequence elements in their 3' UTRs contain multiple and redundant localization 'zipcodes' [20]. Thus the genetic effects of deleting the terminal sequences of the *CG1847* 3' UTRs are likely to be mild, but nevertheless one must remain cognizant of these issues when characterizing the function of *Vab2* by determining the phenotypes of *Vab2*^{115} flies.

Two alleles to study Vab2 function

While the *Vab2*^{115} allele represents a *bona fide* genetic null of *Vab2* and an almost ideal deletion for determining the role of *Vab2* and its relationship to canonical metazoan BLOC-1, the *Vab2*^{114} allele remains of interest for future investigation of *Vab2* function. Although beyond the scope of the studies described here (*c.f.* Chapter 4 – Phenotypic characterization of Vab2, Kxd1 and Bos3 gene deletion mutants), the reduced Vab2 mRNA accumulation of the *Vab2*^{114} allele presents an opportunity to characterize the gene dosage requirements for Vab2 function and for any protein interactions in which it engages. In combination with the *Vab2*^{115} allele (a *Vab2* deficiency), a second allele of *Vab2*^{114}, or a wildtype copy of *Vab2*, the *Vab2*^{114} allele presents a tool for controllably reducing the natural expression levels of *Vab2* in an endogenous setting. In this sense, both *Vab2*^{114} and *Vab2*^{115} represent gene deletions for determining the function of *Vab2* in metazoans.

Total founders	**189**
Infertile founders	12
Heterozygous only lines	6
Lines screened by PCR	168
Unscreened lines	3

Lines screened by PCR	**168**
Putative precise excisions	123
Anomalous excisions	45

Anomalous excisions	**45**
Type 1 (P elem residual)	20
Type 2 (P elem residual)	20
Large deletion	2
Complex/mixed	1
^{3}*114 Vab2* Promoter Deletion	1
^{3}*115 Vab2* ORF Deletion	1

Table 2.1. Results of *Vab2* imprecise excision. A total of 189 w^- ; $\Delta 2\text{-}3^-$ founders were obtained and characterized from P{EPg}HP10420 ; $\Delta 2\text{-}3^+$ females that were crossed to FM6 males (upper box). Most of the females giving rise to w^- ; $\Delta 2\text{-}3^-$ founders showed no evidence of mosaicism and had uniformly red pigmented eyes. w^- ; $\Delta 2\text{-}3^-$ founders were individually crossed to FM6 balancer stocks to generate 177 lines with putative P element excision events. 168 of the resulting lines were screened by PCR (center box). 123 lines showed molecular evidence of precise (or nearly precise) P element excision. 45 lines showed evidence of anomalous P element mobilization. These lines 45 lines were characterized further by additional PCR screens and (in some cases) by direct sequencing. This revealed that the majority of the anomalous P element mobilization events were instances of incomplete removal of P element sequences with no accompanying deletion of *Vab2* sequences (Type 1 and Type 2 events). Two lines had large deletions that extended into both genes adjacent to *Vab2*, and two of the lines (^{3}114 and ^{3}115) had *Vab2* deletions.

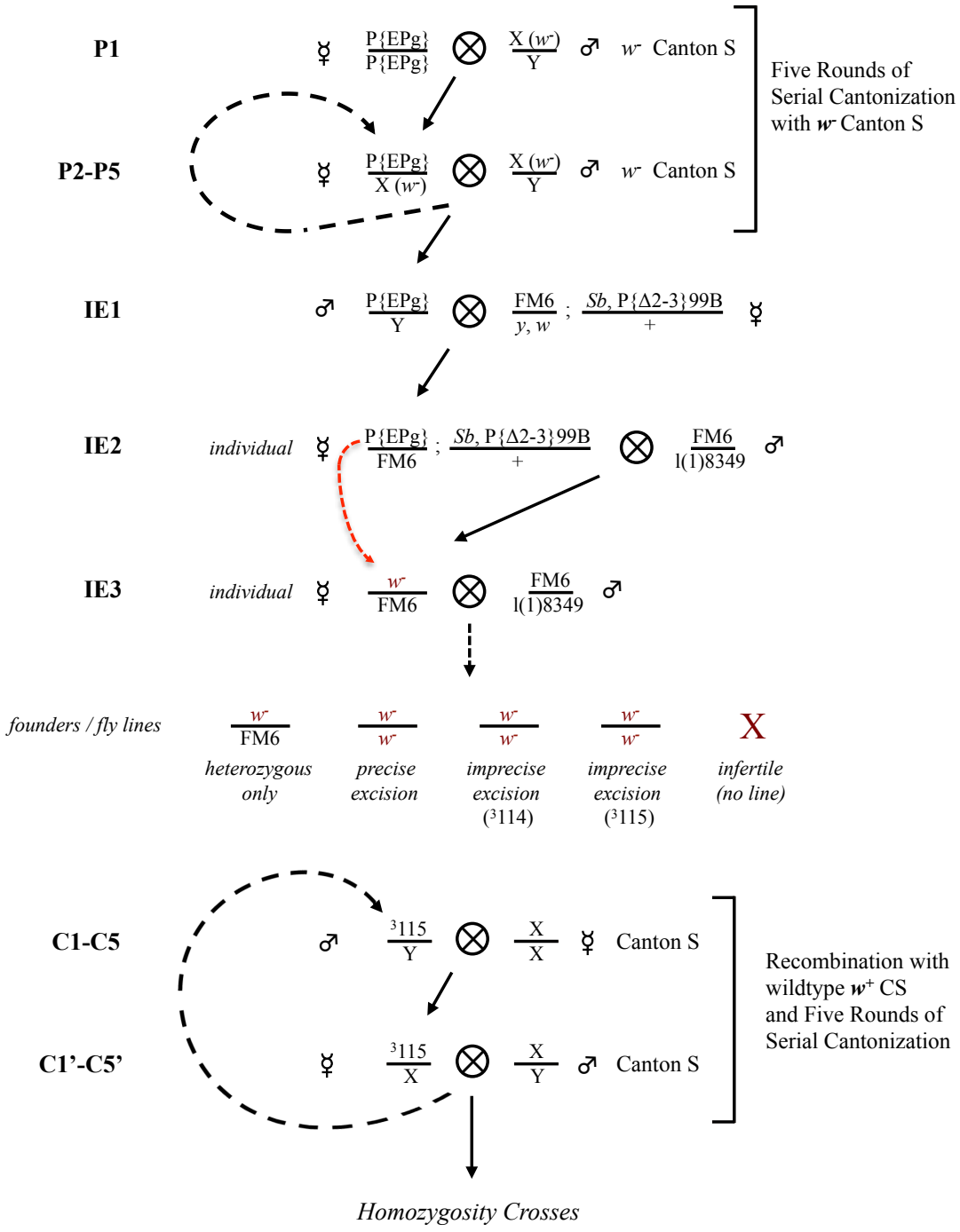

Figure 2.1. Schematic of pre-Cantonization, imprecise excision and Cantonization crosses.

Figure 2.1. Schematic of pre-Cantonization, imprecise excision and Cantonization crosses. A schematic of the pre-Cantonization crosses (P1-P5), the imprecise excision crosses (IE1-3), and the subsequent Cantonization crosses (C1-C5'). The first two lines (P1 and P2-P5) show pre-Cantonization crosses. Crosses P2-P5 utilize a heterozygous w^-, P{EPg}CG11802^{HP10420}/ w^- female from the preceding cross as one of the parents. Δ2-3 transposase is introduced to the pre-Cantonized P{EPg} line in cross 1 of the imprecise excision steps (IE1). Cross 2 of the imprecise excision crosses shows the female in which mobilization of P{EPg}CG11802^{HP10420} took place (IE2). In cross 3, a w^- F1 female arising from P element mobilization is shown mated to an FM6 balancer male (IE3). The red dotted arrow between cross IE2 and cross IE3 indicates that the w^- chromosome in cross IE3 is the same P{EPg}-insertion X chromosome in cross IE2 that has lost expression of the w^{+mC} gene construct carried by P{EPg}, presumably due to P element mobilization. The line under cross IE3 illustrates a sample of the assortment of P element mobilization events that were observed and collected (*founders / fly lines*). Crosses C1-C5 and C1'-C5' are paired crosses, each constituting one cross of a two-step X chromosome Cantonization strategy (C1-C5 and C1'-C5', respectively).

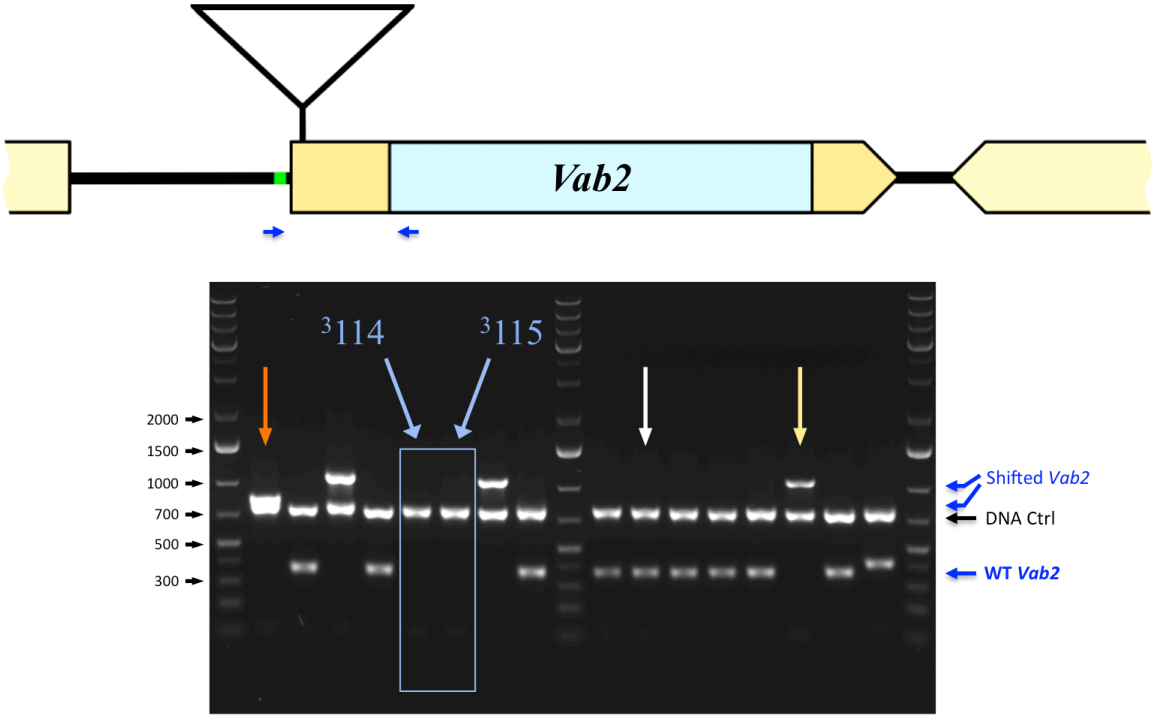

Figure 2.2. PCR screening of *Vab2* P element excision lines. Representative PCR screening reactions resolved by agarose gel electrophoresis. A total of 168 homozygous lines that were established from individual w^- founders isolated following Δ2-3 mediated mobilization of P{EPg}HP10420^{CG11802} were screened by PCR for loss of *Vab2* DNA sequences. Two sets of primers were used to screen each DNA sample. Control primers amplifying a 760 b.p. *Rabaptin-5* band (DNA Ctrl) were used to determine the quality of each DNA sample. A *Vab2*-specific pair of primers (CDS-108/CDS-144 – dark blue arrows under gene schematic), flanking the *Vab2* upstream promoter elements (green line), the *Vab2* transcriptional start site, and the first 24 codons of the *Vab2* open reading frame, was used to identify lines carrying deletions of *Vab2* that resulted from P element imprecise excision. In several instances the *Vab2*-specific band was seen shifted from the 371 b.p. wildtype size (white arrow) to 1099 b.p. (yellow arrow) or 844 b.p (orange arrow), indicative of Type 1 and Type 2 excision events, respectively. In rare instances the DNA sample was able to amplify the *Rapabtin-5* control band but did not generate a *Vab2*-specific PCR product (blue boxed lanes). All samples that generated this banding pattern were characterized further. The two blue boxed lanes shown here correspond to *Vab2* excision lines ^{3}114 and ^{3}115; a *Vab2* promoter deletion line and a *Vab2* ORF deletion line, respectively.

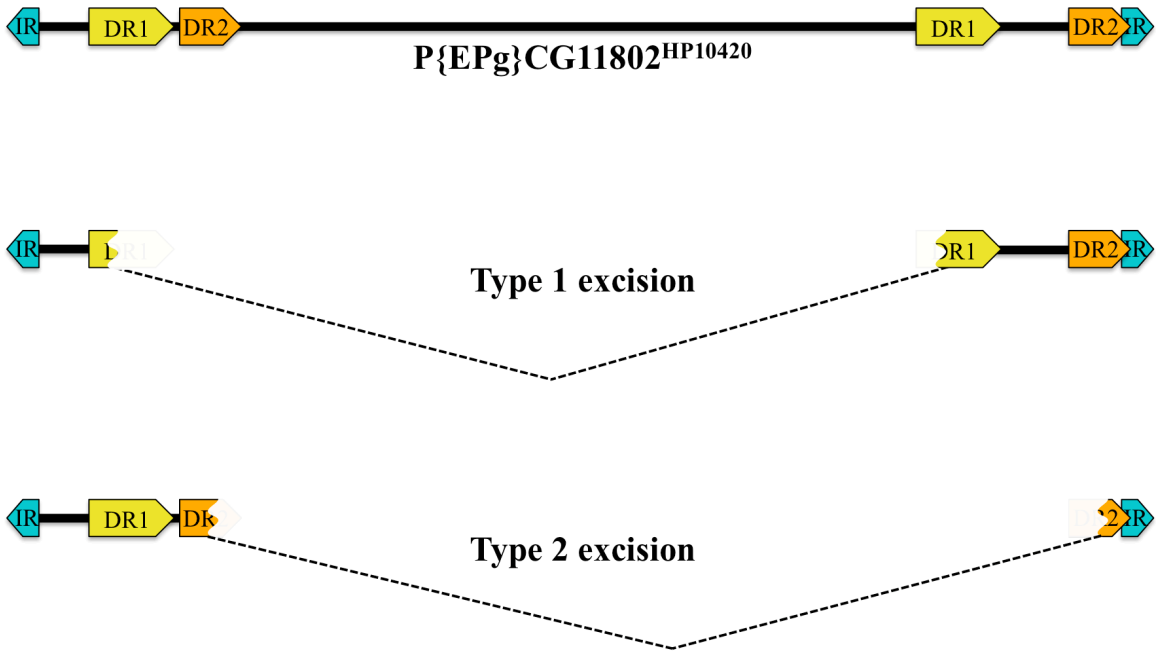

Figure 2.3. Type 1 and Type 2 imprecise excision alleles. Two types of common imprecise excision alleles were identified among flies lines established from w^- founders in which P{EPg}HP10420^{CG11802} had been mobilized: Type 1 and Type 2. Both allele types lacked the w^{+mC} gene construct carried by P{EPg}HP10420^{CG11802} but otherwise exhibited incomplete removal of all P element sequences. The upper gene schematic shows the arrangement of repeat elements within P{EPg}HP10420^{CG11802}. The ends of the P element are defined by 31 b.p. inverted repeats (IR) that are inserted into an 8 b.p. *Vab2* target sequence (not illustrated) that was duplicated during the original insertion event. Nested within the termini domains of the P{EPg} transposon are two sets of longer direct repeats (DR1 and DR2 – 133 b.p. and 98 b.p., respectively). Type 1 alleles (middle schematic) are characterized by genetic recombination at an unspecified location within the 5' and 3' DR1 sequences to leave a single intact copy of DR1 with all of the intervening P element sequences removed. Type 2 alleles (lower schematic) exhibit a similar recombination event between the DR2 repeats resulting in a single remaining DR2 element while deleting the intervening sequences.

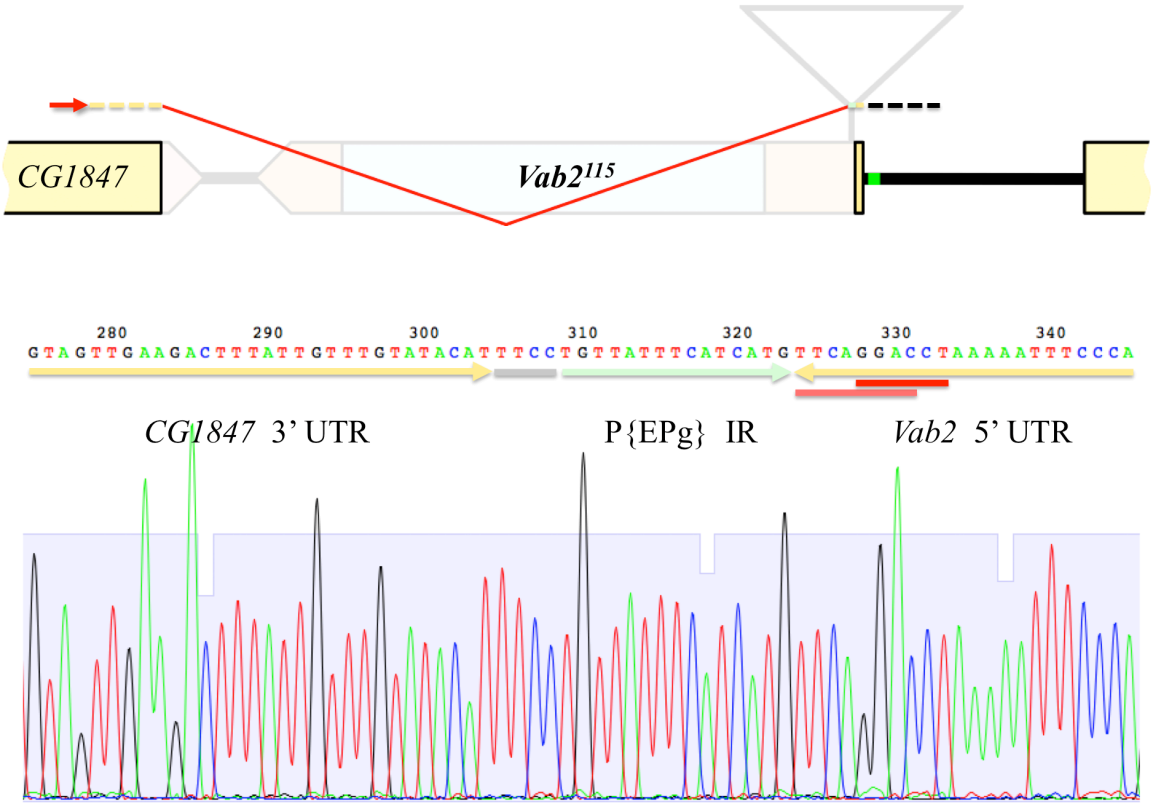

Figure 2.4. Sequencing electrophoregram of *Vab2*^{115} allele. A schematic of the *Vab2*^{115} allele is shown above a section of the electrophoregram generated by sequencing DNA isolated from flies homozygous for *Vab2*^{115}. CDS-149 (red arrowhead) extends a sequencing product in the orientation opposite of *Vab2* transcription (discontinuous dashed line above *Vab2* gene schematic). Regions of *Vab2* missing from *Vab2*^{115} are shown whited-out on the gene schematic. The electrophoregram shows the junction between intact *CG1847* 3' UTR bases and the remaining intact *Vab2* 5' UTR bases. Above each color-coded electrophoregram peak is the corresponding base called by the sequencing software. *CG1847* 3' UTR bases are underlined with a yellow arrow as are the remaining *Vab2* 5' UTR bases. The salmon underlined nucleotides are the 8 bases (TTCAGGAC) duplicated by P{EPg}HP10420 insertion. The red underlined nucleotides (GGACCT) are the *Vab2* downstream promoter element bases. The intervening 15 bases underlined in green are terminal nucleotides from one of the P{EPg}HP10420 inverted repeats as found adjacent to the duplicated *Vab2* bases in the parental Bloomington line. The 4 bases underlined in gray are of an unspecified origin.

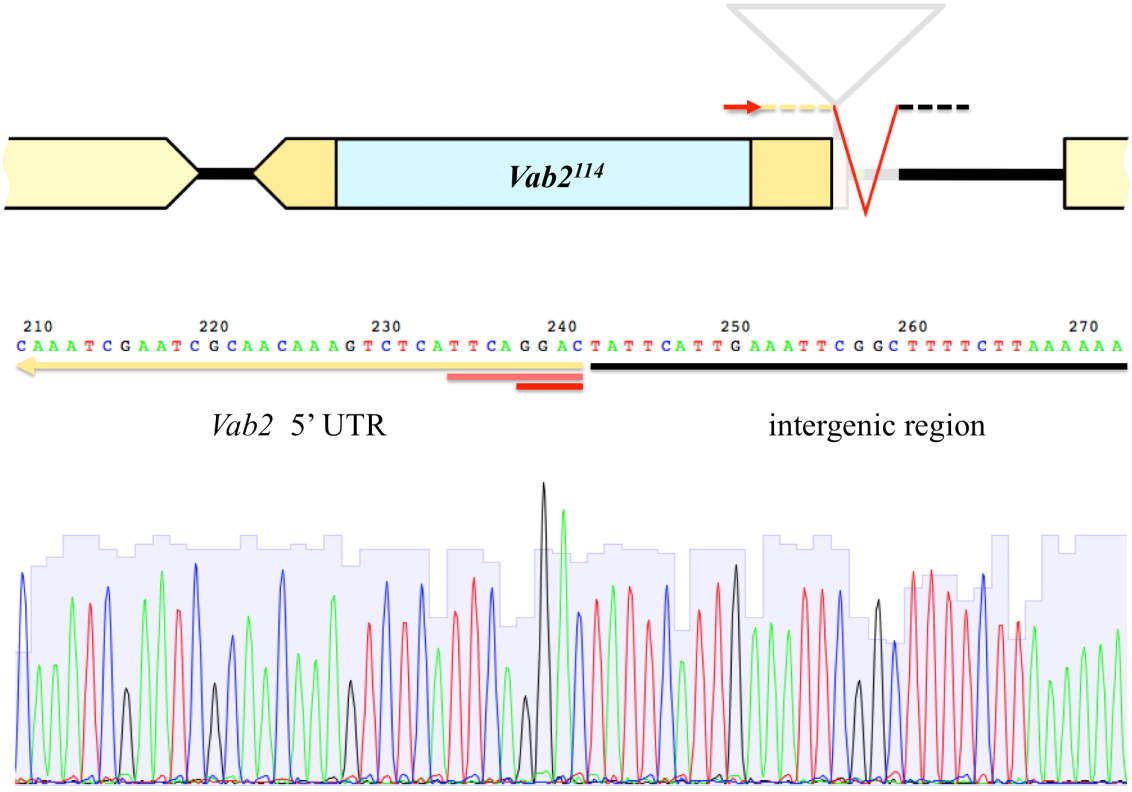

Figure 2.5. Sequencing electrophoregram of *Vab2*^{114} allele. A schematic of the *Vab2*^{114} allele is shown above a section of the electrophoregram generated by sequencing the *Vab2* locus from DNA isolated from flies homozygous for the *Vab2*^{114} allele. CDS-108 (red arrowhead) extends a sequencing product in the orientation opposite of *Vab2* transcription (discontinuous dashed line above *Vab2* gene schematic). Regions of *Vab2* missing from *Vab2*^{114} are shown whited out on the gene schematic. The portion of the electrophoregram shown represents the junction between intact *Vab2* 5' UTR bases and the proximal intact upstream intergenic bases present in the *Vab2*^{114} allele. Above each color-coded electrophoregram peak is the corresponding base called by the sequencing software. *Vab2* 5' UTR sequences are underlined with a yellow arrow. The salmon underlined nucleotides are the 8 bases (TTCAGGAC) duplicated by P{EPg}HP10420 insertion. The red underlined nucleotides (GGAC) are the remaining bases of the partially deleted downstream promoter element. The remaining adjacent intergenic bases are underlined in black.

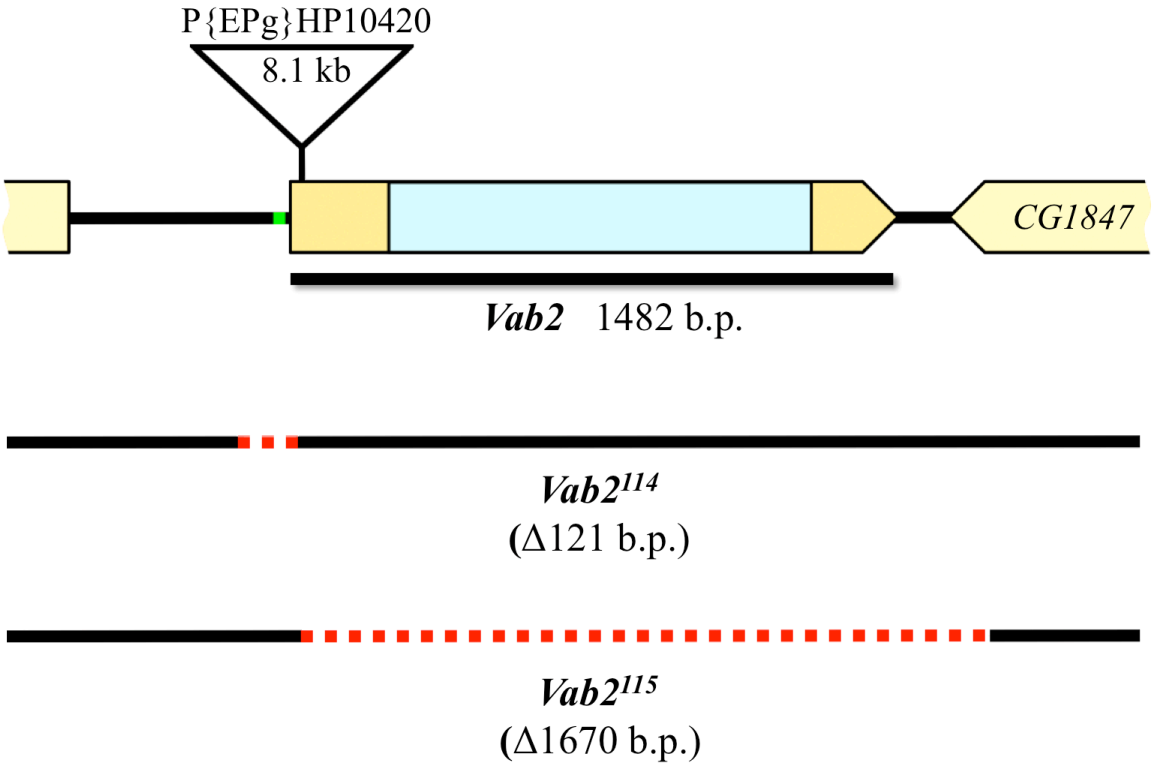

Figure 2.6. *Drosophila Vab2* gene and *Vab2* P element deletion alleles. *CG11802* (*Vab2*) is located on the minus strand of the *Drosophila* X chromosome at cytological position 10F2. It is shown here 5' to 3'. The light blue region corresponds to the *Vab2* open reading frame (ORF). Yellow segments represent untranslated regions (UTRs) of *Vab2* and of the neighboring genes: *CG15739* (5' of *Vab2*) and *CG1847* (3' of *Vab2*). *CG15739* and *CG1847* are transcribed oppositely of *Vab2*. Bloomington line 21873 harbors a P element insertion in the 5' UTR of *Vab2,* P{EPg}CG11802^{HP10420}. The small green box shows predicted *Vab2* upstream promoter elements in the intergenic region. The two lower black lines illustrate deletion mutants of *Vab2* generated by imprecise excision of P{EPg}CG11802^{HP10420}. The dotted red regions represent the deleted sequences of each allele. The *Vab2^{114}* allele is missing 121 b.p., that include predicted *Vab2* upstream promoter elements, the *Vab2* transcriptional start site and a portion of the *Vab2* 5' UTR and downstream promoter element. The *Vab2^{115}* allele is missing 1670 b.p., including a portion of the *Vab2* 5' UTR, the entire *Vab2* ORF, the *Vab2* 3' UTR, the downstream intergenic region, and 95 b.p. of the 734 b.p. 3' UTR of *CG1847*.

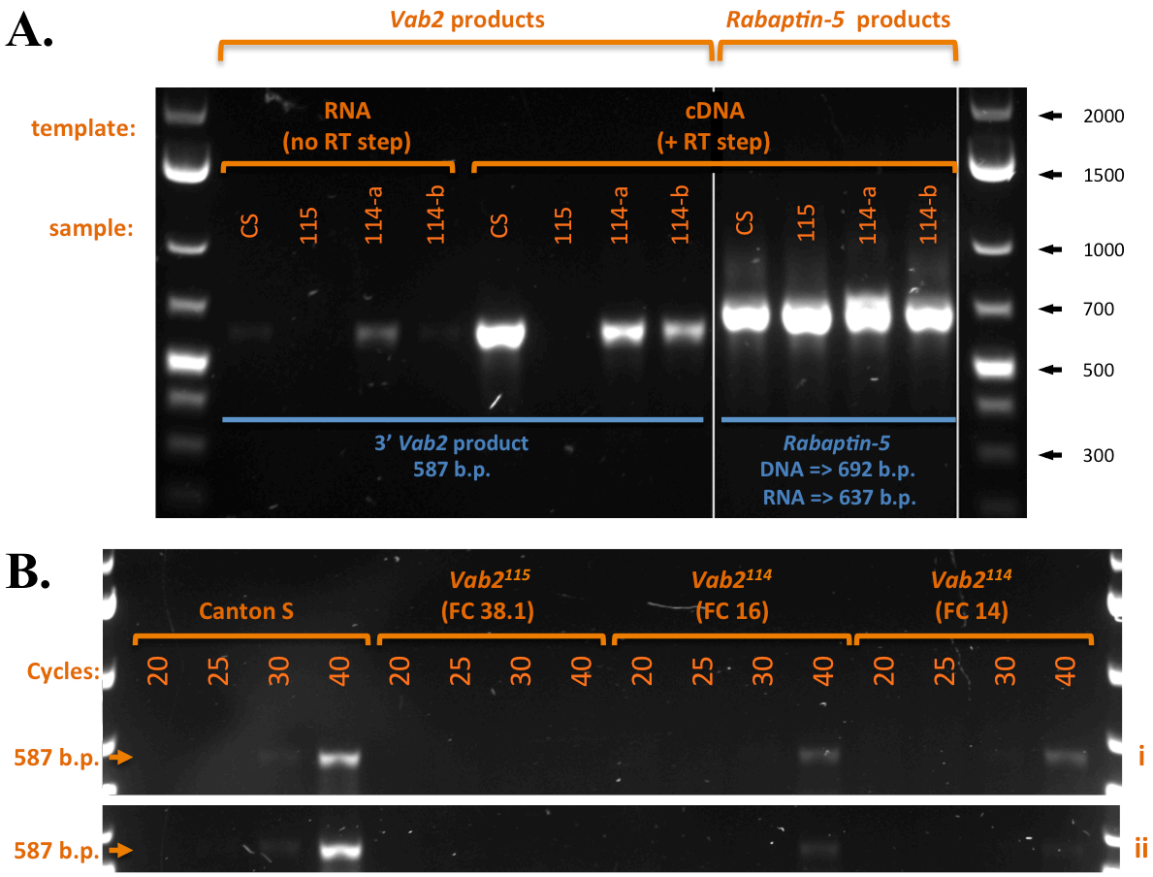

Figure 2.7. Vab2 mRNA expression from *Vab2*^{114} and *Vab2*^{115} alleles. (**A**) Total RNA was purified from Canton S (CS), *Vab2*$^{115•FC38.1}$ (115), *Vab2*$^{114•FC16}$ (114-a) and *Vab2*$^{114•FC14}$ (114-b) flies. cDNA was generated from each RNA sample by reverse-transcription using poly-dT and random hexamer primers. The presence of *Vab2* mRNA in each fly line was determined by PCR amplification of a *Vab2* transcript target from the corresponding cDNA sample (center four lanes). To control for *Vab2* amplification from contaminating genomic DNA, *Vab2* screening was also carried out using the un-reverse-transcribed RNA samples as templates (first four lanes). The *Vab2* ORF is missing in the *Vab2*^{115} allele. Accordingly, *Vab2* PCR products were not generated when using *Vab2*^{115} RNA or cDNA templates. As a positive control, *Rbpn-5* was PCR amplified from each cDNA sample (right four lanes), and the major PCR product for each reaction was the size expected of a spliced *Rbpn-5* transcript. *Vab2*$^{114•FC16}$ (114-a) also amplified a less intense genomic-sized *Rbpn-5* PCR band, and a more intense *Vab2* band than the other samples using the RNA-only template; both observations are consistent with a greater amount of genomic DNA in this specific preparation of *Vab2*$^{114•FC16}$ RNA. (**B**) Semi-quantitative *Vab2* mRNA screen. *Vab2* transcript was detected in Canton S, *Vab2*$^{114•FC16}$ and *Vab2*$^{114•FC14}$ cDNA samples using a high-stringency PCR amplification protocol. Quadruplicate PCR reactions were set-up for each cDNA

sample, and reactions were extended for 20, 25, 30 or 40 cycles. The 587 b.p. *Vab2* product was readily observed at later cycles from Canton S cDNA, and it was detected, but less abundant, in cDNA preparations from both $Vab2^{114}$ lines. Results from two independently prepared sets of RNA/cDNA samples are shown: Set **i** (upper panel) and Set **ii** (lower panel).

REFERENCES

1 Hayes MJ, Bryon K, Satkurunathan J, Levine TP. Yeast homologues of three BLOC-1 subunits highlight KxDL proteins as conserved interactors of BLOC-1. Traffic. 2011 Mar;12(3):260-8.

2 Cheli VT, Daniels RW, Godoy R, Hoyle DJ, Kandachar V, Starcevic M, Martinez-Agosto JA, Poole S, DiAntonio A, Lloyd VK, Chang HC, Krantz DE, Dell'Angelica EC. Genetic modifiers of abnormal organelle biogenesis in a Drosophila model of BLOC-1 deficiency. Hum Mol Genet. 2010 Mar 1;19(5):861-78

3 Beall EL, Rio DC. Drosophila P-element transposase is a novel site-specific endonuclease. Genes Dev. 1997 Aug 15;11(16):2137-51.

4 Ryder E, Russell S. Transposable elements as tools for genomics and genetics in Drosophila. Brief Funct Genomic Proteomic. 2003 Apr;2(1):57-71.

5 Laski FA, Rio DC, Rubin GM. Tissue specificity of Drosophila P element transposition is regulated at the level of mRNA splicing. Cell. 1986 Jan 17;44(1):7-19.

6 Robertson HM, Preston CR, Phillis RW, Johnson-Schlitz DM, Benz WK, Engels WR. A stable genomic source of P element transposase in Drosophila melanogaster. Genetics. 1988 Mar;118(3):461-70.

7 Thibault ST, Singer MA, Miyazaki WY, Milash B, Dompe NA, Singh CM, Buchholz R, Demsky M, Fawcett R, Francis-Lang HL, Ryner L, Cheung LM, Chong A, Erickson C, Fisher WW, Greer K, Hartouni SR, Howie E, Jakkula L, Joo D, Killpack K, Laufer A, Mazzotta J, Smith RD, Stevens LM, Stuber C, Tan LR, Ventura R, Woo A, Zakrajsek I, Zhao L, Chen F, Swimmer C, Kopczynski C, Duyk G, Winberg ML, Margolis J. A complementary transposon tool kit for Drosophila melanogaster using P and piggyBac. Nat Genet. 2004 Mar;36(3):283-7.

8 Mackenzie SM, Howells AJ, Cox GB, Ewart GD. Sub-cellular localisation of the white/scarlet ABC transporter to pigment granule membranes within the compound eye of Drosophila melanogaster. Genetica. 2000;108(3):239-52.

9 Takasu-Ishikawa E, Yoshihara M, Hotta Y. Extra sequences found at P element excision sites in Drosophila melanogaster. Mol Gen Genet. 1992 Mar;232(1):17-23.

10 Takara Bio Inc. PrimeSTAR® Max DNA Polymerase Product Manual. (Cat.# R045A) v1108Da. (URL: http://www.takara-bio.com)

11 Starcevic M, Dell'Angelica EC. Identification of snapin and three novel proteins (BLOS1, BLOS2, and BLOS3/reduced pigmentation) as subunits of biogenesis of lysosome-related organelles complex-1 (BLOC-1). J Biol Chem. 2004 Jul 2;279(27):28393-401.

12 Cooley L, Kelley R, Spradling A. Insertional mutagenesis of the Drosophila genome with single P elements. Science. 1988 Mar 4;239(4844):1121-8.

13 Spradling AC, Stern D, Beaton A, Rhem EJ, Laverty T, Mozden N, Misra S, Rubin GM. The Berkeley Drosophila Genome Project gene disruption project: Single P-element insertions mutating 25% of vital Drosophila genes. Genetics. 1999 Sep;153(1):135-77.

14 Bellen HJ, Levis RW, Liao G, He Y, Carlson JW, Tsang G, Evans-Holm M, Hiesinger PR, Schulze KL, Rubin GM, Hoskins RA, Spradling AC. The BDGP gene disruption project: single transposon insertions associated with 40% of Drosophila genes. Genetics. 2004 Jun;167(2):761-81.

15 Kutach AK, Iyama S, Kadonaga JT. Drosophila Core Promoter Database (DCPD). http://labs.biology.ucsd.edu/Kadonaga/DCPD.html

16 Butler JE, Kadonaga JT. The RNA polymerase II core promoter: a key component in the regulation of gene expression. Genes Dev. 2002 Oct 15;16(20):2583-92.

17 Juven-Gershon T, Kadonaga JT. Regulation of gene expression via the core promoter and the basal transcriptional machinery. Dev Biol. 2010 Mar 15;339(2):225-9.

18 Gotea V, Petrykowska HM, Elnitski L. Bidirectional promoters as important drivers for the emergence of species-specific transcripts. PLoS One. 2013;8(2):e57323.

19 Preker P, Nielsen J, Kammler S, Lykke-Andersen S, Christensen MS, Mapendano CK, Schierup MH, Jensen TH. RNA exosome depletion reveals transcription upstream of active human promoters. Science. 2008 Dec 19;322(5909):1851-4.

20 Xing L, Bassell GJ. mRNA localization: an orchestration of assembly, traffic and synthesis. Traffic. 2013 Jan;14(1):2-14.

CHAPTER 3

Deletion of the *Drosophila Kxd1* and *Blos3* genes by CRISPR-mediated genomic editing

ABSTRACT

The *Saccharomyces cerevisiae KXD1* gene encodes one of the protein subunits of the heterohexameric yeast BLOC-1, which differs in composition and subunits from the canonical metazoan BLOC-1. KXD1 is not one of the eight proteins that constitute BLOC-1 described in mammals and insects. To determine if loss of *Kxd1* in *Drosophila* phenocopied the loss of canonical BLOC-1 subunits, even in a mild manner as is reported for loss of *Kxd1* in mice, I used a CRISPR genomic editing approach to delete *Kxd1* in flies. Following the process described in the literature, I targeted *Kxd1* in a line of flies that harbored a PBac insertion in the 5' UTR of *Kxd1*. Deletion of w^{+mC}, a dominant marker carried by PBac, was observed with high frequency, but deletion of *Kxd1* remained elusive due to an unforeseen *Kxd1* gene duplication in this line. Since I observed that the limiting factor for deletion of *Kxd1* was the genetic background in which *Kxd1* was targeted, I used the same approach and reagents to delete *Kxd1* in wildtype Canton S flies. This avoided the extensive backcrossing that was anticipated for a deletion of *Kxd1* in the PBac insertion background. In a similar manner, I used CRISPR reagents to delete *Blos3* in Canton S flies and obtained three independent *Blos3* deletion alleles. Biochemically, BLOS3 is a member of the metazoan BLOC-1 protein complex. However, loss of *BLOS3* in mice (*Bloc1s3 – reduced pigmentation*) elicits a noticeably mild BLOC-1 phenotype. By deleting *Blos3* in *Drosophila*, I aimed to determine if the loss of *Blos3* elicits mild BLOC-1 phenotypes as an intrinsic characteristic of BLOS3 function rather than as a species-specific effect. If so, *Blos3* would also provide a direct genetic comparison for the deletion of *Kxd1*.

INTRODUCTION

The CRISPR/Cas9 (clustered regularly interspaced short palindromic repeats / CRISPR associated protein 9) system is a remarkably flexible set of tools to carryout targeted genomic editing across a wide spectrum of organisms and cell types. Fundamentally, the system consists of the bacterial Cas9 RNA-guided endonuclease and the targeting CRISPR RNAs – the target specific crRNA and the crRNA-maturation trans-activating RNA (tracrRNA) [1]. The utility of the CRISPR/Cas9 system, however, has been due to the reagents and protocols developed and described by a variety of groups [2-4]. The seminal work describing the use of CRISPR reagents to perform genomic editing in *Drosophila* was published in a 2013 Genetics article by Gratz *et al*. [5]. According to this study, a desirable procedure for gene deletion/genomic editing in *Drosophila* includes taking advantage of the vast transposon insertions resources that mark almost every genetic locus in *Drosophila* and are available through the commonly accessible collections.

Although transposon insertions have traditionally been used as starting points for reverse genetics studies involving transposon-mediated gene deletion, in the context of CRISPR technologies individual transposon insertions can serve as visible markers for recognizing gene deletion after CRISPR-mediated gene targeting. As with traditional transposon-mediated gene deletion, the loss of a transposon-carried dominant marker (often w^{+mC}) serves as an indicator of the loss of the surrounding genomic locus. In this manner, individual animals in which the gene of interest has been deleted can be visually identified and mated before being molecularly screened for loss of the gene of interest and/or for a targeted gene-replacement event.

I set out to delete *Drosophila Kxd1* to determine if loss of *Kxd1* phenocopied the loss of the BLOC-1 subunit gene, *blos1*. In mice, loss of *Kxd1* was reported to elicit BLOC-1 phenotypes [6], and the product of *KXD1* in yeast is a subunit of yeast BLOC-1 [7, 8]. However, unlike loss of canonical BLOC-1 subunit genes, *Kxd1* was reported to cause only mild and partial BLOC-1

phenotypes [6]. These observations seeded the interest in targeting *Kxd1* for characterization in *Drosophila*, a model organism where BLOC-1 phenotypic differences would be directly comparable. However, when deletion of *Kxd1* was first considered, it was noted that there were no available P element insertions in *Kxd1*, making deletion by imprecise excision not an option. Nevertheless, a line carrying a piggyBac insertion in the 5' UTR of *Kxd1* could be obtained and would serve to monitor CRISPR-mediated deletion of *Kxd1*.

At the same time as I was considering using CRISPRs to delete *Kxd1* I realized that a similar approach could be used to target *Blos3* for deletion in *Drosophila*. Like *Kxd1*, *Blos3* was anticipated to have mild BLOC-1 phenotypes based on the well established phenotypes of the 'reduced pigmentation' mouse that harbors a mutation in the gene encoding BLOS3 (*Bloc1s3*) [9, 10]. However, it had never been clear if the 'reduced-pigmentation' phenotype in mice is due to an intrinsic property of the BLOS3 protein, or if the attenuated phenotype of *Bloc1s3* mutation is due to a species-specific characteristic. By targeting *Blos3* for deletion in *Drosophila* along side *Kxd1* I could validate the role of BLOS3 in BLOC-1 function and would possibly be generating an internal control for assessing the anticipated attenuated BLOC-1 phenotype of *Kxd1*.

MATERIAL AND METHODS

Fly Stocks

Flies were maintained and bred in a dedicated room maintained at 20-24°C on media prepared by the UCLA Drosophila Media Facility. Canton S and w^+ ; TM3/TM6 fly stocks were obtained from Bloomington Stock Center. FlyBase (http://flybase.org) was used to identify available fly lines of interest. Harvard line 21873 harbors a P{EPg} P element insertion in the 5' UTR of *Vab2* [11] and was obtained from Exelixis at Harvard Medical School.

CRISPR reagents

CRISPR reagents, pHsp70-Cas9 and pU6-BbsI-chiRNA, were described by Gratz *et al.* [5] and were obtained from Addgene (http://www.addgene.org).

chiRNA targets were identified and designed using the UCSC Genome Browser (http://genome.ucsc.edu) with the "SpCas9_Dm-targets" custom track and using the FlyCRISPR online CRISPR Optimal Target Finder tool [12, 13].

The *Kxd1* chiRNA targets were a 5' target in exon 2 of *CG10638* (GCATATCTGTACAGG AAˇTGA AGG – PAM underlined, ˇ site of DNA cleavage), and 3' target near the end of *Kxd1* exon 3 (GTGCAGTCGGAGGAATCˇ ATT GGG – 3' "NGG" PAM sequence underlined, ˇ represents site of DNA cleavage).

The *Blos3* chiRNA targets were a 5' target at the start of the *Blos3* ORF (GTATTTAATAAA CTGAAˇTG*A TG*G – PAM sequence underlined, ˇ site of DNA cleavage, blue italics *Blos3*

initiation codon. There are two in-frame ATG codons at the start of the *Blos3* ORF. The second ATG, highlighted in blue, is the annotated translational start site.), and a 3' target in *Blos3* exon 3 (GCTGCGAGTGAAAGCGGˇTAA GGG – PAM sequence underlined, ˇ site of DNA cleavage).

Injection services were contracted from Rainbow Transgenic Flies.

PCR screening

DNA was prepared from samples screened by PCR using the Macherey-Nagel NucleoSpin Tissue XS spin column kit according to the manufacturer's protocol, except that columns were eluted with 20 µl of BE (Buffer Elution) per fly used. PCR screening reactions were carried out using Bioland Scientific 2 X Taq PCR Premix reagent according to the manufacturer's protocol.

Putative *Kxd1* CRISPR-deletion flies were screened with primers CDS-179 (ACCATCTTGGG TTCGTGGTATATGTCCCACAG), CDS-180 (AGGCTTAACCTGTATCCTCGGATGTGCA GTC) and CDS-181 (GCTCAGCTACGATGGTCGCGTCATAATCTC) to identify *Kxd1* NHEJ deletions. Primers CDS-175 (GTGTTCTCCCTTATTATAAACAAATAAATTCTAGGCTACA ATGAGCCACTTG) and CDS-176 (ATCGAGGGACTAAAGCTAATTAGGCTTAACCTGTA TCCTC) were used to screen for the presence of *Kxd1* or *emGFP* gene replacement sequences, and primers CDS-177 (ACTTCCAAGGG CGAGGAGCTGTTCAC) and CDS-178 (GTACAG CTCGTCCATGCCGAGAGTGAT C) were used to specifically detect emGFP coding DNA.

The 5' *Kxd1* CRISPR target sites were differentially PCR amplified using CDS-179 (ACCATCT TGGGTTCGTGGTATATGTCCCACAG) as the 5' primer and either CDS-170L (GTTAATTA TGTTATCTGTAGTTAAAGAAGTCTCGCTGTGAG), CDS-183S (CGCCTTAAGCTGCAG

TAGGAAGACGAATAGGTG) or CDS-185 (ACATCCGCAAGGCCCAAGTGGCTCATTG TAG) as the 3' primer.

Deletion of *Blos3* was assessed using primers CDS-199 (TGGCACTGACATCAAACGAATGT TCGAGACA) and CDS-200 (GAGGACGAAACTATACCCCAGTCACCTGA G) to amplify *Blos3* wildtype or *Blos3* CRISPR-deletion alleles.

DNA sequencing

Sequencing services were contracted through Laragen Inc. (Culver City, CA) or through the UCLA GenoSeq core facility. "Purified Template" full service Sanger sequencing was ordered from Laragen Inc., and "Full Service" Sanger sequencing service was ordered from GenoSeq. In both cases, purified DNA and primers were provided.

Kxd1 PCR products were sequences with primers CDS-179 and CDS-170L. Blos3 PCR products were sequenced with primers CDS-199 and CDS-200. (c.f. above for primer nucleotide sequences).

RESULTS

CRISPR/Cas9 Kxd1 gene deletion strategy

The *Drosophila Kxd1* gene is on the third chromosome at cytological position 69C4. I had previously used P element imprecise excision to delete the *Drosophila Vab2* gene, however the FlyBase reference resource indicated that the only available transposon insertion proximal to *Kxd1* was the insertion of a PBac{WH} construct in the 5' UTR of *CG10681* (*Kxd1*) [14]. PBac{WH} is a piggyBac-based construct that contains the w^{+mC} dominant marker [11]. Due to the low frequency of piggyBac imprecise excision, piggyBac insertions are not considered useful starting points for gene deletion by imprecise excision – piggyBac was initially thought to always excise in a precise manner [15-17]. However the w^{+mC} marker carried by PBac{WH} did fulfill the criteria outlined by Gratz *et al*. of serving as a visible indicator of targeted locus retention or deletion when using a CRISPR-based method of gene deletion. To this end, Harvard line f00719, which harbors a PBac{WH} insertion in *Kxd1,* was used as the genetic background in which to target *Kxd1* for CRISPR/Cas9-mediated deletion.

Selection of Kxd1 CRISPR target sites

I used the UCSC Genome Browser with the "SpCas9_Dm-targets" custom track to identify and evaluate possible CRISPR target sites flanking *Kxd1*. This custom track identifies unique genome-wide 20 b.p. sequences that are followed by a 3 b.p. Cas9 3' "NGG" protospacer adjacent motif (PAM). The sequences identified by the SpCas9_Dm-targets track should represent CRISPR targets sites that are unique throughout the *Drosophila* genome. Rather than expressing separate crRNAs and tracrRNAs, the *Drosophila* CRISPR reagents described by Gratz *et al.* make use of a DNA plasmid, pU6-chiRNA, to express a single chimeric RNA (chiRNA)

that directs Cas9 endonuclease activity to the specific genomic sequence matching the chiRNA. The use of two such pU6-chiRNA plasmids can express chiRNAs that direct Cas9 DNA cleavage to locations upstream and downstream of a genomic target. A significant consideration is that the Gratz *et al.* pU6-chiRNA plasmid uses the *Drosophila snRNA:U6:96Ab* promoter to drive transcription of the cloned target DNA to be expressed as a chiRNA. One caveat of the *snRNA:U6:96Ab* promoter is that Pol III transcription of this promoter initiates with a G nucleotide. Since chiRNA generation from this plasmid initiates directly with the 5' base of the 20 b.p. sequence that is being targeted, this limits the 20 b.p. target sequences that can be selected for chiRNA production to those targets that start on their 5' end with a G nucleotide. Otherwise one introduces a 5' mis-match that reduces Cas9 targeting efficiency. With these limitations in mind I was able to identify a 3' *Kxd1* CRIPSR target that directed Cas9 double-stranded DNA (dsDNA) cleavage activity to a site 33 b.p. from the end of the *Kxd1* ORF.

The PBac{WH} insertion in *Kxd1* is between nucleotides 83 and 84 of the *Kxd1* transcript within the *Kxd1* 5' UTR. Although a suitable 20 b.p. 5' CRISPR target site exists within exon 2 of *Kxd1*, 8 nt into the *Kxd1* ORF, this is 196 b.p. downstream from the PBac insertion. Using this target site would leave the PBac{WH} insertion intact after CRISPR gene deletion and, procedurally, would not incorporate the loss of PBac{WH}CG10681^{f00719} as a marker of *Kxd1* deletion. Upstream of PBac{WH}, the next suitable CRISPR target site is located in the second exon of the upstream adjacent gene, *CG10638*.

CG10638 encodes a pair of putative alditol-oxidoreductases and is transcribed in the opposite orientation of *Kxd1*. Using the 3' *Kxd1* CRISPR target site and the 5' *CG10638* CRISPR target site would effectively eliminate the *Kxd1* gene, but would also eliminate critical portions of *CG10638* at the same time (Fig. 3.1). On the other hand using these CRISPR target sites also removes PBac{WH}CG10681^{f00719} which thus acts as a visible marker of *Kxd1* deletion, in accordance with the general strategies outlined by Gratz *et al.*

Template for gene replacement by homologous recombination

Because the desired end product was a deletion of *Kxd1* that did not delete adjacent gene sequences, I also incorporated the co-injection of a template for DNA break repair by homologous recombination (HR) as described by Gratz *et al*. who used a single-stranded oligodeoxynucleotide (ssODN) as an HR donor. Their goal was to replace the CRISPR-deleted *yellow* gene with a relatively short 50 nt Φ-C31 phage attP site. Introducing a short gene replacement allowed the use of a synthetic oligonucleotide as an HR template. In the case of *Kxd1,* my goal was to restore the 5' *CG10638* sequences that would be deleted using the 5' and 3' *Kxd1*·chiRNAs that I had selected. Gene replacement templates (*i.e.* HR donors) should incorporate stretches of homology to the genomic sequences flanking both ends of a DSBs to allow the donor to base pair with flanking genomic sequences by strand invasion or Holliday junction formation [18]. The sequences between the regions of homology can serve as a template for gene replacement by strand exchange or synthesis dependent strand annealing. In the case of an ssODN donor, 60 b.p. of homology were found to be sufficient to direct gene replacement [5]. However, currently, commercially available ssODNs are limited to 200 nt [19]. These lengths do not approach the lengths needed to replace the deleted *CG10638*, intergenic and *Kxd1* sequences.

Beumer *et al.* found that, like ssODNs, dsDNA templates are effective gene replacement donors but work better with 1 kb stretches of homology, and closed circular DNAs are more efficient than linear dsDNA [18]. To engineer a suitable HR donor to restore the deleted *CG10638* sequences and to replace *Kxd1* with *emGFP*, I constructed a plasmid template. For homologous flanking sequences I cloned 984 b.p. of genomic DNA upstream of the 5' CRISPR cut site and 1336 b.p. of genomic DNA downstream of the 3' CRISPR cut site into a pBluescriptSK(+) vector backbone. Between these I inserted the deleted *CG10638* and *CG10638-Kxd1* intergenic sequence, *Kxd1* exon 1 (encoding most of the *Kxd1* 5' UTR) and intron1, and the first 19 b.p. of *Kxd1* exon 2 (which included the first four codons of *Kxd1*). This was joined in-

frame to an FRT-flanked *emGFP* coding sequence to create a *Kxd1* gene replacement. The last 12 codons of *Kxd1* (11 of which are downstream of the 3' CRISPR cut site) finished the ORF which ended with the natural *Kxd1* stop codon followed by the *Kxd1* 3' UTR. The deduced translation product was an emGFP protein flanked N-terminally by the first 4 a.a. of Kxd1 and an FRT translation product (GSSYSLESIGTS), and C-terminally by a similar FRT translation product (RSSYSLESIGTS) and the last 12 a.a. of Kxd1.

The donor plasmid can be schematized as follows:

pBS-KpnI-[984 b.p. 5']-*CG10638*-intg-*Kxd1*-FRT-*emGFP*-FRT-[1336 b.p. 3']-SacI-pBS

(The **bracketed segments** are homologous genomic DNA. ***CG10638*** shows the deleted *CG10638* sequences, ***intg*** is the *CG10638-Kxd1*intergenic region. ***Kxd1*** is exon 1, intron 1 and the first 19 b.p. of exon 2 of *Kxd1*, **FRT** represent the 34 b.p. FLP-recombinase target sites. ***emGFP*** is the *emGFP* ORF, **KpnI** and **SacI** are restriction enzyme sites, and **pBS** is the pBluescriptSK(+) vector backbone.)

The gene replacement vector also modified the nucleotide sequences of the 5' and 3' CRISPR target sites so that these sites no longer matched the chiRNAs that directed Cas9 endonucleolytic activity to these locations. Since both of the *Kxd1*·CRISPR target sites fall within coding sequences, this was accomplished by making silent b.p. mutations taking into account codon usage frequencies. DSB repair and gene replacement directed by this donor template would generate a CRISPR-resistant *Kxd1* gene replacement allele (Fig 3.1 – lower schematic).

Putative gene replacement animals might be identifiable by screening them for expression of emGFP. Similarly, expression of emGFP could, in later experiments, serve as a visual marker of sites of *Kxd1* gene expression, and finally, *Kxd1*-linked expression of *emGFP* could be eliminated from these flies by expressing FLP recombinase in *trans*. The FRT sites

flanking the *emGFP* ORF in this construct are oriented as direct repeats, such that introduction of FLP recombinase would cause looping out and removal of the *emGFP* sequences [20, 21] leaving only a vestigial 16 a.a. encoding remnant of *Kxd1* (first 4 a.a. of *Kxd1*, 12 FRT encoded a.a., last 12 a.a. of *Kxd1*).

CRISPR injection of Drosophila embryos

CRISPR reagents were introduced into *Drosophila* by injecting 0-4 hour old embryos collected from Harvard f00719 flies. Injection services were contracted from Rainbow Transgenic Flies, Inc (Camarillo, CA). A total of 1218 embryos were injected with a cocktail of DNA including a pHSP70 plasmid directing the synthesis of an NLS-tagged Cas9 protein, two pU6-chiRNA plasmids directing the expression of the 5' and 3' *Kxd1* chiRNAs, and the pKxd1::emGFP gene replacement plasmid. Of the injected embryos, a total of 326 flies matured to adulthood (Table 3.1).

A subset of these flies displayed a distinctive eye color phenotype suggesting that they had lost one copy of the w^{+mC} dominant marker carried by the PBac{WH} transposon. Another subset of injected flies exhibited an eye color identical to that of the parental line, Harvard f00719, suggesting that these flies retained a homozygous PBac{W} insertion in the 5'UTR of *Kxd1*. To determine the genetic basis for the aberrant "heterozygous" eye color among some of the injected "founders", I crossed these flies individually to w^- balancer flies in order to segregate the third chromosomes that carried the *Kxd1* locus.

The heterozygous founders gave rise to an equal number of white-eyed flies, and progeny that displayed a w^{+mC} eye color identical to that of the heterozygous injected founders. In contrast, the subset of injected founders that displayed a parental eye color (*i.e.* identical to uninjected Harvard f00719 flies) gave rise entirely to F1 progeny that displayed the heterozygous eye color when crossed to w^- balancer flies. This implied that the offspring were heterozygous for the w^{+mC}

marker after their parents were crossed to w^- balancer flies that did not carry the w^{+mC} dominant marker. The Mendelian inheritance pattern of the eye color indicated that aberrant eye color observed of some of the injected flies was indeed a consequence of being heterozygous for the PBac-associated w^{+mC} marker, and mechanistically, loss of one copy of w^{+mC} in these injected individuals was best explained by an early heterozygous deletion of the genomic locus delineated by the 5' and 3' *Kxd1*·CRISPR target sites, including PBac{WH} and *Kxd1*.

Besides the prevalent heterozygous eye color phenotype (Table 3.1), there was a high incidence of premature mortality among the CRISPR-injected flies that matured to adulthood (roughly 28% - Table 3.1). These flies died within a day of eclosure and prior to successfully breeding with the balancer flies to which they were mated. Another group of injected flies did not exhibit early mortality but never successfully bred. In fact, sterility was the second most commonly observed phenotype of the CRISPR-injected animals (The most frequently observed phenotype was heterozygous loss of w^{+mC}). (Table 3.1).

emGFP expression and PCR screening of PBac^{f00719} Kxd1·CRISPR-deletion flies

CRISPR-injected founders that showed the heterozygous eye color phenotype and their w^- F1 progeny were screened for expression of emGFP under a dissecting fluorescent microscope. I reasoned that if an animal expressed emGFP, this would indicate that this individual harbored a *Kxd1::emGFP* gene replacement. Although some flies were initially set aside as putative emGFP-expressing transgenics, a comparison of these animals to verified eGFP expressing control flies and to non-GFP parental Harvard f00719 flies and the w^- balancer stock indicated that none of the injected flies, nor their F1 progeny, exhibited fluorescence above background. This did not rule out that these individuals were gene replacement carriers. I had not verified that emGFP expressed from the donor plasmid was functional, nor was it certain that emGFP expression levels from the native *Kxd1* promoter elements were sufficient to be seen using the visual screen

that I employed. To definitively determine the genetic status of these animals, these animals were screened by PCR after they had been successfully mated to establish F1 lines.

Screen for NHEJ repair of PBac^{f00719} Kxd1

Two F1 lines derived from each heterozygous (+/- eye color) injected founder were screened with four sets of primers. Two of the primer pairs annealed to sequences outside of the 5' and 3' *Kxd1*·CRISPR target sites. The third primer pair annealed within the *Kxd1* ORF (at the beginning of exon 2, and at the end of the *Kxd1* ORF in exon 3), and the fourth primer pair annealed within the emGFP coding sequence. The first two primer pairs (CDS-179/CDS-180 and CDS-179/CDS-181) were used to identify non-homologous end joining (NHEJ) DNA repair products of a CRISPR-mediated *Kxd1* deletion. Briefly, these DNA structures could be expected to consist of end-to-end joining of the blunt DSBs made by Cas9 at each CRISPR-target site, with or without some degree of end processing (base pair resection) prior to end-joining and chromosomal repair. The two sets of screening primers were slightly further spaced from each other in order to decrease the chances of missing a NHEJ product that included substantial end-resection prior to end-joining. At the same time, if an F1 line did not harbor a NHEJ deletion product, these PCR primers would generate products of different sizes depending on whether the amplified a product was generated from a wildtype copy of *Kxd1* or from a *Kxd1*::*emGFP* gene replacement allele.

Screen for emGFP gene replacement of PBac^{f00719} Kxd1

Because the DNA encoding *Kxd1* and that encoding the *Kxd1*::*emGFP* gene replacement construct differed only slightly in overall length – 133 b.p. (*i.e.* 695 b.p. wildtype *Kxd1* vs. 828 b.p. *Kxd1*::*emGFP* fusion), and because the first two sets of PCR screening primers annealed

outside of the *Kxd1*·CRISPR cut sites, both pairs of primers generated large PCR products if they amplified wildtype *Kxd1* or the *Kxd*::*emGFP* gene replacement. The exact size of the products that were generated by these PCR reactions was not always easily determined or unequivocal (1711 b.p., wildtype *Kxd1* vs 1844 b.p., *Kxd1*::*emGFP* – primer pair-1 [CDS-179/CDS-180]; and 1926 b.p,, wildtype *Kxd1* vs 2059 b.p., *Kxd1*::*emGFP* – primer pair-2 [CDS-179/CDS-181]). To resolve this issue I also screened these F1 lines with PCR primers that annealed to sequences between the *Kxd1*·CRISPR cut sites. Primer pair-3 (CDS-175/CDS-176) annealed to *Kxd1* sequences in exon 2 and exon 3, and primer pair-4 (CDS-177/CDS-178) annealed to *emGFP* sequences that were introduced by HR with the gene replacement donor. Both pairs were used to generate smaller products that could unequivocally distinguish between a wildtype *Kxd1* allele and a *Kxd1*::*emGFP* gene replacement allele.

Results of PCR screen of PBac^{f00719} Kxd1 F1 lines

I opted to screen only two F1 lines from each heterozygous injected founder since I was confident that each of the heterozygous founders harbored some form of a *Kxd1* gene deletion. I expected that the challenge of the molecular screen would be to identify a line of flies that carried a *Kxd1* gene replacement that restored the upstream *CG10638* sequences. In point of fact, none of the 146 F1 lines that I screened generated a NHEJ PCR product (120 *w*¯ F1 lines from heterozygous founders [+/- founders], 6 F1 lines from founders with an undetermined eye color [N.D. founders], and 20 F1 lines from founders with a parental eye color [+/+ founders]). Further, all of the lines that I screened generated a wildtype *Kxd1* PCR product and not a *Kxd1*::*emGFP* PCR product from primer pair-3, and none of the lines generated an *emGFP* product from primer pair-4, indicating that none of the lines had incorporated *emGFP* as part of a gene replacement, but all of the lines harbored a wildtype *Kxd1* allele.

Furthermore, a subset of these lines were characterized with three additional pairs of primers. Two sets of these primers showed that, in addition to carrying a wildtype copy of *Kxd1* without a PBac insertion, these lines carried this copy of *Kxd1* in the context of the annotated 5' and 3' genomic sequences: 1540 b.p. of annotated genomic sequence upstream and 1128 b.p. of annotated genomic sequence downstream. The third additional primer pair confirmed that these lines did not harbor an *emGFP* coding sequence inserted into *Kxd1* by amplifying across the expected *Kxd1*/*emGFP* junction of the gene replacement allele using a forward primer in *Kxd1* exon1 and a reverse primer in the coding sequence of *emGFP*.

PCR characterization of injected PBac·Kxd1 flies and parental Harvard f00719 flies – [Wildtype Kxd1]

In addition to screening two of the F1 lines that were generated from each injected Pbac·*Kxd1* founder, I collected some of the injected founders themselves and extracted their DNA after they had been bred to balancer flies. Both heterozygous eye color injected founders [+/- founders] and parental eye color injected founders [+/+ founders] were collected for DNA extraction. These flies were screened with the same four primer pairs that were used to screen the F1 lines. Representative screening results are shown in Figure 3.2. In agreement with the screening results of the F1 lines, all of the injected PBac·*Kxd1* founders that were tested amplified a robust wildtype *Kxd1* PCR band when screened with the primer pairs that annealed outside of the CRISPR cut sites (CDS-179/CDS-180 and CDS-179/CDS-181). This was observed for each of the +/- founders as well as for each of the +/+ injected founders that was screened. As a negative control, DNA from the parental Harvard f00719 line of flies was extracted and screened with the same set of PCR primers. Like the injected founders, the parental Harvard f00719 line of flies also amplified a robust wildtype *Kxd1* PCR product with these two pairs of PCR primers (Fig. 3.2 – gel, right hand side, upper blue arrow, blue "CG10638-*Kxd1*" bracket).

Notably, just as none of the F1 lines should have amplified a wildtype *Kxd1* PCR product from any of these PCR screens, neither should any of the CRISPR-injected founder flies. Like the uninjected parental line, the CRISPR-injected individuals were homozygous for PBac insertions in *Kxd1* before the introduction of the *Kxd1*·CRIPSR reagents. The *Kxd1*·CRISPR reagents injected into these flies directed DNA breaks 639 b.p. 5' of the PBac^{f00719} insertion and 844 b.p. 3' of the PBac insertion. The entire *Kxd1* gene spans 1135 b.p., 927 b.p. of which falls between the 5' and 3' *Kxd1*·CRISPR targets. The PBac{WH} transposon containing the w^{+mC} construct is 7234 b.p. in length and has no homologous sequences to either of the *Kxd1*·CRISPR targets. Therefore there is no CRISPR-mediated process that could explain removal of Pbac{WH} (and the associated w^{+mC} construct) without concomitant removal of *Kxd1*, and wildtype *Kxd1* PCR products could not have been amplified from the homozygous PBac^{f00719}·*Kxd1* allele that these animals harbored. Moreover, the observation that the parental Harvard f00719 flies also amplified a robust wildtype *Kxd1* PCR band indicated that the template for this band existed in PBac·*Kxd1* flies prior to introduction of CRISPR reagents. Finally, the amplification of a wildtype *Kxd1* band from all of the CRISPR-injected founders suggested that the template for this PCR product was likely unaffected by the *Kxd1*·CRISPR reagents despite their removal of w^{+mC} in over 60% of the injected flies (Table 3.1).

PCR characterization of injected PBac·Kxd1 flies and parental Harvard f00719 flies – [emGFP]

When DNA from the CRISPR-reagent injected flies was tested with primer pair-4 (CDS-177/ CDS178) that anneals within the emGFP coding sequence, each of the injected Pbac^{f00719} flies amplified a weak *emGFP* PCR product regardless of whether the flies displayed the parental red eye color or a heterozygous eye color (Fig. 3.2 – gel, left hand side, green arrow, green "emGFP" bracket,). This was in direct contrast to the lack of *emGFP* amplification from these sample samples when screened with primer pair-1 or -2, which would have indicated

emGFP incorporation into the CRISPR-cut *Kxd1* locus by gene replacement. On the other hand, the uninjected Harvard f00719 flies did not amplify emGFP. Thus, generation of this PCR product correlated with injection status. Because none of the F1 progeny lines amplified *emGFP* (screening negative by multiple PCR assays), I interpreted these results to mean that donor template had persisted in the injected individuals in an episomal state but was not passed on in the germline. This interpretation was somewhat remarkable as it implied that the screened individuals had maintained detectable quantities of episomal DNA throughout the larval stages, through metamorphosis and into adulthood despite having being injected as single-celled embryos.

PCR characterization of injected PBac·Kxd1 flies and parental Harvard f00719 flies - [NHEJ]

The last notable result from the PCR screening of the CRISPR-injected founders was that the majority of the screened heterozygous founders (four out of six), in addition to amplifying a robust wildtype *Kxd1* PCR band, amplified a trace band corresponding in size to that expected of a NHEJ DNA repair product of *Kxd1*. In addition, the putative NHEJ bands amplified by these samples were of distinct sizes for each of the samples but of heterologous sizes between samples. Two of the four injected founders amplified putative *Kxd1* NHEJ DNA repair bands close in size to the expected NHEJ band of 443 b.p. (the calculated size of direct end joining of the 5' and 3' CRISPR-generated DSBs). The remaining two injected founders amplified a NHEJ PCR bands that were both smaller than 443 b.p.: the larger of the two migrating at approximately 415 b.p. and the smaller of the two migrating at just under 400 b.p. ~ approximately 395 b.p. (Fig 3.2 – gel, right hand side, lower purple arrows, blue "CG10638-*Kxd1*" bracket).

Smaller NHEJ products were expected in cases where the Cas9-cut DNA ends were resected before final end joining. This indicated that the *Kxd1* locus had been deleted, as anticipated, in most of the injected founders but in a minority of the cell of these animals.

Alternatively, these PCR bands could have been generated from CRISPR-cut donor plasmid that persisted in these animals as episomal DNA and that was similarly repaired by cellular NHEJ repair pathways, despite the donor plasmid not having sequence-matched 3' and 5' *Kxd1*·CRISPR targets. This later explanation becomes quite unlikely when one considers the heterologous distinct sizes of the NHEJ bands that were amplified from these animals, unless one proposes that some of these bands were products of single DNA templates. The injected HR donor plasmids are non-replicative in *Drosophila* cells, and although they may persist for extended periods of time in an injected individual, they do not have the capacity to propagate. Thus specific genetic editing events experienced by individual donor plasmids, such as CRISPR-mediated cutting and specific degrees of DNA end resection, would not be present in more than a single copy per fly.

Sequencing of Harvard f00719 Pbac·Kxd1 locus proximal DNA

To examine the precise genetic structure and sequence of the PBac·*Kxd1* allele in the Harvard f00719 flies, given the observation that PCR bands consistent with the presence of a wildtype *Kxd1* gene (non-PBac) were generated from these flies, I sought to generate PCR products for DNA sequencing from these flies that were specific to both the annotated PBac insertion in *Kxd1* and to the observed wildtype, non-PBac, *Kxd1* allele.

Prior to injecting the Harvard f00719 flies with the *Kxd1*·CRISPR reagents, I had sequenced the DNA regions that were selected as targets in order to make sure that the target sites existed in the Harvard f00719 flies and that they matched the FlyBase reference sequence against which the CRISPR target sites were originally designed. Whereas the 3' CRISPR target site and the surrounding DNA matched the FlyBase reference sequence perfectly, the results for the 5' CRIPSR site were ambiguous. The 8th position of the 5' CRISPR target site generated base peaks for two different nucleotides. Both a C and a T peak of equal intensity were recorded, and the

automatic base-calling algorithm called this position a Y (pyrimidine – Figure 3.3, center). When this was first observed it stood out as highly irregular that an establish line that had been maintained by inbreeding (Harvard F00719) would harbor two equally prevalent alleles without one of them having gone to fixation and the other disappearing from the population. Nevertheless, it was decided that even if half of the chromosomes were recalcitrant to CRISPR-mediated *Kxd1* deletion, the other half would be subject, and the resistant and subject chromosomes could be subsequently segregated and isolated to establish a *Kxd1* deletion line.

When I observed that all of the chromosomes segregating from the *Kxd1*·CRISPR-injected animals retained a wildtype *Kxd1* allele regardless of whether the PBac w^{+mC} marker was retained, I hypothesized that the equivalent intensity C and T peaks found in position 8 of the 5' CRISPR site represented evidence of a prior *Kxd1* gene duplication event and that the duplicated alleles harbored a distinguishing single nucleotide polymorphism (SNP) within the target sequences of the 5' chiRNA. This interpretation was bolstered by the observation that a wildtype *Kxd1* allele was also present in the parental PBac line. To test this hypothesis I generated 5' *Kxd1*·CRISPR target site PCR products for sequencing using three different sets of primers, each of which had different template specificities (Fig. 3.3).

The original set of primers that I used to amplify the 5' *Kxd1*·CRIPSR target site for sequencing annealed 5' and 3' of the CRIPSR target site in *CG10638* sequences. These primers amplified a product from Harvard f00719 flies that always showed an ambiguous Y (pyrimidine) base upon sequencing (or an R [purine] if sequenced from the other direction). No other ambiguous base calls or peaks were generated when sequencing this PCR product. The most parsimonious explanation of this result, after considering the characteristics of the flies that were generated by *Kxd1*·CRISPR injection, was that a PCR product was being amplified from two copies of *Kxd1* in these flies and that the two copies of *Kxd1* differed from each other with respect to the base identity at position 8 of the 5' *Kxd1*·CRISPR target site.

To specifically amplify any 5' *Kxd1*·CRISPR target sequences proximal to the annotated PBac{WH} insertion, I generated a PCR product by paring the previously used upstream primer that annealed in *CG10638* sequences with a downstream primer that annealed within the terminal base pairs of PBac{WH} (Fig 3.3 – upper right gene schematic, orange arrows). This generated a 1610 b.p. PCR product consistent with the annotated location of PBac{WH} insertion in *Kxd1*. When sequenced, this 1610 b.p. product showed only a T in position 8 of the 5' *Kxd1*·CRISPR target site (Fig. 3.3 – lower right electropherogram). Reciprocally, to specifically amplify 5' *Kxd1*·CRISPR target sequences that were proximal to wildtype *Kxd1* sequences, I used the same upstream *CG10638* primer as used previously but shifted the downstream primer to a position in *Kxd1* exon 1 downstream of the annotated PBac{WH} insertion (Fig 3.3 – upper left gene schematic, green arrows). In this case the primers pair would generate a 1038 b.p. PCR product from a wildtype copy of *Kxd1*, but would not generate a PCR product from *Kxd1* with PBac{WH}CG10681^{f00719} insertion because the intervening PBac sequences comprised an additional 7234 b.p. between the primers. Indeed, a 1038 b.p PCR product was observed, and when this PCR product was sequenced it only yielded a C base peak at position 8 of the 5' *Kxd1*·CRIPSR target site (Fig. 3.3 – lower left electropherogram).

Together, these results indicated that the parental Harvard f00719 line of flies, indeed, harbored two distinct copies of *Kxd1* that were differentiable by sequence polymorphisms. One of the copies of *Kxd1* contained the annotated PBac{WH} insertion and was proximal to a 5' *Kxd1*·CRIPSR target that conformed to the FlyBase reference sequence. The second copy of *Kxd1* did not harbor a PBac{WH} insertion (the "wildtype" copy of *Kxd1*) and was proximal to a 5' *Kxd1*·CRIPSR target that did not match the FlyBase reference sequence. The location of the SNP between these two copies of *Kxd1*, at the 8th nucleotide from the 3' end of the CRISPR target site, 5 base pairs from the location of Cas9 DNA cleavage, meant that the 5' *Kxd1*·CRISPR target site proximal to the wildtype copy of *Kxd1* was unlikely to be efficiently targeted by the 5' *Kxd1*·chiRNA.

Although CRISPR/chiRNA targets tolerate some sequence variability in terms of serving as Cas9 cleavage targets, the 12 nt closest to the PAM are the most critical determinants of Cas9 targeting [22-24]. In this case the mis-match in the 5' *Kxd1*·CRISPR target proximal to the wildtype copy of *Kxd1* is 8 nt away from the PAM sequence. Therefore the 5' target sequence proximal to the wildtype copy of *Kxd1* in these flies is unlikely to serve as an efficient target for Cas9 cleavage.

CRISPR-mediated loss of w^{+mC}

Before proceeding further with a CRISPR-mediated attempt to delete *Kxd1*, I sought to understand what had occurred in the Harvard f00719 flies after injection of the *Kxd1*·CRISPR-reagents. Figure 3.4 illustrates a *Kxd1* gene duplication arrangement in which injection of *Kxd1*·CRISPR reagents would delete the PBac-associated w^{+mC} marker and create a gene deletion product which, if repaired by NHEJ, would reconstitute a pseudo-wildtype copy of *Kxd1* since DNA end resection prior to DSB repair would have likely introduced micro-deletions [25]. The loss of a handful of bases from NHEJ-associated end resection would not have been discernable within the context of a 2 kb diagnostic PCR product. Thus, the conditions proposed by the gene arrangement shown in Figure 3.4 are consistent with the phenotypic and molecular data obtained from characterizing the *Kxd1*·CRISPR-injected Harvard f00719 flies: Phenotypically the majority of the CRISPR-injected flies had lost a single copy of the w^{+mC} dominant marker, but all of the flies amplified a wildtype copy of *Kxd1* regardless of exposure to *Kxd1*·CRISPR-reagents.

Importantly none of the CRISPR-injected Harvard f00719 flies underwent gene conversion by incorporating the *emGFP*::*Kxd1* gene fusion. If the gene structure postulated in Figure 3.4 was reflective the actual situation, the DNA cuts made by the injected *Kxd1*·CRISPR reagents would not have generated a chromosomal substrate amenable to gene replacement. CRISPR-mediated cuts on this structure would be topologically equivalent to making a single

DSB in a wildtype copy of *Kxd1* (Fig. 3.4 – lower gene schematic), and the HR donor plasmid that I co-injected did not have regions of homology to both sides of the 3' CRISPR cut site.

Finally, it must be considered that alternative gene arrangements were possible for the duplication event discovered in the Harvard f00719 flies (Fig. 3.5). These alternative duplication arrangements would have generated distinct diagnostic PCR products when the injected Harvard f00719 flies and the F1 progeny from these flies were screened for *Kxd1* deletion. However, only the gene arrangement shown in Figure 3.4 was consistent with the PCR screening results. Notably, there were trace *Kxd1* gene-deletion (NHEJ) PCR products generated from the majority of the injected founders that were screened. This trace amount of NHEJ is consistent with a diminished rate of CRISPR cutting at the divergent 5' *Kxd1* CRISPR-target site proximal to the wildtype copy of *Kxd1* in the gene arrangement illustrated in Figure 3.4. Such CRISPR mis-targeting events would generate substrates for the trace amounts of *Kxd1* NHEJ products that were observed.

CRISPR targeting of Kxd1 in wildtype Canton S flies

Although the Harvard line f00719 flies proved to be unsuitable for CRISPR-mediated deletion of *Kxd1* with the reagents in hand, the genetic evidence of CRISPR-mediated w^{+mC} loss indicated that the targeted locus was effectively deleted when the flanking target sites matched the injected chiRNA sequences. Furthermore, the rate of w^{+mC} loss suggested that it was not necessary to identify putative gene deletion flies by the loss of a visible phenotypic marker (*e.g.* eye color), but that gene deletion events occurred frequently enough that they could be isolated without the use of a visual marker. I therefore opted to target *Kxd1* in wildtype Canton S flies using the same *Kxd1*·CRISPR reagents. If I successfully deleted *Kxd1* in a Canton S background I would also not need to Cantonize the resulting knockout animals. By eliminating several generations of outcrossing to Canton S this would shorten the time needed before the phenotypic

effects of *Kxd1* deletion could be tested, and, if multiple independent deletions of *Kxd1* were obtained, phenotypic consistency between the deletion alleles would serve to distinguish veritable *Kxd1* deletion phenotypes from phenotypic changes that occurred due to second site mutations.

Before having Canton S flies injected with the cocktail of *Kxd1*·CRISPR DNAs, I generated PCR products of the 5' and 3' *Kxd1*·CRIPSR target sites in Canton S flies for DNA sequencing to verify that the target sequences existed without sequence changes in these flies. Both the 5' and 3' target sites matched the FlyBase reference sequence and were therefore exact matches to the *Kxd1*·chiRNAs that targeted these loci. Following the same approach that I had used to target *Kxd1* in the Harvard f00719 flies, I mated all of the *Kxd1*·CRISPR-injected flies that matured to adulthood to w^+ ; TM3/TM6 balancer flies to establish collections of F1 flies from each injected founder. Instead of establishing individual F1 lines I pooled the F1 progeny from each founder and screened them collectively. My screening assumption was that if *Kxd1* deletion rates approached the rate that was previously observed for CRISPR-deletion of PBac·*Kxd1* allele in Harvard f00719 flies, a large percentage of CRISPR-injected Canton S flies could be expected to experience at least heterozygous deletion of *Kxd1*, and *Kxd1* deletion would be likely to have occurred in a nearly completely heterozygous manner such that close to half of the resulting F1 progeny would carry the segregated deletion allele or gene replacement.

PCR screening of Kxd1·CRISPR-injected Canton S flies

For unrelated logistical reasons I was unable to screen all of the pooled collections of F1 flies that had been established from the *Kxd1*·CRISPR-injected Canton S founders. Therefore I cannot report the rate or frequency of *Kxd1* deletion that resulted from this round of CRISPR injection. Nevertheless I was able to screen roughly 80 of the F1 populations using a subset of the same primer pairs described above. In each case I screened pools of 5 representative animals to look for putative *Kxd1* deletions and/or *Kxd1* gene replacement. Two of the pools amplified a

Kxd1 NHEJ PCR product indicating that some of the animals in these populations were carrying a CRISPR-mediated *Kxd1* deletion. To isolate the putative deletions, I established a collection of sublines by individually crossing all of the remaining individuals in these pools to w^+ ; TM3/TM6 balancer flies in order to segregate the putative deletion chromosomes. I subsequently purified DNA from each subline and screened the sublines by PCR. Four of the 14 sublines that were generated from pool 76i amplified a *Kxd1* NHEJ deletion PCR band (Fig. 3.6). The remaining sublines only gave rise to PCR bands indicative of wildtype *Kxd1*.

Kxd1 deletion allele in Canton S

To determine the molecular structure of the *Kxd1* deletion allele that was recovered from pool 76i of Canton S CRISPR-injected progeny, I established homozygous lines from the four $Kxd1^{76i}$ sublines that amplified a NHEJ deletion product. After purifying DNA from $Kxd1^{76i}$ subline 2, I submitted the NHEJ PCR product from this subline for bidirectional DNA sequencing. The results of this analysis indicated that $Kxd1^{76i}$-2 harbored a 1486 b.p. deletion that originated at the 5' *Kxd1*·CRIPSR target cut site and extended through the 3' *Kxd1*·CRIPSR target cut site. However, prior to DNA end joining the $Kxd1^{76i}$-2 substrate DNA was resected at both the 5' and 3' blunt-end DSBs (Fig 3.7): at least one base pair was removed from the 5' CRISPR-generated DSB (5' TTCA 3'-end – the underlined base pair having being resected), and at least two base pairs were removed from the 3' CRISPR-generated DSB (end-5' GATTC 3' – the underlined two base pairs having been resected). This DNA end processing left the trinucleotide base pair, TTC, at the terminus of both DSBs and was apparently the substrate for microhomology end-pairing as only one copy of this terminal trinucleotide is present in the DNA junction between the resected 5' and 3' DSBs in this allele.

Because I was unable to establish the individual sublines from pool 76i until more than 2 months after the Canton S founders were injected with CRISPR reagents, and because at the time

of subline separation the pools consisted of limited numbers of remaining individuals due to the nutritional status of each vial, I established sublines from the remaining flies of pool 76 with the goal of isolating the *Kxd1* deletion chromosomes that had been identified in the initial screening reactions. In other words, I was not attempting to segregate multiple putative deletion alleles but to rescue the deletion allele that had given rise to the screening NHEJ PCR product. I considered it unlikely that more than one deletion allele was present in this population given that the pool was screened a likely three generations away from the injected Canton S founder, and that it has most likely experienced a severe genetic bottleneck prior to the separation of the individual subline founders. However, formally, I did not determine if the individual sublines of $Kxd1^{76i}$ ($Kxd1^{76i}$-2, $Kxd1^{76i}$-3, $Kxd1^{76i}$-13 and $Kxd1^{76i}$-14) represented the same or different *Kxd1* deletion alleles.

CRISPR-targeted deletion of Blos3

Because I observed a high rate of loss of the w^{+mC} marker from *Kxd1*·CRISPR-injected Harvard f00719 flies, I opted to generate additional *Drosophila* BLOC-1 gene deletions by targeting BLOC-1 subunit genes in Canton S wildtype flies as undertaken for *Kxd1*. Among the BLOC-1 subunit genes characterized in mice, the gene encoding BLOS3 *(Bloc1s3*) is notable because it produces an attenuated BLOC-1 phenotype [9]. By making a *Blos3* deletion in *Drosophila*, a phylogenetically-distant species from mice, I aimed to robustly test the hypothesis that *Blos3* is a non-canonical BLOC-1 subunit gene and that loss of *Blos3* elicits BLOC-1 phenotypes of a less severe nature.

Selection of Blos3 CRISPR target sites

Using the UCSC Genome Browser with the SpCas9_Dm-targets custom track, I examined the genomic region around *Drosophila Blos3* to identify putative CRISPR target sequences. *Drosophila Blos3* is located on the third chromosome at cytological position 75E2, but *Blos3* is small genetic target and is located in a genetically compact region of chromosome 3. The *Blos3* gene spans a mere 645 b.p. and produces a 533 nt transcript composed of three exons. *Blos3* is transcribed in the positive direction, but it is entirely overlapped with and located within the coding sequence of *Rad9*, which is transcribed in the negative direction of the same span of DNA (Fig. 3.8). RNAi driven inactivation of *Rad9* causes partial lethality [26, 27] but an imprecise excision of *Rad9* that did not disrupt *Blos3* was reported to be viable (other than viability, no phenotypic description of *Rad9* was reported in the techniques paper that described deletion of the upstream *Rad9* coding sequences) [28]. In any case, my goal was to identify CRISPR target sites that would delete *Blos3* without disrupting *Rad9.*

I was able to identify genome-wide unique CRISPR target sites that deleted the first half of the *Blos3* ORF (the first 76 codons of 144 codons total) without deleting coding sequences of *Rad9* (Fig 3.8 – gene schematic). The 5' CRIPSR target site that I identified directs Cas9 DNA cleavage two base pairs before the ATG initiation codon of the *Blos3* ORF. With regards to *Rad9*, this CRISPR target site cut 47 nt into *Rad9* exon 6, which encodes most of the *Rad9* 3' UTR. The *Rad9* 3' UTR is 340 nt long. The first 31 nt of the *Rad9* 3' UTR are encoded by *Rad9* exon 5. The remaining 309 nt are encoded in exon 6. The 3' *Blos3* CRISPR target site cut within the *Blos3* ORF in exon 3. With regards to *Rad9*, this CRISPR target site directed Cas9 activity one nucleotide into *Rad9* intron 5 (between exon 5 and exon 6). This removed the downstream consensus 5' intron splice site [29]. Together these target sites eliminate the majority of the *Blos3* ORF. Of the remaining 68 *Blos3* codons (codons 77-144) another in-frame initiation codon does not occur until codon 98.

In terms of *Rad9* expression, most of the 341 b.p. that fall between the 5' and 3' *Blos3*·CRISPR target sites are located within intron 5 of *Rad9*. Only 47 b.p. are within *Rad9* exon 6. Furthermore, because all of *Rad9* intron 5 and the beginning of Rad9 exon 6 are removed, this also first eliminates the 5' and 3' consensus splicing signals of *Rad9* intron 5. The remaining bases of *Rad9* exon 5 and exon 6 are likely to be transcriptionally fused and transcribed as a single exon that is missing as few as 47 bases from the beginning of the *Rad9* 3' UTR but that contains the remaining 293 nt of the *Rad9* 3' UTR. In other words, although it is almost impossible to engineer a *Blos3* deletion that does not also affect *Rad9* without invoking a gene replacement strategy, the aforementioned *Blos3*·CRISPR target sites are predicted to virtually eliminate *Blos3* while minimally affecting expression of *Rad9*.

Blos3·CRISPR injection and PCR screening of Blos3 deletion flies

After having Canton S flies injected with *Blos3*·CRISPR DNAs, a total of 30 injected embryos matured to adulthood. These injected founders were individually mated to w^+ ; TM3/TM6 balancer flies to generate F1 progeny. Nine produced offspring within the same initial period. I separated out the injected founders and extracted DNA from these animals and from a pooled group of five F1 progeny from each founder. Using a pair of primers that annealed in the two adjacent genes (upstream primer, CDS-199, annealing in exon1 of *CG6852*; downstream primer, CDS-200, annealing in *Rad9* exon 4) I screened each of the 18 DNA samples, in a pairwise fashion (injected founder and 5 pooled F1 progeny), for amplification of a *Blos3* wildtype or NHEJ PCR product (Fig. 3.8 – gel). Using this primer pair, wildtype *Blos3* was expected to generate a 1125 b.p. band while the anticipated *Blos3* NHEJ deletion allele was expected to generate a 784 b.p. band. Indeed, three of the paired DNA samples generated *Blos3* NHEJ amplification products from the pooled F1 progeny. Canton S·*Blos3* lines 7, 8 and 13 (CSB3-7, CSB3-8 and CSB3-13) each generated the 784 b.p. *Blos3* deletion bands from the F1

progeny samples. Interestingly, among the DNAs isolated from the injected founders of these three groups, only CSB3-13 gave rise to a strong *Blos3* deletion band. Nevertheless, these results indicated that the *Blos3*·CRISPR reagents that I used deleted *Blos3* in a genetically inheritable manner roughly a third of the time.

Blos3 deletion alleles

To isolate the *Blos3* deletion alleles that were identified in the screening assays described above, the remaining F1 progeny from the pooled F1 offspring of CSB3-7, CSB3-8, and CSB3-13 were individually crossed to w^+ ; TM3/TM6 balancer flies to establish sublines and segregate the wildtype and NHEJ *Blos3* alleles in the population. When the resulting sublines were screened for deletion of *Blos3*, almost precisely half of them had inherited a *Blos3* NHEJ chromosome. This indicated that the *Blos3* deletions identified in the pooled screening assays probably originated from injected founders that were heterozygous for *Blos3* deletion (despite the inconsistent amplification of a *Blos3* deletion band from the DNAs extracted from these three animals) and that the inherited Blos3 deletions alleles were likely identical among the sublines of each group. The sublines that screened positive for a Blos3 deletion gene were backcrossed to eliminate the balancer chromosomes and to generate sublines that were homozygous for *Blos3* deletion. Homozygous *Blos3* deletion of each subline was confirmed by PCR screening.

Sequencing of Blos3 deletion alleles

To determine the exact DNA sequence of each of the *Blos3* deletion alleles I generated PCR products from a homozygous subline of each of the three *Blos3* alleles and submitted these for bidirectional sequencing. Each of the three deletion alleles, $Blos3^7$, $Blos3^8$ and $Blos3^{13}$, was molecularly distinct and showed evidence of NHEJ DNA repair that followed DSBs caused by

the injected CRISPR reagents (Fig. 3.9). The sequence differences between each allele all occurred at the location of DNA end joining and appeared to have resulted from different degrees of DNA end processing before final DNA end joining. For example, *Blos3*^{7} appears to have been repaired by blunt end ligation after three base pairs had been resected from the 3' Cas9 DNA cut site (end-3' ACCGCTT 5' – underlined bases resected). *Blos3*^{8} appears to have been repaired following microhomology-driven end pairing. The exact extent of microhomology end pairing that took place prior to end joining is ambiguous: Two base pairs appear to have been resected from the 5' Cas9 cut site DSB (5' ACTGAA 3'-end – underlined bases resected), and – either three bases were resected from the 3' Cas9 DNA cut site and the DNA ends were joined following single base end pairing (end-3' ACCGCTT 5' – underlined bases resected), – or the 3' Cas9 DNA cut site was not resected and the DNA ends were joined following a four base stretch of microhomology-driven end pairing that included a one base pair mis-match (end-3' AC*C*GCTT 5' – italicized C mis-matched to T in resected 5' Cas9 DNA end). If the latter interpretation is true then the mis-matched C:T base pair was likely replicatively converted to the A:T base pair that is seen in the sequence data of the *Blos3*^{8} deletion allele. Finally, *Blos3*^{13} appears to have been repaired by a NHEJ processes that involved one base pair of microhomology end pairing without prior end processing or base pair removal (5' ACTGA**A** 3'-end – annealed to – end-5' **A**CCGCT 3'). A single A:T base pair is missing from the DNA junction between the 5' and 3' CRISPR cut sites of *Blos3*^{13} indicative of single base end annealing prior to end joining. I did not formally determine whether the different sublines of each *Blos3* deletion line harbor the identical deletion allele, but the Mendelian segregation patterns argue that each of the *Blos3* lines is derived from a single event.

DISCUSSION

In this chapter I describe the targeting and deletion of the *Drosophila Kxd1* and *Blos3* genes using a CRISPR/Cas9 strategy of genomic editing. In both cases, the anticipated deletion products were generated relatively quickly, and were obtained in a common isogenic Canton S background. This significantly simplified the post-genomic- editing handling of the deletion lines. For *Blos3,* multiple alleles of the gene deletion were obtained in parallel, further strengthening the interpretation of any phenotypic characterization that would be pursued with these alleles. Finally, although the CRISPR-mediated deletion of *Kxd1* also deleted sequences of the adjacent upstream gene, the use of CRISPR reagents to target both *Kxd1* and *Blos3* resulted in precise genetic lesions not easily accomplished with other approaches.

Deletion of Drosophila Kxd1

When I set out to delete *Drosophila Kxd1* in order to characterize its function in relation to BLOC-1, a survey of available *Drosophila* transposon-insertion lines revealed that the P element insertion closest to *Kxd1* was in the neighboring upstream gene, *CG10638*. The next closest P element insertion was in the 5' UTR of the gene downstream of *Kxd1*, *CG10646*, which is transcribed in the opposite orientation of *Kxd1* making this second P element insertion significantly further away than that in *CG10638*. However, in the previous year Gratz *et al.* had reported the construction and use of CRISPR reagents for heritable genomic editing in *Drosophila*. One of the considerations that they mention is the use a visible genetic marker to detect deletion of the targeted genetic element [5, 25]. Although there were no P element insertions in *Kxd1*, I did find an annotated piggyBac insertion in *Kxd1* that was available from the Exelixis Collection at the Harvard Medical School [11]. The *Kxd1* PBac insertion was a

PBac{WH} construct meaning that it carried a w^{+mC} dominant marker that fulfilled the criteria of providing a visible marker of *Kxd1* locus retention.

Using a combination of online resources (UCSC Genome Browser with the SpCas9_Dm-targets custom track and the FlyCRISPR online CRISPR Optimal Target Finder tool) I was able to identify chiRNA target sites compatible with the Cas9 *Drosophila* CRISPR reagents described by Gratz *et al*. [5]. Notably, this necessitated selection of a CRISPR target that initiated with a G nucleotide at the 5' end of the chiRNA target, opposite the end where the Cas9 DSBs are made [5, 25]. Although the 3' *Kxd1* CRISPR target site fell near the end of the *Kxd1* ORF, the 5' CRISPR target site was in the second exon of the adjacent upstream gene, *CG10638.* Although at this juncture use of a CRISPR-mediated gene deletion approach was ostensibly no longer at an advantage relative to attempting to delete *Kxd1* by P element imprecise excision using the P element inserted in the 5' UTR of *CG10638* exon 1 – both strategies would delete portions of the upstream adjacent gene – using a CRISPR approach promised a defined *Kxd1* deletion while attempting the same procedure by imprecise excision would generate a fundamentally more random spectrum of deletions and potentially involved a considerably larger amount of screening. Secondly, although the CRISPR-based approach similarly removed portions of *CG10638,* the precise genomic cuts that were would be generated had the distinct advantage of creating a substrate for genomic editing and gene replacement by homologous recombination [5, 18]. This meant that it was reasonable to attempt restoring the deleted *CG10638* sequences upstream of *Kxd1* without restoring deleted *Kxd1* sequences, arriving at a precise genomic deletion of interest.

Deletion of Kxd1 in Harvard line f00719 flies

Harvard line f00719 flies harbor a PBac{WH} insertion in the 5' UTR of *Kxd1* making this line seemingly ideal for monitoring the deletion of *Kxd1* when using CRISPRs. As detailed in the Results section above, it was determined that these flies had experienced a gene duplication

event that resulted in f00719 flies having two copies of *Kxd1*. The annotated copy of *Kxd1* had the PBac{WH}CG10681^{f00719} insertion, and the second copy of *Kxd1* lacked a PBac insertion. Furthermore, while the PBac-inserted copy of *Kxd1* was adjacent to a 5' CRISPR target site that matched the annotated FlyBase genomic sequence (and hence the 5' *Kxd1* chiRNA), the second copy of *Kxd1* that did not have PBac insertion was proximal to a 5' CRISPR target site that differed from the 5' *Kxd1* chiRNA. This made the target site 5' of the second, wildtype, copy of *Kxd1* unamenable to Cas9 DNA cleavage.

Targeting *Kxd1* for deletion using the selected CRISPR target site resulted in the highly efficient elimination of w^{+mC} – the visible dominant marker carried by PBac{WH} but did not result in genomic deletion of *Kxd1*. After becoming aware of the *Kxd1* gene duplication in line f00719 and the sequence variation that characterized this gene duplication, these were the expected results of targeting *Kxd1* in line f00719 flies using the chiRNA targets for which I had built reagents. Although these particular gene deletion efforts did not eliminate *Kxd1*, they did demonstrate the efficiency with which the CRISPR/Cas9 system honed in on and deleted the targeted genomic elements, and the success of these results encouraged me to consider directly targeting *Kxd1* in a wildtype Canton S background.

CRISPR-mediated deletion of Kxd1 in wildtype Canton S flies

Given the efficiency with which w^{+mC} was eliminated from Harvard line f00719 flies, I used the same CRISPR reagents that I had built to eliminate *Kxd1* in those flies to target *Kxd1* for deletion directly in wildtype Canton S flies. By selecting Canton S flies as the genetic background in which to eliminate *Kxd1,* I lost the advantage of visually monitoring the efficiency with which *Kxd1* was eliminated. Instead, unless loss of *Kxd1* manifested a visually assessable haploinsufficiency phenotype, I would have to identify *Kxd1* deletion mutants by molecular screening. Nevertheless, if the rate of deletion of *Kxd1* in a Canton S background approached that

observed in the Harvard line f00719 flies, I reasoned that I could identify and rescue any putative deletion alleles by undirected screening. The frequency of gene deletion (w^{+mC}) was high enough in the previous *Kxd1*·CRIPSR experiments to anticipate encountering one or more Kxd1 deletion alleles in Canton S flies by even a low density molecular screen, *i.e.* PCR screen. I reasoned that I could accomplish this by segregating the third chromosomes of the CRISPR-injected Canton S flies and establishing F1 lines and then screen the resulting lines for the presence of a *Kxd1* deleted allele. I further reasoned that this could even be accomplished without producing homozygous deletion lines, if I was looking for diagnostic PCR products that were kinetically favored over wildtype *Kxd1* PCR products as the diagnostic PCR products that I was looking for were.

This last point was of particular interest because it was not clear if deletion of *Kxd1* in *Drosophila* would be homozygous viable. It was theoretically possible that *Kxd1* was duplicated in Harvard line f00719 flies because piggyBac insertion had disrupted expression of *Kxd1,* and flies that had experienced a *Kxd1* duplication were at a selective advantage. Notably, a second annotated line of PBac insertion in the 5' UTR of *Kxd1* (also an Exelixis pBac{WH} insertion line) was no longer available.

The purpose for targeting *Kxd1* for deletion directly in Canton S was that my ultimate goal was to obtain a *Kxd1* mutant in a wildtype genetic background that was isogenic with the previously characterized canonical BLOC-1 mutant, *blos1* [30], to allow direct and quantitative comparison between the effects of these mutations. It is notable that previous characterization of loss of *Kxd1* in mice had not been performed in a directly comparable quantifiable manner, much confusing the interpretation of these results [6]. Directly deleting *Kxd1* in a background isogenic to a previously generated mutation of BLOC-1 had the advantage of eliminating multiple downstream steps of outcrossing *Kxd1* mutants generated in a genetically isolated line, such as Harvard line f00719, in order to bring it into a common genetic background. Avoiding these 'Cantonization' steps also had the advantage of potentially avoiding molecular screening of the

progeny from each outcross if, as was seen of *Vab2*, a visible phenotype was not available to follow the gene deletion through the crosses.

Unfortunately, due to unrelated circumstances, I was not able to determine the efficiency with which *Kxd1* was targeted and eliminated in Canton S flies, but by screening individuals from the sublines that did remain after I was able to return to following up on these injection experiments, I identified and isolated a NHEJ genomic deletion mutant of *Kxd1*. I found the *Kxd1* deletion allele harbored by these mutants in a heterozygous state, but I was able to segregate the allele and establish it homozygously. No eye color phenotype was apparent when the deletion allele, $Kxd1^{76i}$, was brought to homozygosity. Nevertheless, $Kxd1^{76i}$ had the anticipated DNA structure that eliminated the vast majority of the *Kxd1* ORF along with critical portions of the neighboring upstream CG10638 gene indicating that the allele had been generated by DNA cleavage at the Cas9 target sites and had been repaired by NHEJ after limited DNA end resection to a stretch of three base microhomology (Fig. 3.7).

As no other genomic *Kxd1* sequences were detectable in the strain harboring this allele, this meant that $Kxd1^{76i}$ was a *bona fide* genetic null of *Kxd1*, but it was also a likely genetic null of *CG10638*. Thus $Kxd1^{76i}$ could be used to identify putative *Kxd1* deletion phenotypes – it had already been used to show that deletion of *Kxd1* was homozygous viable – but verification of these phenotypes would require additional steps such as genetic complementation using endogenously expressed '*Kxd1* and *CG10638*' constructs and '*CG10638* only' constructs. Alternatively, a second deletion allele of *Kxd1* that did not also eliminate *CG10638* sequences could be used to validate the *Kxd1* deletion phenotypes observed of $Kxd1^{76i}$.

CRISPR deletion of Blos3

With similar considerations in mind to those for deleting *Kxd1* in Canton S flies, I set out to delete *Blos3* in a Canton S background. Although *Blos3* is situated in a complex genetic locus

– it is entirely overlapped by *Rad9* [26, 28] – I was able to identify CRISPR target sites that eliminated over half of the *Blos3* coding region, including the *Blos3* initiation codon, without affecting the open reading frame of *Rad9*. Cas9 cutting at these CRISPR target sites did eliminate 47 b.p, of the *Rad9* 3' UTR (prior to the removal of any additional bases by DNA end resection and NHEJ), but it otherwise did not delete *Rad9* coding sequences. Therefore, in this case, I did not construct and co-inject a gene replacement template with the *Blos3* CRISPR reagents.

I was able to immediately establish and screen F1 flies from the injected founders, and I identified multiple instances of heritable *Blos3* deletion among the F1 flies from individual injected founders. In each case the *Blos3* deletion allele was inherited in Mendelian ratios indicating that the individual deletions had been created at an early, probably single cell, developmental stage in the injected founders and that the injected founders that harbored the individual *Blos3* gene deletions were probably heterozygous.

Since I had identified in this manner three *Blos3* deletion alleles among the first nine injected flies that successfully mated, I deemed it unnecessary to screen additional flies. Each of the isolated alleles was created from a unique genomic editing event (a unique *Blos3*·CRISPR embryo injection) in a Canton S background, and each of the alleles was molecularly distinct. This greatly diminished the chances of later erroneously characterizing the effects of *Blos3* mutation due to a random second site mutation in one of the lines, and the creation of the deletion alleles in a Canton S background allowed for the immediate characterization of loss of *Blos3* with a high degree so long as identical phenotypes were observed from each individual deletion line.

CRISPR gene targeting and deletion efficiencies

The rate of success and ease of isolating *Blos3* CRISPR-generated deletions was on par with the efficiency with which w^{+mC} was seen to have been eliminated from the Harvard f00719

flies when they were injected with *Kxd1* CRISPR reagents. This efficiency of gene deletion, along with the advantages of not having to isogenize deletion alleles generated in a non-related background, argued that CRISPR-mediated genomic editing in *Drosophila* was efficient enough to target gene deletion directly in the genetic background of interest. The lack of a visibly scorable marker, as has traditionally been a practical requirement for gene deletion strategies such as P element imprecise excision and as still recommended by Gratz *et al*. [25], is practically unnecessary and even burdensome. Instead, CRISPR-mediated gene deletion events that occur at the frequencies observed here can be identified by undirected screening, and there is no reason to not directly target genes in the background of interest. A visibly scorable marker becomes even less necessary, if one is targeting a gene on the X chromosome that is expected to elicit a visible phenotype when deleted. In these cases, one might identify gene deletion events directly in injected animals if, for instance, hemizygous males are generated by CRISPR-mediated gene deletion.

In this vein, it was notable that despite the high frequencies observed of CRISPR-mediated gene deletion, I did not observe any instances of homozygous gene deletion. Despite 60% of the *Kxd1*·CRISPR-injected flies appearing to be heterozygous for w^{+mC} and at least 30% of the *Blos3*·CRISPR-injected flies seeming to be heterozygous for *Blos3*, homozygous deletion flies were never observed or isolated.

I also never obtained reliable data about the efficiency of gene replacement using the Gratz *et al*. set of CRISPR reagents. Gene replacement is supposed to be relatively efficient using the proper approaches and the Gratz *et al*. complement of CRISPR tools [5, 13, 25]. However, gene replacement was unlikely to have occurred in the original CRISPR-injection experiments that I performed targeting *Kxd1* in Harvard f00719 flies due to lack of homology between the *Kxd1*::*emGFP* gene replacement vector and the Cas9 DNA cuts that likely occurred in the Harvard f00719 flies (*c.f.* Fig 3.4 and the *CRISPR-mediated loss of* w^{+mC} section of the Results). I was not able to adequately screen the later *Kxd1*·CRISPR injections of Canton S flies, and I did

not co-inject a gene replacement donor when I deleted *Blos3* by CRISPR-mediated gene targeting. Therefore I did not have sufficient data to make conclusions about the efficiency of gene replacement in CRISPR-injected flies using long circular dsDNA donor templates, although these were recently reported by others to work efficiently [13].

Lastly, the parameters of CRISPR reagents injection appear to matter significantly. After realizing that it was optimal to directly inject the *Kxd1*·CRIPSR reagents into Canton S flies in order to obtain a *Kxd1* deletion, I revisited the design and selection of the *Kxd1* CRISPR target sites. As mentioned in the Results section, in addition to the 5' *Kxd1* target site in *CG10638* that was used to target *Kxd1* in Harvard f00719 flies, and which, in combination with the selected 3' Kxd1·CRISPR target site, effectively deleted w^{+mC} and generated $Kxd1^{76i}$, a second 5' *Kxd1*·CRIPSR target site existed in exon 1 of *Kxd1* at the start of the *Kxd1* ORF. I generated a chiRNA-encoding plasmid to produce this new 5' CRISPR target site and had it injected into Canton S flies along with the original 3' *Kxd1*·CRISPR chiRNA plasmid and pHsp70-Cas9 (without co-injection of a gene replacement donor since *CG10638* was left untouched by these CRISPR reagents and DNA deletion was entirely limited to *Kxd1* sequences).

The quantities of DNA that I had injected in this round of CRISPR DNA-injections were in excess of those normally used to generate CRISPR-mediated gene deletions. Despite injecting 245 embryos, only 7 of these matured to adulthood and only 2 of those successfully bred to establish F1 lines (Both of these were *Kxd1* wildtype). This indicated that the quantities of injected DNA were likely critical to successfully deleting a genomic target without causing excess mortality and sterility – problems that were endemic throughout these experiments.

Finally, the specific chiRNAs that are used likely have a profound effects on the efficiency of targeted gene deletion. In addition to attempting to delete *Kxd1* and *Blos3* in Canton S flies, I targeted *Muted*, a canonical BLOC-1 subunit gene that, in mice, shows a typical BLOC-1 phenotype [31, 32]. Although I validated that both the *Muted* CRISPR target site existed in Canton S flies, as annotated in FlyBase, as I had previously done for *Kxd1* and *Blos3*, and despite

performing three rounds of CRIPSR injection into Canton S flies with these reagents, I never observed a targeted gene deletion of *Muted* even though I screened all of the injected founders that had bred F1 lines. Although viability and sterility were again issues with these rounds of CRISPR injection, I nevertheless PCR-characterized over 50 sample pairs (paired samples of injected-founders and 5 pooled F1 progeny) without observing any evidence of *Muted* gene deletion. This argued that at least one of the *Muted* chiRNAs had not efficiently targeted the intended cut site or that one of the cut sites was somehow resistant to Cas9 activity. It was possible that some of the *Muted*·CRISPR-injected flies harbored NHEJ frame-shift mutations of *Muted*, but given the simplicity and ease of creating large gene deletions using the Gratz *et al.* *Drosophila* CRISPR reagents, the take-home lesson from targeting *Kxd1*, *Blos3* and *Muted* was that specific chiRNAs may not efficiently target the intended locus but that the CRISPR approach of heritable genomic editing in *Drosophila* is a revolutionary break-through in terms of experimental design and execution.

Adult Animals Recovered from *Kxd1* CRISPR/Cas9 Injected Embryos						
Animals by Gender	Deduced genotype (by eye color)			% Bred	% Sterile	% Died
173 ♂	+/-	104	(60%)	45	41	14
	+/+	64	(37%)	43	9	48
	N.D.	5	(3%)	40	0	60
153 ♀	+/-	96	(63%)	15	58	27
	+/+	50	(33%)	2	50	48
	N.D.	7	(4%)	14	14	72
All genotypes sorted by sex						
173 ♂	all genotypes			44	35	21
153 ♀	all genotypes			10	54	36
Both sexes sorted by genotype						
326 ♂ + ♀	+/-	200	(61%)	30	50	20
	+/+	114	(35%)	14	38	48
	N.D.	12	(4%)	25	8	67

Table 3.1 CRISPR deletion of *Kxd1* in Harvard f00719 flies. A total of 326 CRISPR/Cas9-injected embryos matured to adulthood. Injected embryos were homozygous for the PBac{WH} insertion in *Kxd1*. Each embryo was injected with a cocktail of DNA including the gene for the Cas9 endonuclease, genes directing the synthesis of two *Kxd1*-locus targeting chiRNAs, and a plasmid template for *Kxd1* gene replacement. The genotype of each adult fly, with regard to loss or retention of PBac{WH}CG10681^{f00719}, was determined based on eye color: heterozygous PBac (+/-) or homozygous PBac (+/+). The observed eye color differences were deemed to be a function of the intensity of w^{+mC} expression carried by PBac{WH} and, thus, a reflection of PBac copy number. A minority of flies were of ambiguous eye color, and their genotypes could not be determined (N.D.). Flies were individually crossed to w^- FM6 balancer flies, and each of the deduced genotypes bred true: +/- individuals produced equal numbers of w^+ and w^- progeny, +/+ individuals produced only w^+ progeny. A large percentage of the animals did not produce offspring (% Sterile), while others died before mating successfully (% Died).

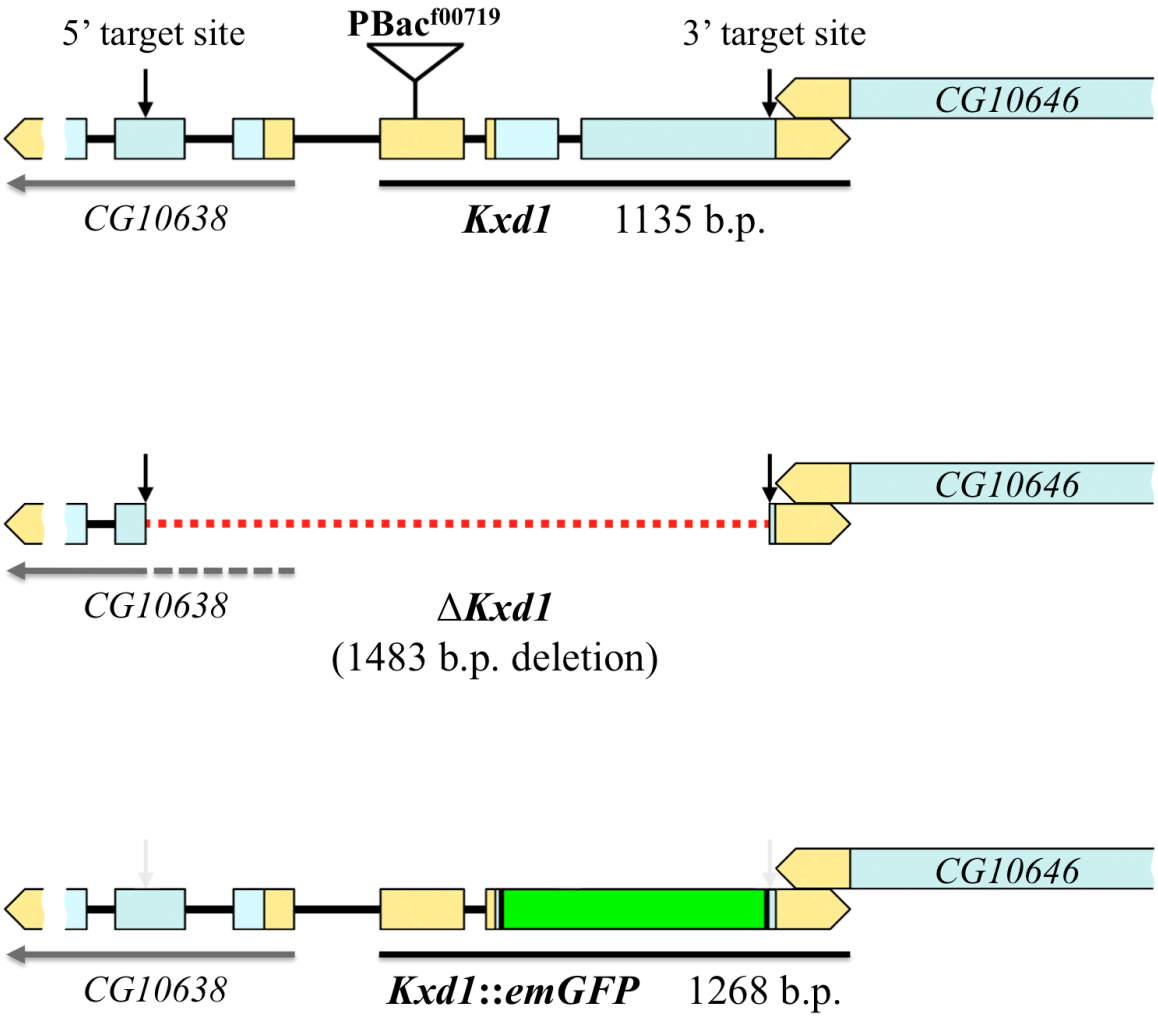

Figure 3.1. Strategy for CRISPR/Cas9-mediated deletion of *Drosophila Kxd1*. Gene schematics illustrating the *Kxd1* genomic locus of Harvard line f00719 and the anticipated CRISPR deletion products. The upper schematic illustrates the exon/intron structure of *Kxd1* and the neighboring genes. The light blue exonic segments correspond to open reading frames (ORFs). Yellow segments represent untranslated regions (UTRs). *Drosophila CG10681* (*Kxd1*) is located on the positive strand of third chromosome at cytological position 69C4. The neighboring genes are transcribed in the opposite direction. *Kxd1* is separated from *CG10638* by an intergenic region, but the 3' UTR of *Kxd1* overlaps with *CG10646*. Harvard line f00719 harbors a PBac{WH} insertion in the 5' UTR of *Kxd1*. Bioinformatically-unique CRISPR/Cas9 target sites were identified upstream of *Kxd1* in the second exon of *CG10638* (5' target site), and near the 3' end of the *Kxd1* ORF (3' target site). The Cas9 gene, chiRNAs specific to 5' and 3' target sites,

and a plasmid template for homologous recombination/repair were injected into embryos to generate a CRISPR/Cas9 deletion allele of *Kxd1* and/or an *emGFP* gene-replacement product. The dotted red line in the middle schematic shows the anticipated non-homologous end-joining (NHEJ) deletion, which includes most of *Kxd1,* as well as portions of *CG10638*. The lower schematic shows the structure of the gene-replacement product, which restores the 5' sequences of *CG10638* and *Kxd1*, replaces the majority of the *Kxd1* ORF with the coding sequence of *emGFP* (green box), and alters the genomic chiRNA target sites by making silent b.p. changes that render them recalcitrant to cutting. The w^{+mC} dominant marker carried by PBac{WH} is removed in both the NHEJ deletion and in the *emGFP* gene-replacement product.

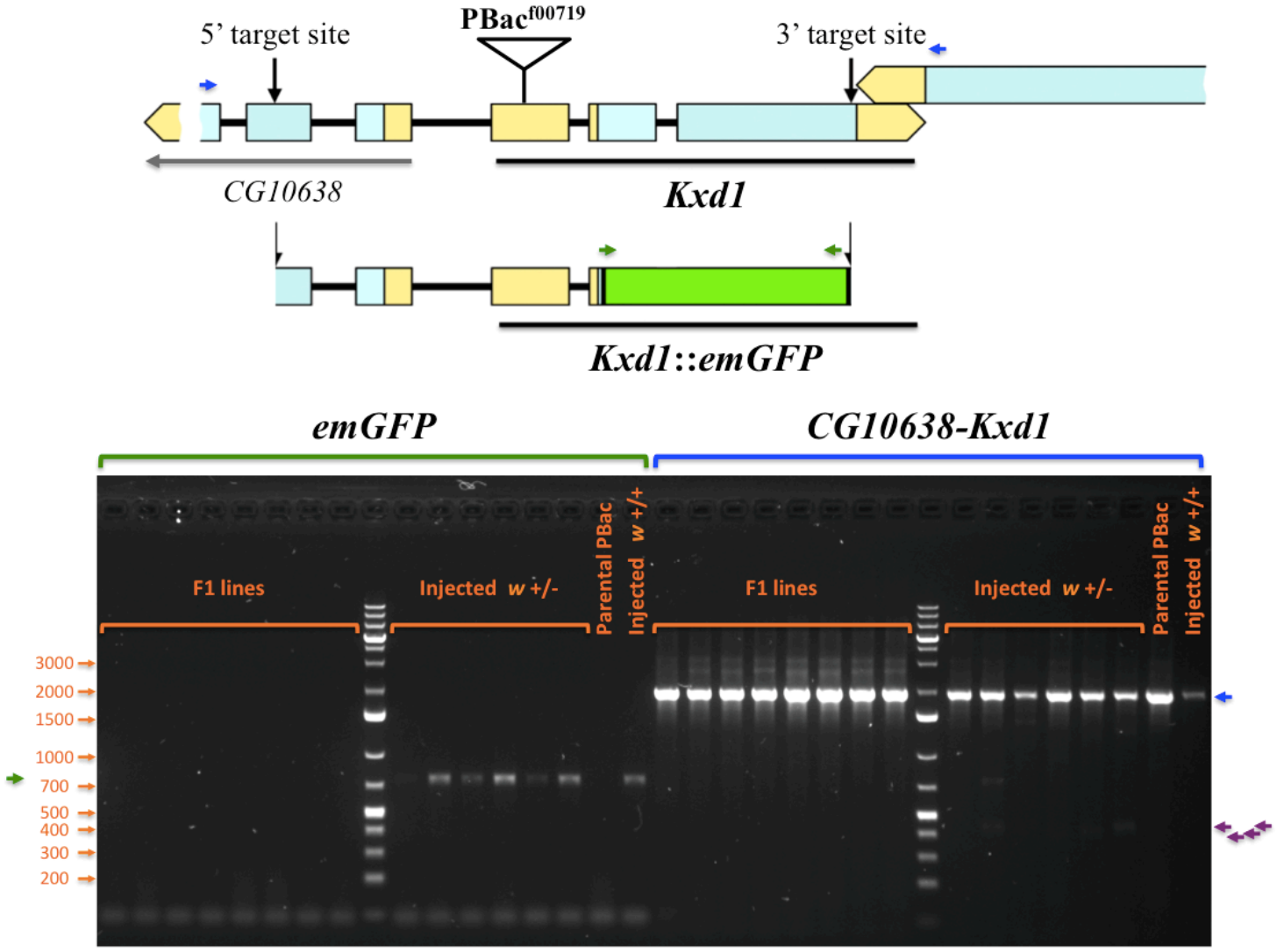

Figure 3.2 PCR screening of PBac^{f00719} *Kxd1*·CRISPR-deletion lines.

Figure 3.2. PCR Screening of PBac^{f00719} *Kxd1*·CRISPR-deletion lines. Representative PCR screening of PBac{WH}CG10861^{f00719} *Kxd1*·CRISPR-deletion flies. PBac{WH} carries the w^{+mC} dominant selectable marker. In the context of PBac{WH}-insertion in *Kxd1* (Harvard line f00719, chromosomal w^- background), w^{+mC} imparts a gene dosage-dependent phenotype. Homozygous PBac{WH}CG10861^{f00719} animals are visually distinguishable from single copy PBac{WH}CG10861^{f00719} animals based on eye color. Lines of w^- flies were established from CRISPR-injected founders that showed a heterozygous w^{+mC} phenotype. These lines (F1 lines) were screened by PCR, using primers that amplified a 711 b.p. emGFP band (green arrows, lower gene schematic) as well as with a set of primers that amplified either a 1926 b.p. wildtype *Kxd1* band, a 443 b.p. (or smaller) *Kxd1*-deletion band, or a 2059 b.p. *Kxd1*::*emGFP* gene-replacement band (blue arrows, upper gene schematic). None of the w^- F1 lines showed evidence of emGFP incorporation (gel, emGFP, F1 lines), and all of the w^- F1 lines amplified only the 1926 b.p. band indicative of wildtype *Kxd1* (gel, *CG10638-Kxd1*, F1 lines, and upper blue arrow, right hand side of gel). The same primer pairs were used to screen a selection of individual *Kxd1*·CRISPR-injected flies, including six that showed a heterozygous w^{+mC} eye color (Injected *w* +/-), and one that showed a homozygous w^{+mC} eye color (Injected *w* +/+). Uninjected parental PBac{WH}CG10861^{f00719} flies were included as a control (Parental PBac). All of the flies that were injected with CRISPR reagents as embryos amplified the emGFP PCR band as adults, but the uninjected parental PBac line did not (green arrow, left hand side of gel). Confoundingly, the $w^{+/-}$ injected founders, primarily amplified the wildtype *Kxd1* band (upper blue arrow, right hand side of gel). This band was also observed from the $w^{+/+}$ injected founder, from the uninjected Harvard f00719 flies, and from all of the w^- F1 lines. This PCR product should not have been generated from any of these flies since the PBac transposon is 7234 b.p. in size, and *Kxd1*·CRISPR-mediated gene deletion should have generated either a *Kxd1* deletion (NHEJ product) or an emGFP gene-replacement product but not a wildtype *Kxd1* locus. Four of the six injected $w^{+/-}$ founders also amplified non-stoichiometric bands of 443 b.p. or smaller, indicative of CRISPR-mediated *Kxd1* gene-deletion and NHEJ (four lower purple arrows, right hand side of gel). Neither the parental PBac line, the $w^{+/+}$ injected founder, nor the F1 lines amplified *Kxd1*-deletion/NHEJ bands.

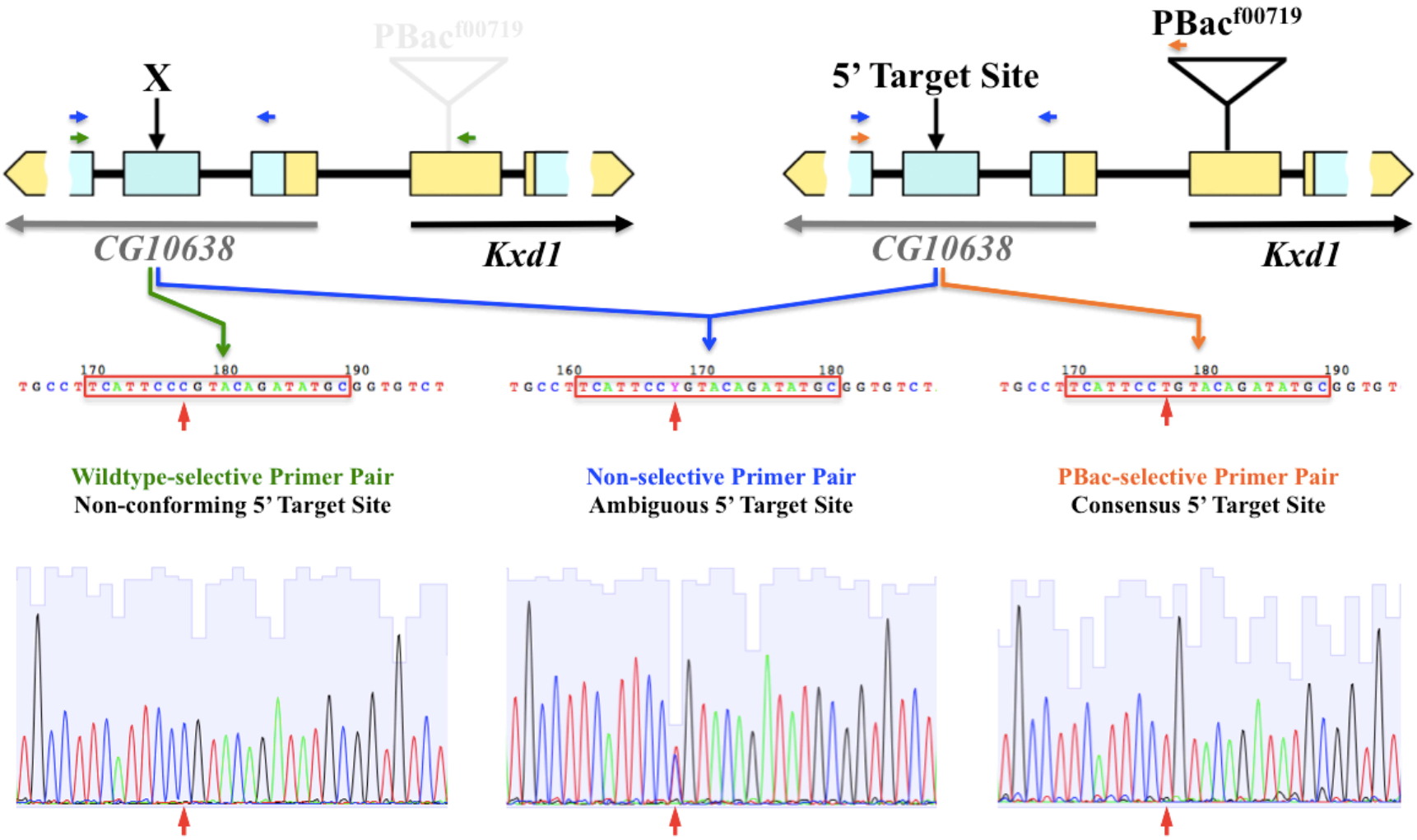

Figure 3.3. Sequencing of the *Kxd1* 5' CRISPR target sites.

Figure 3.3. Sequencing of *Kxd1* 5' CRISPR target sites. Gene schematics and representative sequencing electropherograms. Sequencing analysis revealed that two 5' *Kxd1*·CRISPR target sites exist in the Harvard f00719 line of flies that carry the PBac{WH}10681^{f00719} insertion in *Kxd1*. Both 20 b.p. 5' *Kxd1*·CRISPR target sites are located in exon 2 of the adjacent *CG10638* gene but exists in distinct genomic contexts and have sequence variations. Three different primer pairs were used to PCR amplify these loci for Sanger sequencing. All three primer pairs utilized the same 5' primer, CDS-179, but different 3' primers. The 3' primer CDS-170L anneals in exon 1 of *CG10638*, such that CDS-179/CDS-170L (blue arrows) gave rise to a 294 b.p. PCR product from both genomic templates. The sequencing data from this PCR product (Non-selective Primer Pair) showed C and T peaks of equal intensity at position 8 of the 5' CRISPR target site (lower red arrow). Automatic base-calling deemed this position a pyrimidine (Y – upper red arrow). CDS-183S anneals within the 5' terminal bases of PBac{WH}. The CDS-179/CDS-183S primer pair (orange arrows) amplified a 1610 b.p. PCR product. Only the 5' CRISPR target that was proximal to the PBac{WH} insertion in *Kxd1* served as a template for this PCR product due to the PBac annealing target of CDS-183S. The sequencing electropherogram (PBac-selective Primer Pair) showed a T in position 8 of the 5' CRISPR target site. This matched the FlyBase reference sequence and the 5' *Kxd1* chiRNA. The last 3' primer, CDS-185, anneals in exon 1 of *Kxd1,* downstream of the PBac{WH} insertion site. (The PBac insertion site in the annotated copy of *Kxd1* in is shown whited-out for spatial reference.) Primer pair CDS-179/CDS-185 (green arrows) amplified a 1038 b.p. PCR product. Only the 5' CRISPR target adjacent to the wildtype copy of *Kxd1* served as a template for this PCR product due to the intervening 7234 b.p. PBac{WH}10681^{f00719} insertion in the annotated copy of *Kxd1*. This PCR product was generated from the same templates that gave rise to the other PCR products, and sequencing of this product revealed a C in position 8 of the 5' CRISPR target (Wildtype-selective Primer Pair). This indicated that all of the lines examined (all Harvard f00719 flies or lines established from these flies) contained a second copy of *Kxd1* that did not harbor a PBac{WH} insertion and was proximal to a non-conforming 5' CRISPR target site (left hand gene schematic).

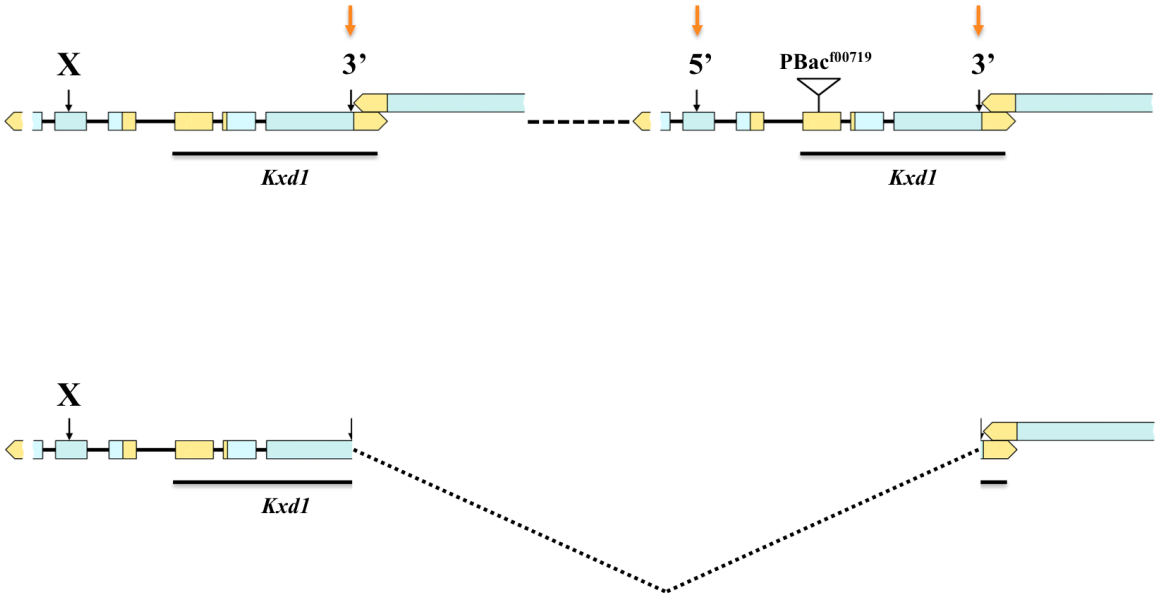

Figure 3.4. Deletion of w^{+mC} and reconstitution of *Kxd1* in CRISPR-targeted Harvard f00719 flies. PCR analysis and sequencing data revealed tandem duplication of *Kxd1* in Harvard f00719 flies. These flies were initially chosen as a genetic background for CRISPR-mediated deletion of *Kxd1* because the w^{+mC} construct carried by the PBac insertion in *Kxd1* served as a visible marker of *Kxd1* deletion or retention. A large number of Harvard f00719 flies displayed a heterozygous w^{+mC} phenotype after CRISPR injection and subsequently segregated the w^{+mC} and w^{-} phenotypes to their F1 progeny in a Medelian manner. The upper schematic shows a tandem duplication of the *Kxd1* locus consistent with the PCR and sequencing data: A wildtype copy of *Kxd1*, without a PBac insertion, is upstream and in the same orientation as the annotated copy of *Kxd1* with a PBac insertion. Injection of CRISPR reagents directs Cas9 endonucleolytic activity to the 5' and 3' CRISPR target sites flanking the PBac-*Kxd1* allele but only to the 3' target site proximal to the wildtype copy of *Kxd1* (orange arrows). The 5' site proximal to the wildtype *Kxd1* allele differs by one nucleotide from the 5' CRISPR chiRNA and therefore makes this site not a target (X). The resulting CRISPR cutting pattern is topologically equivalent to cutting at only the 3' target site proximal to a single copy of *Kxd1*; chromosomal repair reconstitutes *Kxd1* and eliminates the intervening PBac-*Kxd1* allele harboring the w^{+mC} marker (lower gene schematic).

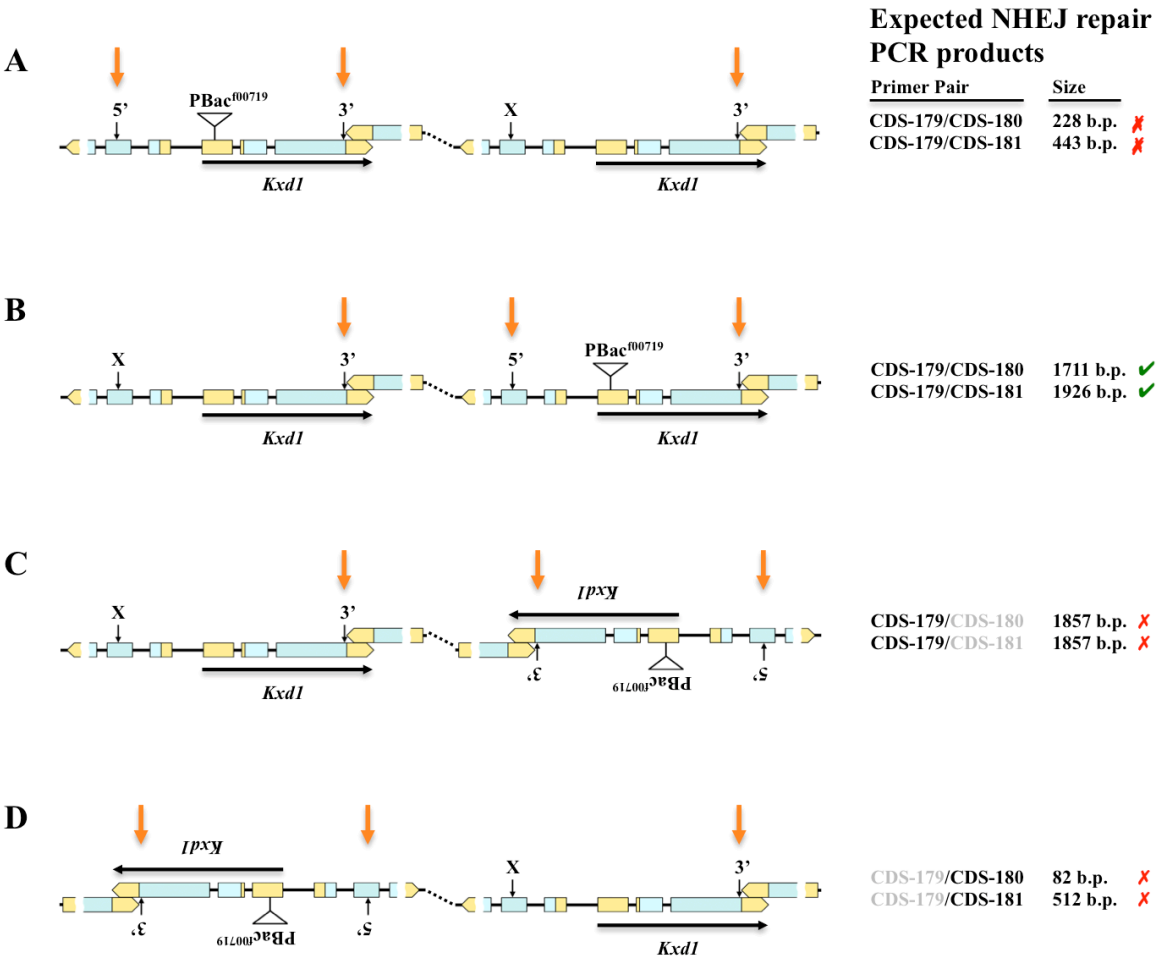

Figure 3.5. Possible *Kxd1* gene duplication arrangements. Four possible arrangements are shown for the *Kxd1* gene duplication in Harvard f00719 flies. Two alleles of *Kxd1* are present in these flies. The *Kxd1* allele with the annotated PBac insertion is flanked by 5' and 3' CRISPR target sites (orange arrows). The second *Kxd1* allele is wildtype, does not have a PBac insertion, and is proximal only to a 3' CRISPR target site (orange arrow). The 5' site next to this allele does not match the FlyBase reference sequence or the 5' CRISPR target sequence (black X). For each arrangement, the size of the PCR bands produced from the NHEJ repair product is shown (✔ indicates observed, ✘ indicates not observed). (**A**) Head-to-tail tandem duplication: PBac-*Kxd1* upstream of wildtype *Kxd1*. CRISPR targeting of this arrangement deletes both copies of *Kxd1*. CRISPR deletion of this duplication arrangement is equivalent to CRISPR deletion of a non-duplicated *Kxd1* gene. (**B**) Head-to-tail tandem duplication: wildtype *Kxd1* upstream of PBac-*Kxd1*. The NHEJ repair of this duplication arrangement produces a single restored copy of *Kxd1* without a PBac insertion (*c.f.* Figure 3.4 – lower gene schematic) The PCR products expected from NHEJ of this arrangement were those observed from Harvard f00719 flies treated

with *Kxd1*·CRISPR reagents. (**C**) Head-to-head inverted duplication. The NHEJ repair product of this arrangement is loss of the PBac-*Kxd1* allele and generation of a single *Kxd1* allele in which the 3' end of *Kxd1* is replaced with the reverse-compliment of the *CG10638* gene. Primer CDS-179 would serve as both a 5' and a 3' primer on this NHEJ product to generate a 1857 b.p. PCR band when using either primer pair CDS-179/CDS-180 or CDS-179/CDS-181. Primers CDS-180 and CDS-181 are whited-out next to this gene duplication arrangement since they would not be involved in generating the diagnostic PCR products anticipated from NHEJ repair of this gene arrangement. (**D**) Tail-to-tail inverted duplication. The NHEJ repair product from this arrangement is deletion of both copies of *Kxd1* and joining of the remaining *Kxd1* 3' UTRs as an inverted repeat. By serving as both 5' and 3' primer downstream of the 3' CRISPR cut site, either CDS-180 or CDS-181 would generate a short PCR product diagnostic of this arrangement. Primer CDS-179 is whited-out next to this gene duplication arrangement because it would not participate in PCR amplification of the NHEJ repair products of this gene arrangement.

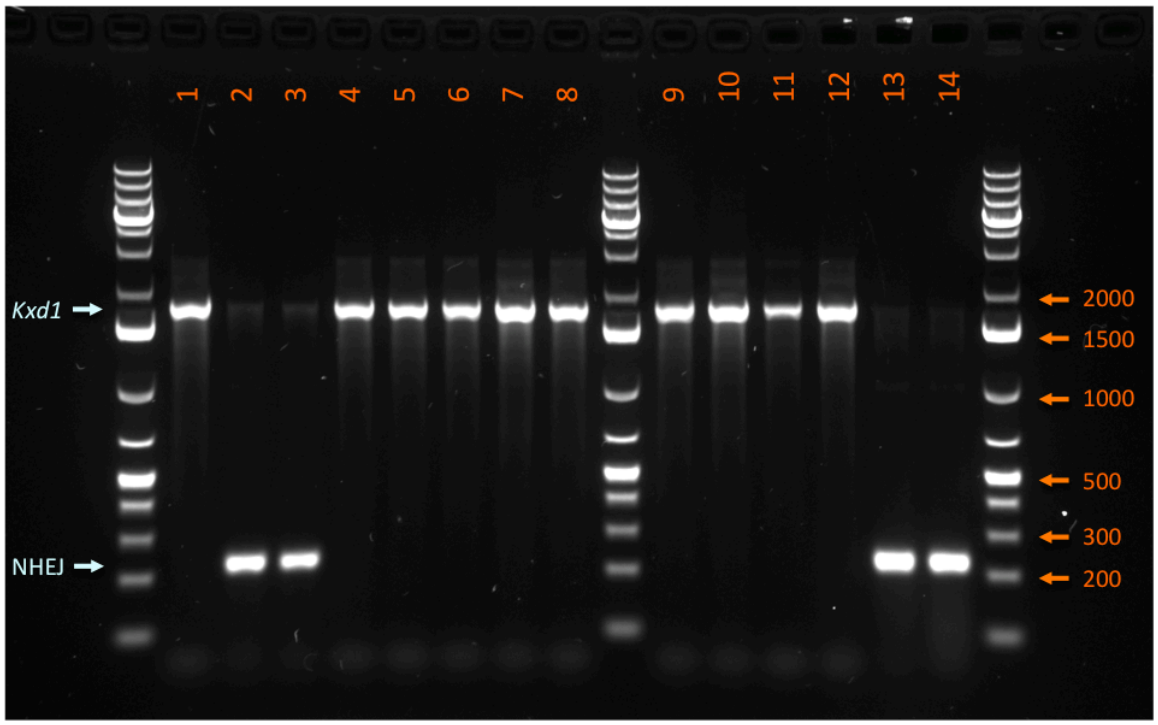

Figure 3.6. PCR screening of *Kxd1* CRISPR-deletion flies (wildtype Canton S background). Wildtype Canton S flies were injected with CRISPR reagents targeting *Kxd1* and crossed to TM3/TM6B balancer flies to generate F1 progeny. F1 animals from individual founders were pooled and screened by PCR. One of the F1 pools (pool 76i) screened positive for a NHEJ *Kxd1*-deletion allele. Individuals from this pool were backcrossed to TM3/TM6B balancer flies to establish sublines and segregate the *Kxd1* alleles in the population. A PCR screen was used to identify sublines that inherited the $Kxd1^{76i}$ deletion allele. Primers CDS-179/CDS-180 amplify a 1711 b.p. product from wildtype *Kxd1* and a 228 b.p. NHEJ product from a CRISPR-deleted *Kxd1* locus. Four of the 14 heterozygous sublines from this group carried the $Kxd1^{76i}$ deletion allele (lanes 2, 3, 13 and 14). DNA from these animals amplified a strong 228 b.p. NHEJ *Kxd1*-deletion PCR product and a less intense 1711 b.p. wildtype *Kxd1* band from the *Kxd1* gene on TM6B. The wildtype *Kxd1* PCR product is kinetically disfavored in these reactions because of its size in comparison to the much shorter NHEJ deletion band.

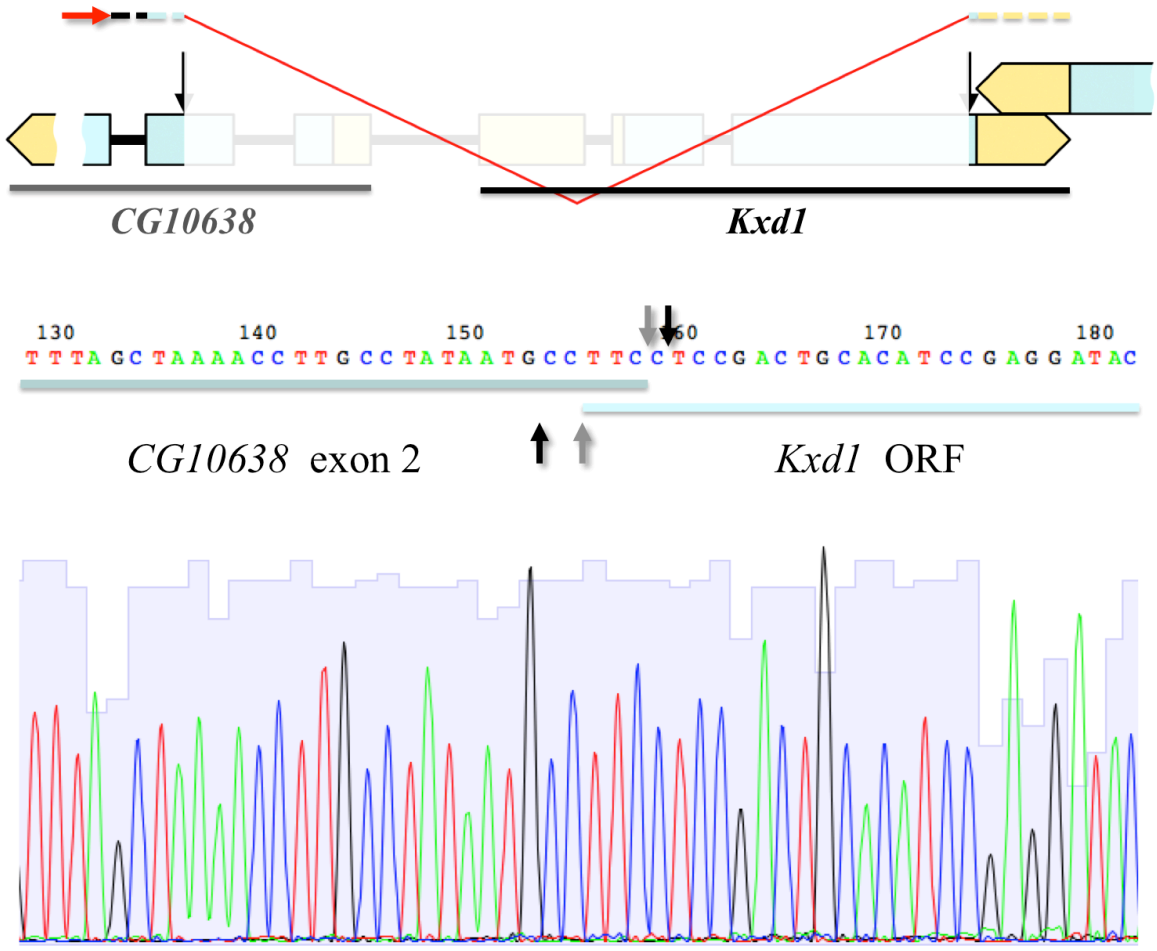

Figure 3.7. Sequencing electrophoregram of *Kxd1*^{76i} allele. A sequencing electrophoregram of the *Kxd1*^{76i} deletion allele is shown below a gene schematic of the *Kxd1* genomic region. Total DNA was purified from *Kxd1*^{76i} homozygous flies and sequenced with primer CDS-179 (red arrow). CDS-179 anneals in exon 2 of *CG10638* and extends a sequencing product in the direction of *Kxd1* transcription (discontinuous dashed line above gene schematic). Genomic regions missing from *Kxd1*^{76i} are shown whited-out on the gene schematic and include portions of *CG10638*, the *CG10638-Kxd1* intergenic region, and most of the *Kxd1* gene – only the last 33 nt of the *Kxd1* ORF and the 3' UTR are intact. Automated base calls are shown above the electrophoregram peaks. *CG10638* bases are underlined in blue-gray. *Kxd1* bases are underlined in baby-blue. The 5' and 3' DNA ends were joined by a three base stretch of microhomology (TTC) common to both DNA ends. Black arrows indicate the location of the CRISPR cut sites. Gray arrows indicate the extent of DNA-end resection (resected bases not shown).

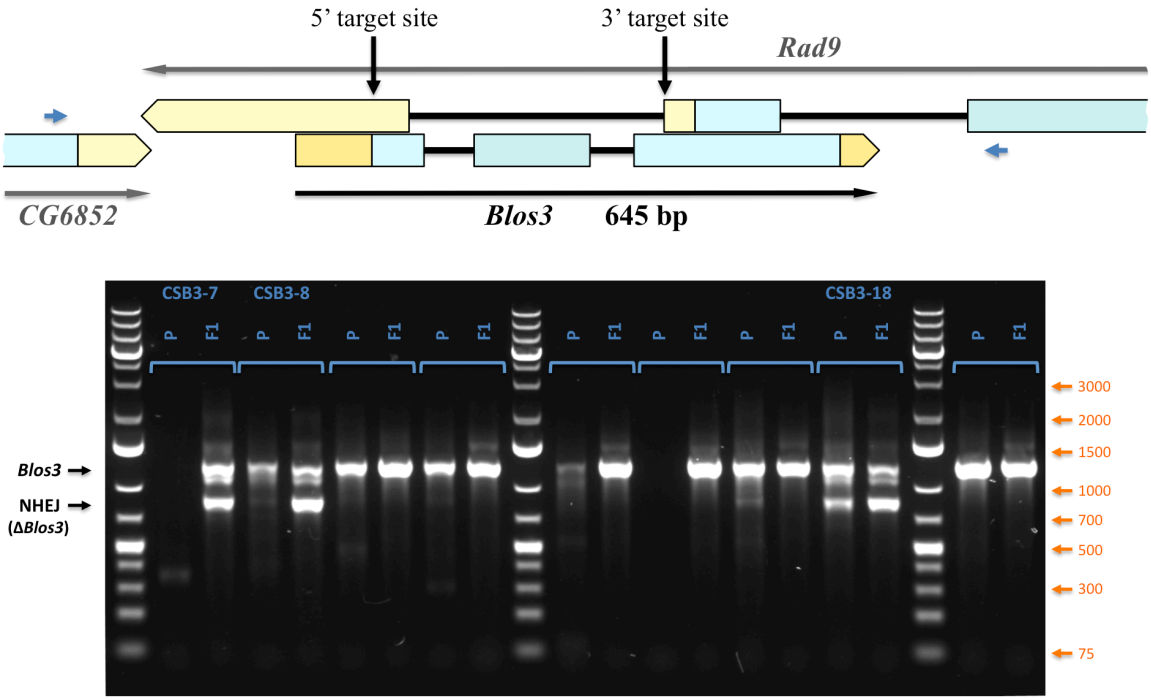

Figure 3.8. PCR screening of *Blos3* CRISPR-deletion flies. Gene schematic showing the *Blos3* genomic region. Exons are boxed: yellow regions are UTRs, blue regions are ORFs. Intergenic sequences are solid lines. Gene spans are shown by arrows that indicate the direction of gene transcription: the span of *Blos3* is black, the partial spans of *Rad9* and *CG6852* are gray. *Blos3* is located on the positive strand of the third chromosome at cytological position 75E2 and is entirely overlapped by *Rad9* from the opposite direction. *Blos3* was targeted in wildtype Canton S flies by designing CRISPR chiRNAs that remove sequences encoding the N-terminal half of Blos3 (amino acids 1-76 out of 144). The deleted sequences fall largely within *Rad9* intron 5 such that *Rad9* intron 5 is deleted and *Rad9* exon 5 and exon 6 are transcriptionally joined. Flies that were injected with *Blos3*·CRISPR reagents were individually crossed to a TM3/TM6B balancer stock to generate F1 progeny and screened by PCR along with a pooled sample of their F1 offspring (gel – P, injected parental fly; F1, F1 progeny). The annealing location of the PCR screening primers is indicated (blue arrows). These primers generated a 1125 b.p. wildtype *Blos3* PCR product and a 784 b.p. *Blos3*-deletion band. Canton S·*Blos3* groups 7, 8 and 18 (CSB3-7, CSB3-8 and CSB3-18) all amplified a robust *Blos3*-deletion band. F1 individuals from these groups were individually crossed to balancer flies and screened to identify sub-lines of each *Blos3*-deletion allele: $Blos3^{7}$, $Blos3^{8}$ and $Blos3^{18}$.

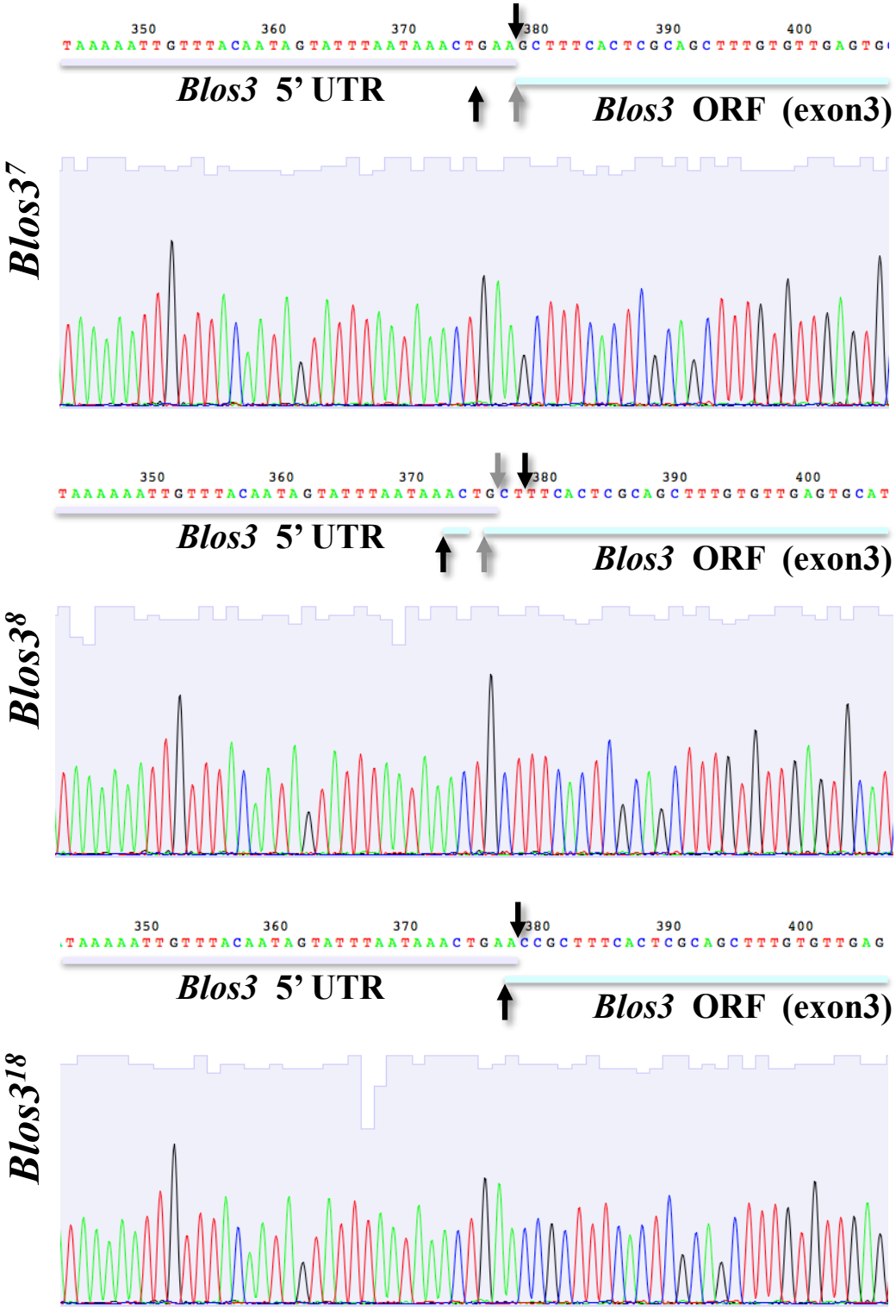

Figure 3.9. *Blos3* CRISPR-deletion electropherograms.

Figure 3.9. *Blos3* CRISPR-deletion electropherograms. DNA was purified from *Blos3*^{7}, *Blos3*^{8} and *Blos3*^{18} homozygous flies and sequenced with primer CDS-199. CDS-199 anneals in exon 1 of *CG6852* and extends a sequencing product in the direction of *Blos3* transcription. The portions of the respective electropherograms that show the junctional repair between the 5' and 3' CRISPR cut sites are shown for each sequencing reaction. Automatic base-calls are shown above the color-coded peaks of each electropherogram. Bases corresponding to *Blos3* 5' UTR sequences are underlined in purple. Bases corresponding to *Blos3* ORF sequences from exon 3 are underlined in baby-blue. Black arrows show the locations of the initial CRISPR cut sites. The locations of the final DNA end resections are shown with gray arrows. (Bases that were removed by DNA end resection are not shown.) *Blos3*^{7} connects the *Blos3* 5' UTR to the *Blos3* 3' ORF bases, apparently without microhomology end annealing, after the removal of three bases from the 3' DNA cut site. The *Blos3*^{8} DNA junction shows evidence of either single-base microhomology or a stretch of four base imperfect microhomology (AC–G) that has been corrected to match the homologous bases of the *Blos3* 5' UTR (ACTG). The DNA end junction in *Blos3*^{18} was presumably made by end annealing involving single-base microhomology (A). Each of the *Blos3* deletion alleles shows different extents of DNA end resection before end-joining was accomplished. *Blos3*^{7} exhibits resection of three bases from the 3' DNA cut site and joining to the unresected 5' DNA end. *Blos3*^{8} shows resection of two bases from the 5' DNA cut site and possibly resection of three bases from the 3' DNA cut site – although the 3' DNA cut site may have been joined without resection to the resected 5' DNA cut site and have then undergone a process of "gene conversion" to modify the terminal nucleotides to match those of the resected 5' DNA cut site. *Blos3*^{18} displays evidence of precise DNA end joining without resection of DNA from either CRISPR cut site; although one base pair is lost from the full complement of bases, presumably due to microhomology end annealing during end-joining.

REFERENCES

1 Jinek M, Chylinski K, Fonfara I, Hauer M, Doudna JA, Charpentier E. A programmable dual-RNA-guided DNA endonuclease in adaptive bacterial immunity. Science. 2012 Aug 17;337(6096):816-21.

2 Chang N, Sun C, Gao L, Zhu D, Xu X, Zhu X, Xiong JW, Xi JJ. Genome editing with RNA-guided Cas9 nuclease in zebrafish embryos. Cell Res. 2013 Apr;23(4):465-72.

3 Hwang WY, Fu Y, Reyon D, Maeder ML, Tsai SQ, Sander JD, Peterson RT, Yeh JR, Joung JK. Efficient genome editing in zebrafish using a CRISPR-Cas system. Nat Biotechnol. 2013 Mar;31(3):227-9.

4 Shen B, Zhang J, Wu H, Wang J, Ma K, Li Z, Zhang X, Zhang P, Huang X. Generation of gene-modified mice via Cas9/RNA-mediated gene targeting. Cell Res. 2013 May;23(5):720-3.

5 Gratz SJ, Cummings AM, Nguyen JN, Hamm DC, Donohue LK, Harrison MM, Wildonger J, O'Connor-Giles KM. Genome engineering of Drosophila with the CRISPR RNA-guided Cas9 nuclease. Genetics. 2013 Aug;194(4):1029-35.

6 Yang Q, He X, Yang L, Zhou Z, Cullinane AR, Wei A, Zhang Z, Hao Z, Zhang A, He M, Feng Y, Gao X, Gahl WA, Huizing M, Li W. The BLOS1-interacting protein KXD1 is involved in the biogenesis of lysosome-related organelles. Traffic. 2012 Aug;13(8):1160-9.

7 Hayes MJ, Bryon K, Satkurunathan J, Levine TP. Yeast homologues of three BLOC-1 subunits highlight KxDL proteins as conserved interactors of BLOC-1. Traffic. 2011 Mar;12(3):260-8.

8 John Peter AT, Lachmann J, Rana M, Bunge M, Cabrera M, Ungermann C. The BLOC-1 complex promotes endosomal maturation by recruiting the Rab5 GTPase-activating protein Msb3. J Cell Biol. 2013 Apr 1;201(1):97-111.

9 Starcevic M, Dell'Angelica EC. Identification of snapin and three novel proteins (BLOS1, BLOS2, and BLOS3/reduced pigmentation) as subunits of biogenesis of lysosome-related organelles complex-1 (BLOC-1). J Biol Chem. 2004 Jul 2;279(27):28393-401.

10 Gwynn B, Martina JA, Bonifacino JS, Sviderskaya EV, Lamoreux ML, Bennett DC, Moriyama K, Huizing M, Helip-Wooley A, Gahl WA, Webb LS, Lambert AJ, Peters LL. Reduced pigmentation (rp), a mouse model of Hermansky-Pudlak syndrome, encodes a novel component of the BLOC-1 complex. Blood. 2004 Nov 15;104(10):3181-9.

11 Thibault ST, Singer MA, Miyazaki WY, Milash B, Dompe NA, Singh CM, Buchholz R, Demsky M, Fawcett R, Francis-Lang HL, Ryner L, Cheung LM, Chong A, Erickson C, Fisher WW, Greer K, Hartouni SR, Howie E, Jakkula L, Joo D, Killpack K, Laufer A, Mazzotta J, Smith RD, Stevens LM, Stuber C, Tan LR, Ventura R, Woo A, Zakrajsek I, Zhao L, Chen F, Swimmer C, Kopczynski C, Duyk G, Winberg ML, Margolis J. A complementary transposon tool kit for Drosophila melanogaster using P and piggyBac. Nat Genet. 2004 Mar;36(3):283-7.

12 CRISPR Optimal Target Finder. http://tools.flycrispr.molbio.wisc.edu/targetFinder/

13 Gratz SJ, Ukken FP, Rubinstein CD, Thiede G, Donohue LK, Cummings AM, O'Connor-Giles KM. Highly specific and efficient CRISPR/Cas9-catalyzed homology-directed repair in Drosophila. Genetics. 2014 Apr;196(4):961-71.

14 Bellen HJ, Levis RW, He Y, Carlson JW, Evans-Holm M, Bae E, Kim J, Metaxakis A, Savakis C, Schulze KL, Hoskins RA, Spradling AC. The Drosophila gene disruption project: progress using transposons with distinctive site specificities. Genetics. 2011 Jul;188(3):731-43.

15 Elick TA, Bauser CA, Fraser MJ. Excision of the piggyBac transposable element in vitro is a precise event that is enhanced by the expression of its encoded transposase. Genetica. 1996 Jul;98(1):33-41.

16 Fraser MJ, Ciszczon T, Elick T, Bauser C. Precise excision of TTAA-specific lepidopteran transposons piggyBac (IFP2) and tagalong (TFP3) from the baculovirus genome in cell lines from two species of Lepidoptera. Insect Mol Biol. 1996 May;5(2):141-51.

17 Witsell A, Kane DP, Rubin S, McVey M. Removal of the bloom syndrome DNA helicase extends the utility of imprecise transposon excision for making null mutations in Drosophila. Genetics. 2009 Nov;183(3):1187-93. doi: 10.1534/genetics.109.108472. Epub 2009 Aug 17.

18 Beumer KJ, Trautman JK, Mukherjee K, Carroll D. Donor DNA Utilization during Gene Targeting with Zinc-finger Nucleases. G3 (Bethesda). 2013 Mar 22. pii: g3.112.005439v2.

19 IDT Ultramer® Oligonucleotides. https://www.idtdna.com/pages/products/dna-rna/ultramer-oligos

20 Turan S, Bode J. Site-specific recombinases: from tag-and-target- to tag-and-exchange-based genomic modifications. FASEB J. 2011 Dec;25(12):4088-107.

21 Bischof J, Basler K. Recombinases and their use in gene activation, gene inactivation, and transgenesis. Methods Mol Biol. 2008;420:175-95.

22 Anderson EM, Haupt A, Schiel JA, Chou E, Machado HB, Strezoska Ž, Lenger S, McClelland S, Birmingham A, Vermeulen A, Smith AV. Systematic analysis of CRISPR-Cas9 mismatch tolerance reveals low levels of off-target activity. J Biotechnol. 2015 Jul 17;211:56-65.

23 Fu Y, Foden JA, Khayter C, Maeder ML, Reyon D, Joung JK, Sander JD. High-frequency off-target mutagenesis induced by CRISPR-Cas nucleases in human cells. Nat Biotechnol. 2013 Sep;31(9):822-6.

24 Cong L, Ran FA, Cox D, Lin S, Barretto R, Habib N, Hsu PD, Wu X, Jiang W, Marraffini LA, Zhang F. Multiplex genome engineering using CRISPR/Cas systems. Science. 2013 Feb 15;339(6121):819-23.

25 Gratz SJ, Rubinstein CD, Harrison MM, Wildonger J, O'Connor-Giles KM. CRISPR-Cas9 Genome Editing in Drosophila. Curr Protoc Mol Biol. 2015 Jul 1;111:31.2.1-31.2.20.

26 Dietzl G, Chen D, Schnorrer F, Su KC, Barinova Y, Fellner M, Gasser B, Kinsey K, Oppel S, Scheiblauer S, Couto A, Marra V, Keleman K, Dickson BJ. A genome-wide transgenic RNAi library for conditional gene inactivation in Drosophila. Nature. 2007 Jul 12;448(7150):151-6.

27 Mummery-Widmer JL, Yamazaki M, Stoeger T, Novatchkova M, Bhalerao S, Chen D, Dietzl G, Dickson BJ, Knoblich JA. Genome-wide analysis of Notch signalling in Drosophila by transgenic RNAi. Nature. 2009 Apr 23;458(7241):987-92.

28 Vanrobays E, Jennings BH, Ish-Horowicz D. Identification and mapping of induced chromosomal deletions using sequence polymorphisms. Biotechniques. 2010 Jan;48(1):53-60.

29 Mount SM, Burks C, Hertz G, Stormo GD, White O, Fields C. Splicing signals in Drosophila: intron size, information content, and consensus sequences. Nucleic Acids Res. 1992 Aug 25;20(16):4255-62.

30 Cheli VT, Daniels RW, Godoy R, Hoyle DJ, Kandachar V, Starcevic M, Martinez-Agosto JA, Poole S, DiAntonio A, Lloyd VK, Chang HC, Krantz DE, Dell'Angelica EC. Genetic modifiers of abnormal organelle biogenesis in a Drosophila model of BLOC-1 deficiency. Hum Mol Genet. 2010 Mar 1;19(5):861-78.

31 Zhang Q, Li W, Novak EK, Karim A, Mishra VS, Kingsmore SF, Roe BA, Suzuki T, Swank RT. The gene for the muted (mu) mouse, a model for Hermansky-Pudlak syndrome, defines a novel protein which regulates vesicle trafficking. Hum Mol Genet. 2002 Mar 15;11(6):697-706

32 Ciciotte SL, Gwynn B, Moriyama K, Huizing M, Gahl WA, Bonifacino JS, Peters LL. Cappuccino, a mouse model of Hermansky-Pudlak syndrome, encodes a novel protein that is part of the pallidin-muted complex (BLOC-1). Blood. 2003 Jun 1;101(11):4402-7.

CHAPTER 4

Phenotypic characterization of *Vab2*, *Kxd1* and *Blos3* gene deletion mutants

ABSTRACT

The loss of *blos1* in *Drosophila* was previously shown to elicit phenotypes analogous to the loss of BLOC-1 subunit genes in mice and humans, namely phenotypes related to the defective biogenesis of lysosome related organelles (LROs) such as the *Drosophila* eye pigment granules. Loss of *blos1* or of genes encoding subunits of other protein complexes involved in LRO biogenesis (e.g. *pink,* a BLOC-2 subunit gene) causes eye color defects. *Vab2* and *Kxd1* are not canonical genes of metazoan BLOC-1, but in yeast the homologs of these genes encode protein subunits of yeast BLOC-1. *Saccharomyces cerevisiae* has a lysosome-like organelle, the yeast vacuole, but does not have LROs *per se*. Thus yeast phenotypes from the loss of yeast BLOC-1 genes cannot be directly paralleled to BLOC-1 phenotypes in mammals and flies. To determine if loss of *Vab2* or *Kxd1* elicited BLOC-1-like phenotypes in *Drosophila*, I tested the eye color phenotypes of these mutations independently and in combination with mutations of *blos1* or *pink*. I also tested the effects of loss of *Blos3* in *Drosophila*. BLOS3 is a BLOC-1 subunit that, in mice, elicits milder BLOC-1-like phenotypes than those caused by mutation of other BLOC-1 subunit genes. I found that mutation or loss of *Vab2* did not have discernable eye color phenotypes nor did it modify the effects of BLOC-1 or BLOC-2 gene deletions. On the other hand, loss of *Kxd1* caused an increased accumulation of red and brown eye pigments, and deletion of *Blos3* showed eye pigment deficits about half as severe as those observed from deletion of *blos1*. These findings suggest that *Vab2* does not influence BLOC-1 function in metazoans, whereas *Kxd1* may negatively regulate LRO accumulation. Finally, these data argue that, as part of BLOC-1, Blos3 may have a distinct role in regulating or guiding BLOC-1 function rather than a primary mechanistic or structural role, as other BLOC-1 subunits appear to have.

INTRODUCTION

Yeast BLOC-1 is a hexameric protein complex composed of three proteins related to constituents of metazoan BLOC-1: Bls1p (a BLOS1 homolog), Snn1p (a Snapin homolog) and Cnlp (a DUF2365 homolog that has Cappuccino-like structural features) – and three additional proteins that are not homologs of metazoan BLOC-1 proteins: Vab2p (an LOH12CR1 homolog), Kxd1p (a KXD1 homolog) and Bli1p (with no metazoan homolog yet identified) [1 and this work]. *Saccharomyces cerevisiae* do not have lysosome related organelles (LROs), but they do have a lysosome-like organelle, the yeast vacuole [2], and, although the phenotypes for deletion of the yeast BLOC-1 proteins have been elegantly tested and demonstrated [3], these phenotypes did not closely parallel metazoan BLOC-1 phenotypes to indicate if the metazoan homologs of the yeast-specific BLOC-1 subunits (Vab2 and Kxd1) had any role in the function of canonical BLOC-1 as characterized in mammals and insects.

Specifically, deletion of any of the six BLOC-1 subunits in yeast affects endocytic flux along the endolysosomal pathway [3]. Yeast that are mutant for BLOC-1 show a decreased sensitivity to the toxic amino acid analogs, canavanine and thialysine. These drug-resistant phenotypes correlate with a lack of plasma membrane (PM) residence of the amino acid permeases, Can1 and Lyp1, respectively. Instead of normally being endocytosed and recycled to the PM, the authors of this study observed that the Can1 and Lyp1 transporters were sorted to the yeast vacuole in BLOC-1 mutants. The authors presented further evidence that this regulation of the endolysosomal pathway by yeast BLOC-1 involved the BLOC-1-mediated recruitment of Msb3, a Vps21 GAP (GTP-ase activating protein), to the endosomes, where it negatively regulates cargo flow to the vacuole by deactivating GTP-bound Vps21, a yeast Rab5 homolog. Thus, loss of yeast BLOC-1 or Msb3 results in the persistence of activated Vps21 and a resultant increased flow to the vacuole. Accordingly, deletion of Msb3 and BLOC-1 are epistatic to each other, but over-expression of Msb3 bypasses the requirement for BLOC-1 as an Msb3 receptor at

the endosomal membrane. At the same time that yeast BLOC-1 regulates flow from the endosome to the vacuole, deletion of yeast BLOC-1 genes does not affect trafficking of GNS (GFP-Snc1-Nyv1 fusion), an artificial AP-3 reporter construct [3].

In contrast, rather than functioning as yeast BLOC-1 does to primarily retard flow along the endolysosomal pathway, metazoan BLOC-1 is involved in directing the maturation of lysosome and LROs. Thus, BLOC-1 deficient mouse or human cells mislocalize the lysosomal markers and AP-3 cargo proteins, LAMP1 and LAMP3, to the plasma membrane [4, 5], and the mutation of BLOC-1 subunits in rodent melanocytes similarly results in mislocalization of Tryp1 to the plasma membrane [6]. On an organellar scale, mutation of BLOC-1 in metazoans results in compromised biogenesis of LROs such as platelet dense granules or melanosomes [7] – definitive defects of Hermansky-Pudlak syndrome (HPS), which is characterized by oculocutaneous albinism and prolonged bleeding [8]. In *Drosophila*, this is paralleled in BLOC-1 mutants by defects in eye pigmentation caused by decreased numbers and density of pigment granules in the sheath cells of the compound eye [9], the class of LRO in which drosopterins and ommochromes are stored and synthesized [10, 11].

Among the spontaneous mouse models of HPS that were found to represent mutations in BLOC-1 subunits, namely sandy, pallid, muted, cappuccino and reduced pigmentation (*rp*), *rp* was the last to be identified and cloned [12, 13]. *rp* mice have an atypical BLOC-1 phenotype that is characterized by mild coat color hypopigmentation and prolonged bleeding [14,15]. On a genetic level, *rp* mice harbor a mutation in the gene encoding BLOS3 [12, 13]. BLOS3 is unique among the BLOC-1 subunits in that it is the only one of the metazoan BLOC-1 proteins that does not contain predicted coiled-coil domains [12, 13]. This raises the intriguing possibility that loss of BLOS3 has a unique function among the BLOC-1 subunits that gives rise to the attenuated phenotypes observed of *rp* mice.

Using the *Drosophila* deletion lines of *Vab2*, *Kxd1* and *Blos3* that I described creating in previous chapters, the experiments that I describe in this chapter aim to address if loss of *Vab2* or

Kxd1 produces BLOC-1-like phenotypes and if the phenotypes of *Blos3* deletion in *Drosophila* indicate that the mouse *rp* phenotypes result from intrinsic characteristics of BLOS3, or if they reflect species-specific effects or artifacts of the specific genetic lesion harbored by *rp* mice.

MATERIAL AND METHODS

Fly Stocks

Flies were maintained and bred in a dedicated room maintained at 20-24°C on media prepared by the UCLA Drosophila Media Facility. The generation of *Vab2*, *Kxd1* and *Blos3* deletion lines was described in previous chapters of this dissertation. $blos1^{ex65}$ flies were described previously [9]. Canton S wildtype, w^- (w^{1118}) and BLOC-2 (p^p) flies were obtained from the Bloomington Stock Center.

Eye Pigment Quantification

Red and brown eye pigments (drosopterins and ommochromes, respectively) were quantified as previously described [16] with the following considerations: Males were collected within 24 hours of eclosure, transferred to another vial and aged for precisely 48 hours, and then frozen at -80°C in 1.5 ml centrifuge tubes until processed. Flies were frozen in groups of 4 per tube in order to facilitate subsequent sample preparation. Heads were isolated by vortexing the frozen flies and then transferring the liberated heads to a fresh, pre-chilled tube. Isolated heads were crushed at room temperature in the appropriate solution (*c.f.* below) using a Kimble Chase® micropestle.

Red pigments were extracted from the heads of four flies per sample, by crushing the heads in 250 µl of 30% (v/v) ethanol acidified to pH 2 with HCl. Crushed heads were tumbled for 20 hours at room temperature in a light-protected enclosure. The extracts were then cleared by centrifugation for 1 minute at 13,000 X *g*. The clarified extracts were transferred to a new tube and quantified by determining their absorbance at 480 nm.

Brown pigments were extracted from the heads of 8 flies per sample, by crushing the heads in 150 µl of 2N HCl, followed by adding 10 µl of 100 g/L sodium metabisulphite and 200 µl butanol and tumbling for 30 minutes at room temperature in a light-protected enclosure. Organic and aqueous phases were then separated by centrifugation at 4000 X *g* for 5 minutes, and the organic phase (upper) was transferred to a new tube, to which 150 µl of 0.66% (w/v) sodium metabisulphite was added. Samples were tumbled for an additional 30 minutes followed by centrifugation for 5 minutes at 4000 X *g*. The upper organic phase was collected and quantified by determining absorbance at 490 nm.

For both red and brown pigment extractions, the absorbance measurements were normalized to average values obtained from samples of wildtype Canton S flies. Average background absorbance values were determined from extractions of w^- (w^{1118}) flies and subtracted from all readings before value normalization.

Weight determination

Fly weights were determined by weighing 2-3 day old adult male flies in groups of 4 in 1.5 ml centrifuge tubes that had been pre-weighed. Handling of tubes was done with gloves or forceps. Flies were weighed alive immediately after collection. Tubes were weighed at least twice when pre-weighed and twice after flies were added.

Fly crosses for Vab2 double mutant lines

To generate F1 generation flies that were heterozygous for *Vab2* and either *blos1* or *pink*, all of the parental line crosses were initiated with *Vab2* virgin females ($Vab2^{114}$ or $Vab2^{115}$) and

blos1^{ex65} or *p*^{p} males, because *Vab2* is on the X chromosome. This was necessary to insure that all of the resulting F1 males were *Vab2* hemizygotes.

Because of the lack of a visibly scorable *Vab2* phenotype, putative F2 generation double mutants were bred in pairs and individually PCR screened after successfully mating to determine the *Vab2* status of each F2 parent. A similar PCR screen was performed to confirm the *blos1*^{ex65} status of each F2 parent. Double mutant flies were maintained as lines after being generated.

RESULTS

Deletion of Vab2 does not affect gross fly phenotypes such as weight

To determine if deletion or mutation of *Vab2* had gross phenotypic effects on *Drosophila,* I examined the 'Cantonized' $Vab2^{114}$ and $Vab2^{115}$ mutant flies for visually obvious phenotypes. No morphological differences or visually discernable pigmentation phenotypes distinguished these animals from wildtype Canton S flies. I also compared the weights of these flies to both wildtype Canton S and w^- flies.

To accurately compare the weights of animals, I collected male flies of each genotype within 24 hours of eclosure and aged them in separate vials for an additional 2 days. This generated populations of 2-3 day old males that were used for further characterization. These flies were weighed in groups of four, and the average weight per individual fly was calculated accordingly. When the distribution and average weights were compared between genotypes, no significant difference was observed between $Vab2^{114}$, $Vab2^{115}$, *blos1*, w^- and Canton S flies (Fig. 4.1).

Although these observations did not elucidate the function of *Vab2*, the fact that there were no gross phenotypic differences between *Vab2*, *blos1*, w^- and Canton S flies indicated that further characterization, such as differences in eye pigment accumulation between the genetic backgrounds, could be reasonably compared between these flies without correcting for differences in size or weight between groups of 2-3 day-old males.

Visible eye phenotypes of Vab2 mutants

The eye pigments of *Drosophila* are biosynthetically and chemically unrelated to mammalian melanins that are synthesized in melanosomes, but, like melanins, the synthesis and

storage of *Drosophila* eye pigments occurs in a class of LRO, *i.e.* pigment granules [11]. In *Drosophila*, mutation of the genes that encode subunits of AP-3, BLOC-1, BLOC-2 or BLOC-3 all affect maturation of these LROs [17, 18, 16, 19, 20]. In particular, loss of *blos1* causes an accumulation of only 30-40% wildtype levels of red and brown eye pigments (drosopterins and ommochromes, respectively) [9]. Despite these reduced levels of eye pigments, the eyes of *Drosophila blos1* mutants are still visibly red; however, they do not appear as "brilliant" as the eyes of wildtype Canton S flies and they lack a pseudopupil. In contrast, the eyes of both $Vab2^{114}$ and $Vab2^{115}$ mutants appeared indistinguishable from the eyes of wildtype Canton S flies: *Vab2* fly eyes were brilliant red and they generated a pseudopupil effect just as effectively as the eyes of Canton S flies.

Red eye pigments of Vab2 mutants

The visible eye color phenotype of *blos1* mutant flies is apparent to the trained observer, but this lack of brilliance and of the pseudopupil effect is the result of a 60-70% reduction in the quantities of eye pigments of wildtype flies. This means that less severe reduction in pigment accumulation may not be visibly discernable, and this could have possibly been the case for flies with a loss or reduction of *Vab2* expression. To determine if either of the *Vab2* mutant alleles carried by the $^{3}114$ and $^{3}115$ lines caused a reduction of drosopterins, I extracted red pigments from isolated heads of $Vab2^{114}$ and $Vab2^{115}$ flies and compared the photometric absorbance of the extracted fractions at 480 nm (A_{480}) to similar extractions performed on Canton S flies. To control for size, sex and developmental considerations, each sample was prepared from the heads of four, 2-3 day-old, males flies. Background absorbance at 480 nm from compounds other than drosopterins was determined by preparing samples from w^{-} flies that accumulate no red eye pigments. These background readings were subtracted from each sample prior to comparing values. *blos1* flies were included as a positive control of reduced drosopterins.

In agreement with a lack of visible eye color defects, the Cantonized $Vab2^{115}$ lines showed no significant change in the accumulation of drosopterins relative to Canton S (Fig 4.2 A). The $Vab2^{114}$ lines, however, showed a modest but statistically significant increase in red eye pigments of about 5%. When these data were re-analyzed by *Vab2* sublines ($Vab2^{114•FC14}$, $Vab2^{114•FC17}$, $Vab2^{115•FC33.2}$ and $Vab2^{115•FC36.2}$) only the $Vab2^{114•FC14}$ showed a statistical difference in the quantities of drosopterins versus those of Canton S flies (Fig 4.2 B). This indicated that mutation of *Vab2* did not affect drosopterins pigment granule biogenesis in the manner that loss of *blos1* does, and it argued that the statistically significant increase in red eye pigments in $Vab2^{114•FC14}$ flies was not due to the $Vab2^{114}$ deletion allele but due to some other event that occurred during partial Cantonization of that subline.

Brown eye pigments of Vab2 mutants

The brown eye pigments of *Drosophila* (ommochromes) are synthesized by a distinct group of enzymes from those responsible for the synthesis of the red eye pigments [10], and it has been proposed that, although the accumulation of both of these pigments are affected by mutations in genes of the 'granule group', they are stored in distinct LROs and each type of LRO is differentially dependent on the assortment of complexes formed by the granule group proteins [20]. Thus, although *Vab2* mutants showed no obvious eye color deficit either by visual examination or by quantification of red eye pigments, I sought to determine if *Vab2* affected ommochrome accumulation by measuring brown pigments in *Vab2* mutants versus wildtype Canton S flies.

The extraction protocol for brown pigments is different from that used to extract red eye pigments, but a similar sample collection protocol was used to control for size, sex and developmental considerations. Ommochromes were extracted from the heads of 2-3 day-old males and quantified by spectrophotometry at 490 nm. Because of the lower absolute absorbance

of brown pigments in comparison to red pigments, each brown pigment sample was composed of eight heads. Absorbance values were normalized to brown pigments extracted from Canton S flies after subtracting background A_{490} from similar extractions on groups of w^- fly heads. Ommochromes were extracted from *blos1* flies as a control showing reduced accumulation of brown pigments.

When measured collectively, neither the $Vab2^{114}$ lines nor the $Vab2^{115}$ lines displayed any significant difference in the accumulation of ommochromes versus Canton S flies (Fig 4.3 A). However the distribution of values obtained from the $Vab2^{114}$ samples was considerably broader than that of any of the other genotypes. When the collected A_{490} values were reexamined based on *Vab2* subline ($Vab2^{114•FC14}$, $Vab2^{114•FC16}$, $Vab2^{114•FC17}$, $Vab2^{115•FC33.2}$ and $Vab2^{115•FC36.2}$), each of the $Vab2^{114}$ sublines showed a statistical difference in the quantity of ommochromes that was extracted from them in comparison to Canton S (Fig. 4.3 B). This was most significant for $Vab2^{114•FC14}$, the same $Vab2^{114}$ subline that showed a statistically significant increase in the accumulation of drosopterins (Fig. 4.2 B). However, both of the $Vab2^{115}$ sublines showed a lack of significant difference in amounts of ommochromes isolated from Canton S (Fig. 4.3 B). These findings indicated that loss of *Vab2* did not phenocopy loss of *blos1* with respect to causing defective pigment granule biogenesis. Furthermore, the differences in brown pigment levels isolated from each of the independently Cantonized $Vab2^{114}$ sublines showed no trend indicative of a *bona fide* effect of *Vab2* on brown pigment accumulation: $Vab2^{114}$ sublines FC14 and FC17 showed increased accumulation of ommochromes relative to Canton S, but FC16 showed decreased accumulation of ommochromes.

Genetic interaction of Vab2 and blos1 – double mutant eclosure

Although neither of the *Vab2* deletion alleles caused a change in red or brown pigment accumulation as independent mutations, it was possible that *Vab2* mediated a compensatory

mechanism when BLOC-1 was defective or that *Vab2* somehow affected the severity of the loss of *blos1* through other genetic interactions. To determine if *Vab2* modified the *blos1* phenotype and to look for synthetic genetic interactions with *blos1*, I introduced the *Vab2* mutations into a line of flies carrying the $blos1^{ex65}$ deletion.

Vab2 is on the *Drosophila* first chromosome (X chromosome) and *blos1* is on the *Drosophila* second chromosome [9]. Accordingly, I was able to generate *Vab2* ; *blos1* double mutants by classical genetic crosses. I crossed females from two sublines of flies homozygous for $Vab2^{114}$, FC14 and FC17, and two lines of flies homozygous for $Vab2^{115}$, FC 33.2 and FC38.1, to male $blos1^{ex65}$ homozygous flies. These crosses established F1 generations of 'double heterozygotes': females heterozygous for one of the *Vab2* alleles and for $blos1^{ex65}$ and males hemizygous for one of the *Vab2* alleles and $blos1^{ex65}$. These 'double heterozygotes' were crossed to their siblings (F1 cross) in order to obtain double homozygotes.

The crosses described above were done without the use of balancers, and to obtain the desired double homozygous flies as lines (without floating wildtype *Vab2* or *blos1* alleles), I crossed individual F2 males to individual F2 females. With this breeding scheme, the desired lines would be obtained if both F2 parents were homozygous double mutants. By selecting animals with a visible *blos1* phenotype, I could limit the crosses that I set-up to the subpopulation of F2 animals that were homozygous for $blos1^{ex65}$. A caveat of this strategy was that if *Vab2* modified the *blos1* phenotypes and made it no longer distinguishable, I risked not crossing *Vab2* ; *blos1* double homozygous parents and only crossing +/+ or *Vab2*/+ ; *blos1* flies. To avoid this I compared the number of observed *blos1* homozygous F2 progeny to the expected number of *blos1* homozygous F2 progeny. The initial progeny counts indicated that *blos1* homozygotes were eclosing at roughly half the frequency at which they were expected. However, when the observation window was extended from 2 days to 6, it was seen that *blos1* homozygotes were eclosing at the ratios expected from the independent assortment of alleles (Table 4.1). This meant that loss of *Vab2* was not modifying the *blos1* phenotype in a manner that rendered it visually

distinguishable from single *blos1* homozygotes nor was *Vab2* causing synthetic lethality with *blos1*. Nevertheless, these data did hint that *blos1* may have a late eclosure phenotype in combination with loss of *Vab2*. However, because I did not determine the genotype the *blos1* animals with regards to whether they eclosed late or on-schedule with their heterozygous siblings, I am unable to state whether late eclosure correlated to *Vab2* status or it is a newly recognized and independent phenotype of *blos1*.

Lack of modifying effects of Vab2 mutation on blos1 reduced red eye pigments

After obtaining the $Vab2^{114}$; $blos1^{ex65}$ and $Vab2^{115}$; $blos1^{ex65}$ double mutant lines, I compared the red pigment levels of these flies to those of wildtype Canton S flies and *blos1* single mutants to determine if *Vab2* modified the *blos1* red pigment phenotype. As was done for the red pigment comparisons described in the previous section, I collected heads from 2-3 day-old males of each genotypes and extracted drosopterins from groups of four heads per sample. Drosopterins were quantified spectroscopically by determining the A_{480} of each sample, and values were normalized to those obtained from Canton S flies after subtracting background A_{480} measurements from w^- flies.

Neither $Vab2^{114}$ nor $Vab2^{115}$ changed the degree of red pigment reduction caused by loss of *blos1*: there was no statistical difference in red pigment accumulation between the $blos1^{ex65}$ single mutant line of flies and either $Vab2^{114}$; $blos1^{ex65}$ double mutants or $Vab2^{115}$; $blos1^{ex65}$ double mutants (Fig 4.4). These findings were consistent with the observations shown in Table 4.1 that indicate that neither allele of *Vab2* affected the *blos1* reduction of eye pigments in a visibly discernable manner. Together, these data indicated that *Vab2* did not act as a genetic modifier of *blos1*.

Lack of modifying effects of Vab2 mutation on BLOC-2 (p^p) reduced red eye pigments

The *pink* gene (*p*) encodes the HPS5 subunit of *Drosophila* BLOC-2 [16, 19]. In both mice and *Drosophila*, the *blos1* phenotype is epistatic to mutations in BLOC-2 (cocoa in mice, p^p in *Drosophila*) [9, 4]. Performing a similar eye color epistasis test between *Vab2* and p^p in *Drosophila* was not possible because *Vab2* alone did not elicit an eye color phenotype. Nevertheless, it remained possible that *Vab2* might modify the p^p eye pigmentation phenotype. To test for this possibility I introduced the *Vab2* alleles into a line of flies homozygous for the p^p allele. Because *p* is on the *Drosophila* third chromosome, *Vab2* could be introduced by standard genetic crosses, and a strategy similar to the one used to generate *Vab2* ; *blos1* double mutant flies was followed (*i.e.* generating 'double heterozygous' F1 animals and performing F1 crosses to obtain double homozygotes that were identified by PCR screening).

p^p homozygotes were obtained from the *Vab2* ; p^p heterozygous F1 crosses at the expected Mendelian frequencies. Once lines of $Vab2^{114}$; p^p and $Vab2^{115}$; p^p double homozygotes had been identified, I tested the effects of *Vab2* on BLOC-2 by determining if loss or mutation of *Vab2* affected the red eye pigment accumulation defects of p^p. As described above, drosopterins were extracted from the heads of 2-3 day-old males flies and quantified by spectrophotometric absorbance at 480 nm. Four heads were used per sample. Absorbance values were normalized to those obtained from Canton S flies and background absorbance was determined from similarly extracted groups of w^- fly heads.

Neither $Vab2^{114}$ nor $Vab2^{115}$ had a statistically significant effect on the reduced accumulation of drosopterins caused by mutation of *p*, *i.e.* both $Vab2^{114}$; p^p and $Vab2^{115}$; p^p flies showed reduced levels of drosopterins that were not statistically different from the reduced levels of red eye pigments extracted from p^p single mutant flies – approximately 25% of Canton S (Fig

4.5). This indicated that *Vab2* did not modify the reduction of red eye pigments caused by the p^p mutation.

Increased accumulation of red and brown eye pigments in Kxd1 mutants

The loss of *Kxd1* in mice was reported to phenocopy the deficiency of canonical BLOC-1 subunit genes in an attenuated manner [21]. However, *Kxd1* mutant flies were visually indistinguishable from wildtype flies. To determine if *Kxd1* mutant flies had BLOC-1-like eye color phenotypes that were not discernable by visual inspection, I extracted and quantified red and brown eye pigments from $Kxd1^{76i}$ flies. Whereas *blos1* deficient flies ($blos1^{ex65}$ homozygotes) show a marked reduction of red eye pigments versus Canton S (only 31% wildtype levels of drosopterins, here), $Kxd1^{76i}$ flies displayed an increased accumulation of red eye pigments in comparison to wildtype Canton S flies (14% more drosopterins than Canton S flies – Fig. 4.6 A). Similarly, when brown eye pigments were extracted and measured from $Kxd1^{76i}$ flies, these were present in quantities roughly 18% greater than those found in wildtype Canton S flies (Fig 4.6 B). Because both pigment types were over-accumulated in *Kxd1* deletion flies relative to Canton S, this indicated that, contrary to the findings reported by Yang *et al*. [12], in insects, *Kxd1* appears to influence the accumulation of LROs (or LRO contents) in a manner opposite of that reported for *Kxd1* in mammals.

Red and brown eye pigments defects of Blos3

'Reduced pigmentation' (*rp*) mice, which harbor a mutation in the gene encoding BLOS3, show a characteristically mild BLOC-1 phenotype [12.] BLOS3 is a *bona fide* subunit of metazoan BLOC-1 [12, 13], but the *rp* phenotype is enigmatic in that it is the only mutation of a BLOC-1 subunit-encoding gene that does not elicit an intense BLOC-1 phenotype in mice. In

lines of flies in which I had deleted *Blos3*, I observed an eye color phenotype that was significantly less severe than the 'dull red eye without a pseudopupil' phenotype caused by loss of *blos1*: *Blos3* mutant flies had bright red eyes that exhibited a pseudopupil and were only slightly less brilliant than the eyes of wildtype flies. To determine if this phenotype represented a classical, but attenuated BLOC-1 phenotype, or if this phenotype represented a different phenomenon, I extracted red and brown eye pigments from *Blos3* deletion flies and quantified them versus pigments extracted from wildtype Canton S flies. Red and brown eye pigments were extracted from $blos1^{ex65}$ flies at the same time to serve as controls for the reduced accumulation of drosopterins and ommochromes.

Both of the alleles of *Blos3* from which red eye pigments were extracted ($Blos3^{7}$ and $Blos3^{8}$) showed a reduced accumulation of drosopterins relative to Canton S (Fig. 4.6 A). However, whereas *blos1* mutant flies accumulated about 31% of the red eye pigments found in Canton S fies, the two lines of *Blos3* mutant flies accumulated roughly 62% of Canton S red pigment quantities. A comparable finding was made when ommochromes were extracted from three lines carrying deletions alleles of *Blos3* ($Blos3^{7}$, $Blos3^{8}$ and $Blos3^{18}$). All of the *Blos3* mutant lines showed reduced accumulation of ommochromes (62-64% wildtype) versus Canton S flies (Fig. 4.6 B). In comparison, $blos1^{ex65}$ flies accumulated only 37% of the brown eye pigments isolated from Canton S flies. By both criteria, deletion of *Blos3* in *Drosophila* phenocopied the mild BLOC-1 phenotypes of *rp* mice, indicating that BLOS3 behaves differently from the majority of the canonical BLOC-1 protein subunits: loss of BLOS3 does not abrogate BLOC-1 function in the same manner as loss of other BLOC-1 subunits does, rather, BLOS3 seems to modulate BLOC-1 function.

DISCUSSION

A lack of genetic interaction of Vab2 with BLOC-1

The findings described here demonstrate that *Vab2* had no detectable effect on *Drosophila* eye pigment accumulation. This argues that *Vab2,* despite being a subunit of yeast BLOC-1 [1], is neither a component of metazoan BLOC-1 nor modifier of BLOC-1 function in higher eukaryotes. The eye pigments of *Drosophila* are stored in a class of LROs called pigment granules [11]. Loss of *blos1* causes a profound reduction of both red and brown eye pigments, and *blos1* mutant flies have fewer pigment granules in the sheath cells of the *Drosophila* compound eye and a reduced electron density of the pigment granules that remain [9]. In mammalian cells, BLOC-1 has been associated with membrane fractions of the tubular early endosome [4] indicating an early role for BLOC-1 in the biogenesis of LROs. Despite the independent enzymatic pathways of red and brown eye pigment synthesis, both compounds rely on pigment granules as a site of storage and biosynthesis [10]. This predicts that mutations of BLOC-1 would have a pleiotropic effect on pigment accumulation, as observed for *blos1* in *Drosophila*. In contrast, mutation of *Vab2* affected neither red nor brown eye pigment accumulation, both of which remained unchanged in a *Vab2* deletion background.

Classical epistasis experiments aim to elucidate gene-gene interactions by comparing the phenotypes of recessive gene single mutants to double mutants. If the double mutant phenotypes resemble one of the single mutant phenotypes, then the genes likely act in a common linear pathway. If the double mutant phenotypes are novel or more severe than the single mutant phenotypes, then the genes likely act in parallel or additive pathways. I initially aimed to determine the epistatic relationship of *Vab2* to *blos1* to determine if they both altered LRO biogenesis by affecting BLOC-1 function. However, this was not possible because mutation of *Vab2* alone did not have a discernable phenotype.

Nevertheless, if the association of Vab2p with yeast BLOC-1 was paralleled in higher eukaryotes, it remained possible that, in metazoans, *Vab2* regulated BLOC-1 function in some other manner and that loss of *Vab2* would modify the *blos1* phenotype when the two mutations existed together. For example, BLOC-1 and AP-3 associate with the tubular early endosome and, at least in part, act in parallel in the biogenesis of LROs such as *Drosophila* pigment granules [9, 4, 22]. If, then, Vab2 facilitated BLOC-1 recruitment to early endosomes and excluded other complexes responsible for LRO biogenesis, such as AP-3, it remained possible that BLOC-1-mutant phenotypes would be less severe when *Vab2* was also mutated. In this case, the additional absence of Vab2 might allow AP-3 to more easily compensate for loss of BLOC-1 by alleviating a Vab2 exclusion of AP-3. When I tested for such interactions by quantifying red eye pigments from *blos1* single mutant flies and *Vab2* ; *blos1* double mutant flies, no difference in pigment accumulation was seen between these genotypes. This indicated that *Vab2* did not modify BLOC-1 function or activity and failed to substantiate the speculative Vab2-BLOC-1 protein-protein interaction in metazoans.

Finally, when loss of *blos1* is combined with a BLOC-2 mutation (p^p) in *Drosophila*, the eye color phenotype is indistinguishable from the eye color defect of single p^p mutant flies, which is more severe than loss of *blos1* alone [9], and reciprocally, the coat color of BLOC-1/BLOC-2 double mutant mice (pallid/cocoa) is indistinguishable from that of BLOC-1 single mutant mice (pallid), which is more severe than the BLOC-2 phenotype alone [4]. This demonstrated that BLOC-1 and BLOC-2 operate in a common pathway. To this end, the speculative interaction between Vab2 and BLOC-1 in metazoans inspired by the inclusion of Vab2p in yeast BLOC-1, might have involved, for example, a role for Vab2 in mediating BLOC-1/BLOC-2 interaction. In this case, loss of *Vab2* in a p^p mutant background might elicit a more severe p^p phenotype if BLOC-1 is no longer waiting to interact with BLOC-2 when Vab2 is present but instead BLOC-1 interacts freely with AP-3 (or does not terminate interaction with AP-3 in order to interact with BLOC-2) and inhibits the independent role of AP-3 in LRO biogenesis. In any case, regardless of

speculative compound phenotypes, when I tested the effects of *Vab2* mutation in combination with p^p, no enhancement or amelioration of the BLOC-2 red eye pigment-accumulation defect was observed. This provided further evidence that *Vab2*, although associated with BLOC-1 in yeast, had no obvious functional interactions with metazoan BLOC-1.

Loss of Kxd1 elicits phenotypes consistent with increased BLOC-1 activity

In addition to being a member of BLOC-1 in yeast [1], in *Drosophila* and mammals the KXD1 protein interacts with BLOS1 [21, 23]. It has been reported that mild LRO defects are characteristic of *Kxd1* knock-out mice [23]. In contrast, visual assessment of the *Drosophila Kxd1* deletion flies that I generated ($Kxd1^{76i}$) showed no evidence of eye pigmentation defects. Strikingly, when I compared red and brown pigment levels of *Kxd1* deletion flies to pigment quantities found in wildtype Canton S flies, I observed an equivalent and statistically significant increase of both types of pigments. Since the biosynthetic pathways of drosopterins and ommochromes are enzymatically distinct [10] the coordinated increase in red and brown pigments argued that the increase was due to changes in LRO biogenesis or turnover. Speculatively, these findings could indicate that *Kxd1* exerts a negative regulatory effect on *Drosophila* BLOC-1 and that the absence of *Kxd1* alleviates a repression of BLOC-1 function. This possibility was a particularly intriguing because, whereas the authors of the mouse *Kxd1* study interpreted their findings to indicate that loss of *Kxd1* causes a mild HPS-like phenotype, they reported an increased number of melanosomes in the retinal pigment epithelium (RPE) and choroid of *Kxd1*−/− mice in comparison to their wildtype littermates [21]. Despite this, the authors also reported that overall eumelanin levels were decreased in the eyes of *Kxd1* knock-out mice – however this comparison was made to a 129/J line of mice that was not syngeneic to the hybrid C57BL/6J-129/J *Kxd1* knock-out mice.

KXD1 was found to associate with BLOS1 in both flies and mammals by yeast two-hybrid studies [21, 23], and the KXD1-BLOS1 interaction was confirmed for the mouse proteins by co-immunoprecipitation [21]. Along with the association of Kxd1p with BLOC-1 in yeast [1, 3], these results strongly implicate that the interaction of KXD1 with some BLOC-1 subunits is biologically consequential. Thus, I favor a model in which *Kxd1* mutant flies accumulated greater quantities of eye pigments because loss of *Kxd1* eliminated an inhibition of BLOC-1 (*i.e.* allowed increased pigment granule biogenesis) rather than loss of *Kxd1* downregulating pigment granule turnover – a process not associated with BLOC-1 function. If this was the case the Kxd1 protein may normally interact with subunits of BLOC-1 and prevent them from assembling fully functional BLOC-1. Loss of *Kxd1* would then allow the BLOC-1 subunits normally sequestered by Kxd1 to avoid being diverted to other processes.

Although the mouse and *Drosophila Kxd1* phenotypes initially appear contradictory, this is not necessarily the case. In *Drosophila*, loss of *Kxd1* caused a stoichiometric increase in red and brown eye pigments (both pigments were over accumulated in proportional quantities). In mice, the loss of *Kxd1* results in increased numbers of melanosomes in the choroid and RPE [21]. In both cases these findings point to an increase of BLOC-1 activity – or, stated otherwise, the elimination of a BLOC-1 inhibitory factor. Thus, loss of *Kxd1* in *Drosophila* might precisely parallel loss of *Kxd1* in mice. As was noted by Chelli, *et al*. when they observed reversal of dominance in the epistatic relationship between BLOC-1 and BLOC-2 in *Drosophila* versus that previously seen in mice [9], these findings illustrate the power and importance of using multiple model systems when trying to understand biological interactions and defining protein function.

Blos3 is an atypical BLOC-1 gene and loss of Blos3 causes mild BLOC-1 phenotypes

I targeted the *Blos3* gene for deletion in wildtype Canton S flies using CRISPR/Cas9 reagents and isolated three independently generated deletion alleles. Each of these alleles showed

a marked decrease in the accumulation of red and brown eye pigments, and in each case both pigments were reduced in equivalent quantities. In this sense, loss of *Blos3* phenocopied the loss of *blos1*. On the other hand, the decrease of both red and brown pigments in the eyes of *Blos3* deletion flies was roughly half as profound as the decrease observed in $blos1^{ex65}$ mutant flies indicating that residual BLOC-1 activity persisted in *Blos3* mutant flies.

In mice, loss of *Bloc1s3* (*Blos3*) causes the abnormal BLOC-1 phenotypes exhibited by the 'reduced pigmentation' (*rp*) mouse [12, 13]. Strains of mice (Sandy, Pallid, Muted, Cappuccino) harboring the classical mutations of BLOC-1 genes exhibit the most pronounced coat color and eye pigmentation defects among the BLOC and AP-3 mouse models of HPS (*i.e.* BLOC-1, BLOC-2, BLOC-3, AP-3), [16, 12, 22]. In contrast, *rp* mice show coat color defects and other pigmentation defects that are significantly less severe than those of the other four mouse models of BLOC-1 deficiency. (For example, the eyes of *rp* mice were originally reported to have normal melanosomes [13].) Nevertheless, as with other BLOC-1 subunits, loss of *Bloc1s3* is associated with a reduced accumulation of the remaining BLOC-1 subunits, and reciprocally, the loss of Pallidin causes decreased accumulation of BLOS3 [12, 22]. Finally, BLOS3, like other BLOC-1 components, is an acidic α-helical protein but it is distinguished by having no predicted coiled-coil domains and by appearing to associate with BLOC-1 in a phosphorylation dependent manner [12, 13].

When I targeted *Blos3* for deletion in *Drosophila* it was unclear whether the mild BLOC-1 phenotypes of *Bloc1s3* mutant mice were indicative of an intrinsic function of the BLOS3 protein or if these phenotypic differences were due to a species-specific effect. The identification of a *BLOC1S3* mutation in humans as the causative mutation of HPS-8 did not clarify this question [24], and a report stating that immortalized *rp* melanocytes showed an equivalent lack of pigmentation to immortalized melanocytes derived from muted and pallid mice further confused the issue [6]. Here, I present the first report of quantitative evidence that, in comparison to other BLOC-1 mutations, loss of *Blos3* elicits an attenuated phenotype. These findings support the

interpretation that, while being a member of BLOC-1, Blos3 is structurally and functionally unique among the BLOC-1 subunits. It raises the interesting possibility that, rather than acting a core structural and functional component of BLOC-1, the primary role of *Blos3* is to regulate BLOC-1 activity: BLOC-1 activity is not abolished when *Blos3* is mutated, but it is significantly reduced. Under normal circumstances Blos3 may regulate BLOC-1 activity as a classical allosteric activator or by targeting BLOC-1 to the proper sites of action, and phosphorylation of Blos3 may play a role in these activities. One last point is that this confirmation that Blos3 functions as a non-canonical subunit of BLOC-1 necessitates re-examining reports of the epistatic relationship between BLOC-1 and BLOC-2: Some groups have reported that mutation of BLOC-2 augments a BLOC-1 phenotype when *Bloc1s3* is the mutated BLOC-1 gene without accounting for the mild BLOC-1 phenotypes caused by loss of *Bloc1s3* [13]. Others have noted that BLOC-1 and BLOC- 2 are epistatic to each other when either *blos1* or *Bloc1s6* (the gene encoding Pallidin) are the BLOC-1 mutation [9, 4, 22].

Double Heterozygote F1 Cross				
Phenotype		$\frac{Vab2^{114}}{+}$; $\frac{blos1^{ex65}}{+}$	$\frac{Vab2^{115}}{+}$; $\frac{blos1^{ex65}}{+}$	
blos1 -/-		**[0.25]**	**[0.25]**	Expct
blos1 +/?		**[0.75]**	**[0.75]**	
♂ *blos1* -/-		40 (21%)	67 (25%)	Observed
♂ *blos1* +/?		148 (79%)	203 (75%)	
♀ *blos1* -/-		17 (20%)	41 (23%)	
♀ *blos1* +/?		69 (80%)	138 (77%)	

Table 4.1. Phenotypic *blos1* flies observed from *Vab2* ; *blos1* heterozygote crosses. F1 'double heterozygous' $Vab2^{114}$; $blos1^{ex65}$ and $Vab2^{115}$; $blos1^{ex65}$ flies were crossed to their siblings, respectively, to obtain double homozygous animals. The number of phenotypic *blos1* animals was determined over a six day period. Based on an assumption of independent segregation, 25% of the F2 progeny from each cross were expected to be homozygous for $blos1^{ex65}$ (Phenotype: *blos1* -/-). The remainder of the animals (75%) were expected to be heterozygous or wildtype for *blos1* (Phenotype: *blos1* +/?). These numbers were expected to differ from the expected ratios if *Vab2* suppressed or modified the *blos1* phenotype. The number of observed phenotypic *blos1* F2 animals is shown under each F1 genotype by sex. The phenotypic ratios of the F2 offspring did not differ significantly by sex for a given genetic background (*i.e.* $Vab2^{114}$ vs. $Vab2^{115}$).

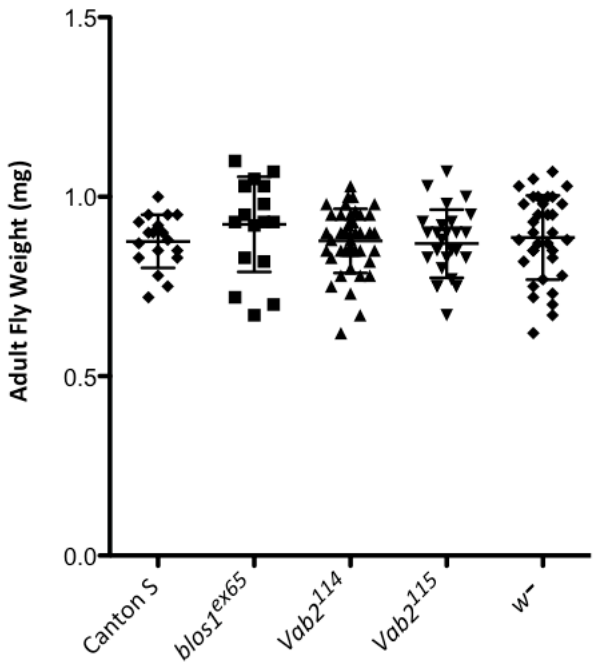

Figure 4.1. Effects of BLOC-1 (*blos1*^{ex65}) and *Vab2* mutations on *Drosophila* weight. Adult male Canton S, *blos1*^{ex65}, *Vab2*^{114}, *Vab2*^{115}, and w^{-} flies were collected 2-3 days after eclosure and weighed. None of the groups showed statistically significant variance by ANOVA.

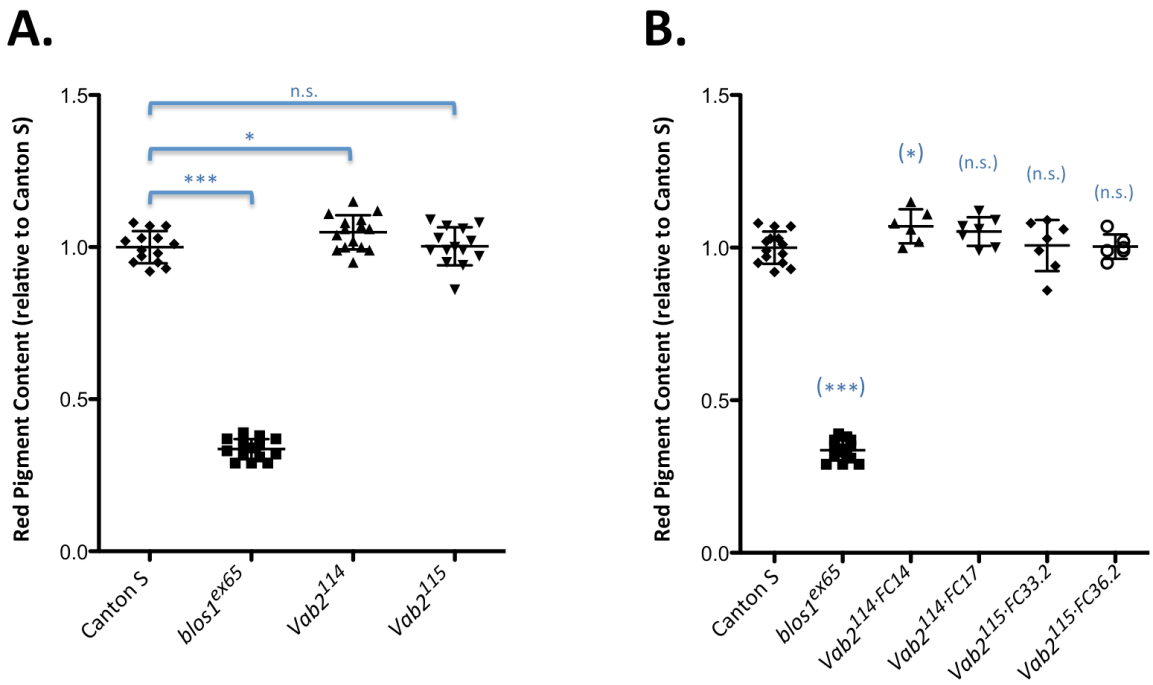

Figure 4.2. Red eye pigments of *Drosophila Vab2* mutants. Red eye pigments (drosopterins) were extracted from groups of four, 2-3 day-old, male Canton S, *blos1*^{ex65}, *Vab2*^{114}, *Vab2*^{115}, and *w*$^{-}$ flies, and quantified spectroscopically at 480 nm. Absorbance values were normalized to red pigment quantities observed in Canton S flies. *w*$^{-}$ flies were used to determine background absorbance. Statistical significance was determined by ANOVA followed by Dunnett's Multiple Comparison Test versus Canton S. (**A**) Homozygous *blos1* deletion flies showed a characteristic 30-40% accumulation of red eye pigments relative to Canton S. In contrast, flies homozygous for the *Vab2*^{115} deletion allele displayed no significant difference in red eye pigments from wildtype Canton S flies, and flies harboring the *Vab2*^{114} promoter deletion allele showed an approximate 5% increased accumulation of red eye pigments relative to Canton S. (**B**) When red pigment levels were examined by *Vab2* subline, the statistically significant increased accumulation of drosopterins seen in *Vab2*^{114} flies was found to be solely due to red pigments in the *Vab2*$^{114\text{•}FC14}$ subline. (n.s. non-significant, * $P \leq 0.05$, *** $P \leq 0.001$)

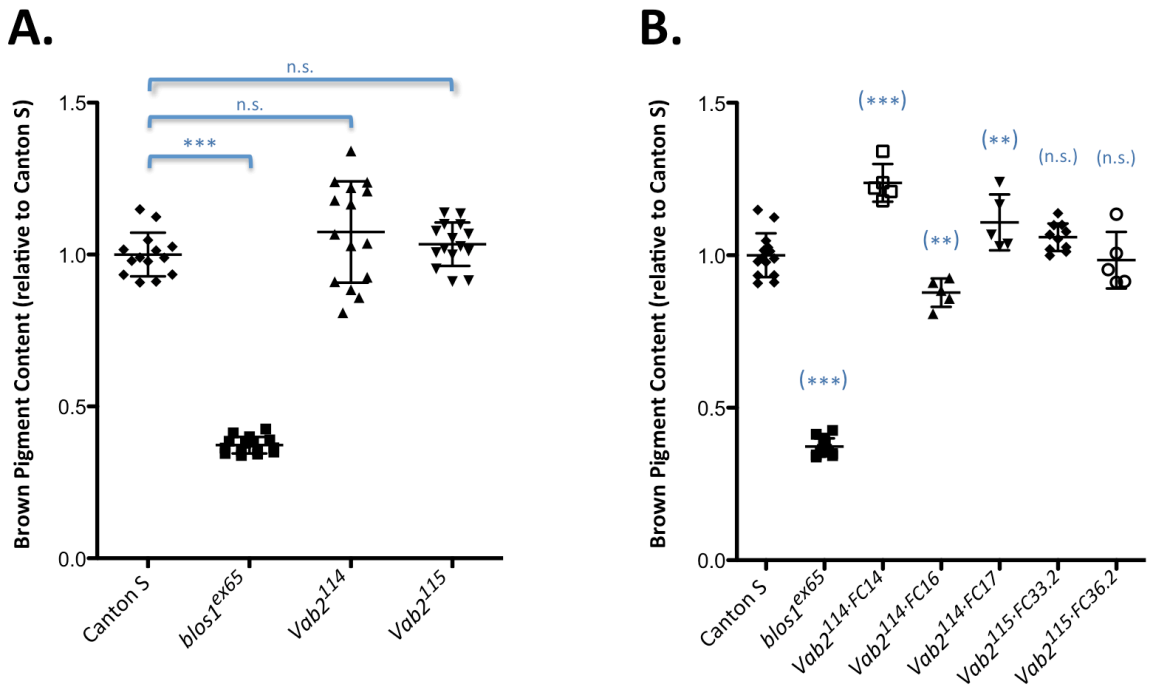

Figure 4.3. Brown eye pigments of *Drosophila Vab2* mutants. Brown eye pigments (ommochromes) were extracted from groups of eight, 2-3 day-old, male Canton S, $blos1^{ex65}$, $Vab2^{114}$, $Vab2^{115}$, and w^{-} flies, and quantified spectroscopically at 490 nm. Absorbance values were normalized to brown pigment quantities observed in Canton S flies. w^{-} flies were used to determine background absorbance. Statistical significance was determined by ANOVA followed by Dunnett's Multiple Comparison Test versus Canton S. (**A**) Homozygous *blos1* deletion flies showed a characteristic 30-40% accumulation of brown eye pigments relative to Canton S. Overall, neither $Vab2^{114}$ nor $Vab2^{115}$ flies displayed a significant difference in brown eye pigment accumulation from wildtype Canton S flies. (**B**) When brown pigments were quantified by *Vab2* sublines, each of the $Vab2^{114}$ sublines ($Vab2^{114•FC14}$, $Vab2^{114•FC16}$ and $Vab2^{114•FC17}$) showed a statistical difference in brown eye pigment accumulation from wildtype. Nevertheless, these differences averaged out when considered collectively (*c.f.* panel A). None of the $Vab2^{115}$ sublines showed a significant difference in the accumulation of ommochromes from Canton S. (n.s. non-significant ** $P \leq 0.005$, *** $P \leq 0.001$)

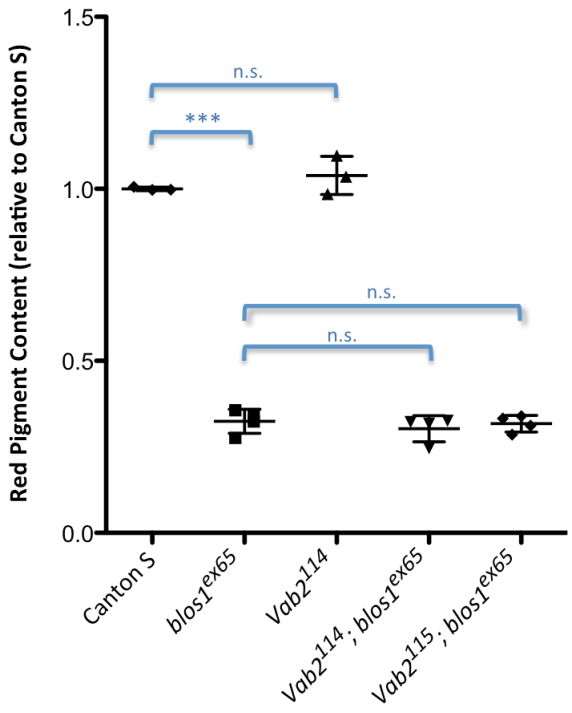

Figure 4.4. Lack of modifying effects of *Vab2* mutations on *blos1* eye pigment phenotype. Red eye pigments (drosopterins) were extracted from groups of four, 2-3 day-old, male flies and quantified spectroscopically at 480 nm to determine if mutation of *Vab2* had any modifying effect on *blos1*. Samples were collected from $Vab2^{114}$; $blos1^{ex65}$ and $Vab2^{115}$; $blos1^{ex65}$ double mutant flies and compared to red eye pigment quantities extracted from $blos1^{ex65}$ single mutant flies. Pigment values were normalized to quantities obtained from Canton S flies after subtracting background absorbance at 480 nm from a similar extraction from w^- flies. Red pigments were also extracted from $Vab2^{114}$ flies as a control. Statistical significance was determined by ANOVA followed by Bonferroni's Multiple Comparison Test. Neither $Vab2^{114}$ nor $Vab2^{115}$ modified red eye pigment accumulation in $blos1^{ex65}$ mutant flies: the *Vab2* ; $blos1^{ex65}$ double mutants of both *Vab2* alleles showed no statistical difference in the accumulation of drosopterins from single mutant $blos1^{ex65}$ flies. (n.s. non-significant, *** $P \leq 0.001$)

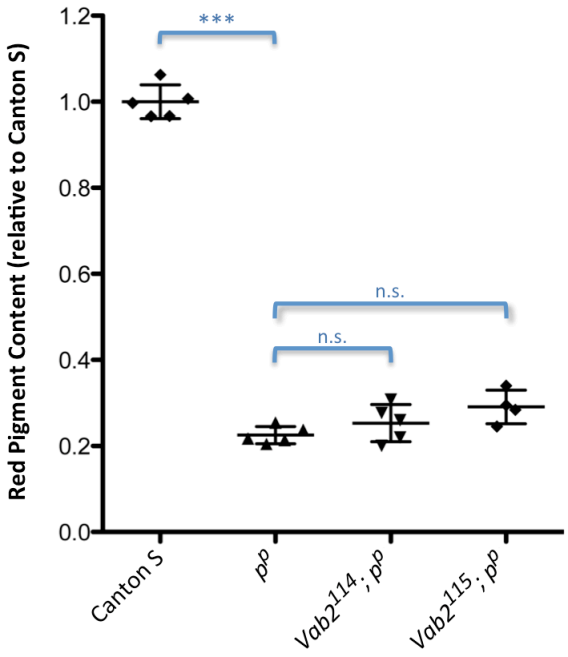

Figure 4.5. Lack of modifying effects of *Vab2* mutations on BLOC-2 (p^p) eye pigment accumulation. Red eye pigments (drosopterins) were extracted from groups of four, 2-3 day-old, male flies and quantified spectroscopically at 480 nm to determine if loss of *Vab2* modified the reduced accumulation of red eye pigments of p^p mutant flies. Red pigments were extracted from p^p single mutant flies and compared to red pigments extracted from $Vab2^{114}$; p^p and $Vab2^{115}$; p^p double mutant flies. Pigment values were normalized to quantities obtained from Canton S flies after subtracting background absorbance at 480 nm from w^- flies. Statistical significance was determined by ANOVA followed by Bonferroni's Multiple Comparison Test. Neither $Vab2^{114}$ nor $Vab2^{115}$ modified red eye pigment levels in p^p mutant flies: the $Vab2^{114}$; p^p and $Vab2^{115}$; p^p double mutants flies showed no statistical difference in the accumulation of drosopterins from single mutant p^p flies. (n.s. non-significant, *** $P \leq 0.001$)

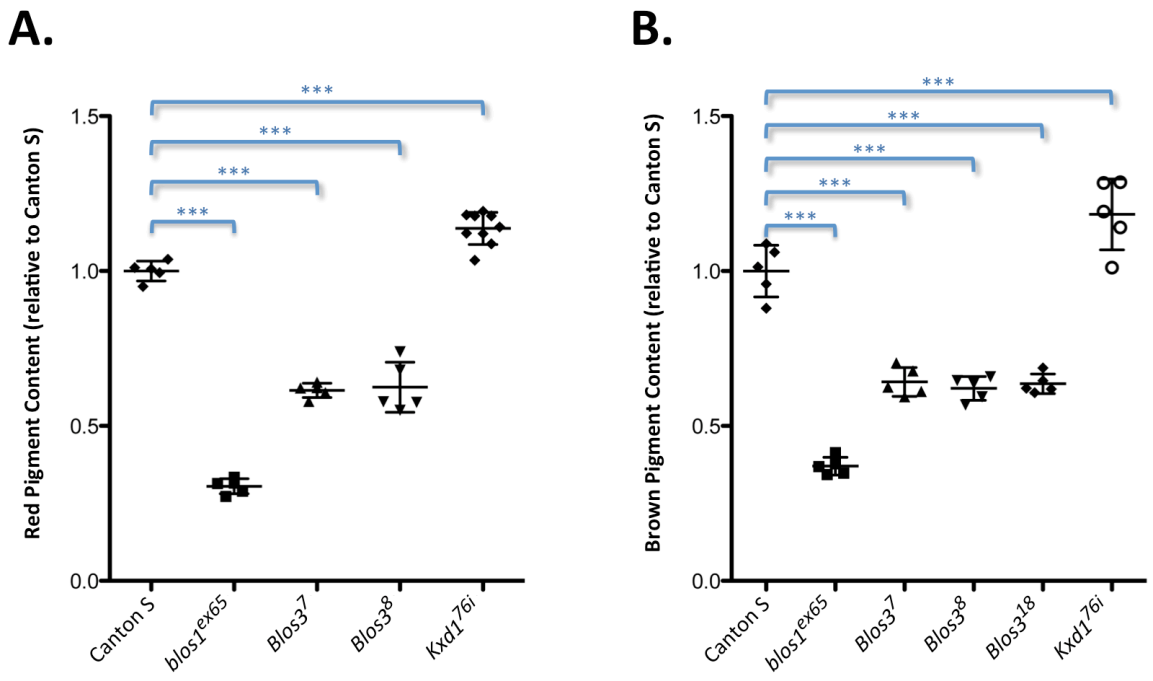

Figure 4.6. Red and brown eye pigments of *Blos3* and *Kxd1* mutants. Eye pigments were extracted from groups of 2-3 day-old adult male flies and quantified by spectroscopic absorbance. Pigment values were normalized to quantities obtained from Canton S flies after subtracting background absorbance from w^- flies. Statistical significance was determined by ANOVA followed by Dunnett's Multiple Comparison Test. (**A**) Red eye pigments (drosopterins) were extracted from groups of 4 flies and measured at 480 nm. $blos1^{ex65}$ mutants showed a characteristic reduction of red eye pigments (approximately 31% of Canton S). Two alleles of *Blos3* showed a reduction of red eye pigments of roughly half of that seen of $blos1^{ex65}$ mutants (*i.e.* approximately 62% of Canton S). In contrast, $Kxd1^{76i}$ flies showed a 14% increase of red eye pigments in comparison to Canton S. (**B**) Brown pigments (ommochromes) were extracted from groups of 8 flies and measured at 490 nm. $blos1^{ex65}$ flies had approximately 37% of the brown eye pigments found in Canton S. All three alleles of *Blos3* showed an average of 63% of the brown pigments found in Canton S flies. $Kxd1^{76i}$ mutants, on the other hand, had an average increase of 18% more brown eye pigments than Canton S. (*** $P \leq 0.001$)

REFERENCES

1 Hayes MJ, Bryon K, Satkurunathan J, Levine TP. Yeast homologues of three BLOC-1 subunits highlight KxDL proteins as conserved interactors of BLOC-1. Traffic. 2011 Mar;12(3):260-8.

2 Li SC, Kane PM. The yeast lysosome-like vacuole: endpoint and crossroads. Biochim Biophys Acta. 2009 Apr;1793(4):650-63.

3 John Peter AT, Lachmann J, Rana M, Bunge M, Cabrera M, Ungermann C. The BLOC-1 complex promotes endosomal maturation by recruiting the Rab5 GTPase-activating protein Msb3. J Cell Biol. 2013 Apr 1;201(1):97-111.

4 Di Pietro SM, Falcón-Pérez JM, Tenza D, Setty SR, Marks MS, Raposo G, Dell'Angelica EC. BLOC-1 interacts with BLOC-2 and the AP-3 complex to facilitate protein trafficking on endosomes. Mol Biol Cell. 2006 Sep;17(9):4027-38.

5 Salazar G, Craige B, Styers ML, Newell-Litwa KA, Doucette MM, Wainer BH, Falcon-Perez JM, Dell'Angelica EC, Peden AA, Werner E, Faundez V. BLOC-1 complex deficiency alters the targeting of adaptor protein complex-3 cargoes. Mol Biol Cell. 2006 Sep;17(9):4014-26.

6 Setty SR, Tenza D, Truschel ST, Chou E, Sviderskaya EV, Theos AC, Lamoreux ML, Di Pietro SM, Starcevic M, Bennett DC, Dell'Angelica EC, Raposo G, Marks MS. BLOC-1 is required for cargo-specific sorting from vacuolar early endosomes toward lysosome-related organelles. Mol Biol Cell. 2007 Mar;18(3):768-80.

7 Falcón-Pérez JM, Starcevic M, Gautam R, Dell'Angelica EC. BLOC-1, a novel complex containing the pallidin and muted proteins involved in the biogenesis of melanosomes and platelet-dense granules. J Biol Chem. 2002 Aug 2;277(31):28191-9.

8 Huizing M, Anikster Y, Gahl WA. Hermansky-Pudlak syndrome and related disorders of organelle formation. Traffic. 2000 Nov;1(11):823-35.

9 Cheli VT, Daniels RW, Godoy R, Hoyle DJ, Kandachar V, Starcevic M, Martinez-Agosto JA, Poole S, DiAntonio A, Lloyd VK, Chang HC, Krantz DE, Dell'Angelica EC. Genetic modifiers of abnormal organelle biogenesis in a Drosophila model of BLOC-1 deficiency. Hum Mol Genet. 2010 Mar 1;19(5):861-78.

10 Kim H, Kim K, Yim J. Biosynthesis of drosopterins, the red eye pigments of Drosophila melanogaster. IUBMB Life. 2013 Apr;65(4):334-40.

11 Lloyd V, Ramaswami M, Krämer H. Not just pretty eyes: Drosophila eye-colour mutations and lysosomal delivery. Trends Cell Biol. 1998 Jul;8(7):257-9.

12 Starcevic M, Dell'Angelica EC. Identification of snapin and three novel proteins (BLOS1, BLOS2, and BLOS3/reduced pigmentation) as subunits of biogenesis of lysosome-related organelles complex-1 (BLOC-1). J Biol Chem. 2004 Jul 2;279(27):28393-401.

13 Gwynn B, Martina JA, Bonifacino JS, Sviderskaya EV, Lamoreux ML, Bennett DC, Moriyama K, Huizing M, Helip-Wooley A, Gahl WA, Webb LS, Lambert AJ, Peters LL. Reduced pigmentation (rp), a mouse model of Hermansky-Pudlak syndrome, encodes a novel component of the BLOC-1 complex. Blood. 2004 Nov 15;104(10):3181-9.

14 Gibb S, Håkansson EM, Lundin LG, Shire JG. Reduced pigmentation (rp), a new coat colour gene with effects on kidney lysosomal glycosidases in the mouse. Genet Res. 1981 Feb;37(1):95-103.

15 Swank RT, Novak EK, McGarry MP, Rusiniak ME, Feng L. Mouse models of Hermansky Pudlak syndrome: a review. Pigment Cell Res. 1998 Apr;11(2):60-80.

16 Falcón-Pérez JM, Romero-Calderón R, Brooks ES, Krantz DE, Dell'Angelica EC. The Drosophila pigmentation gene pink (p) encodes a homologue of human Hermansky-Pudlak syndrome 5 (HPS5). Traffic. 2007 Feb;8(2):154-68.

17 Kretzschmar D, Poeck B, Roth H, Ernst R, Keller A, Porsch M, Strauss R, Pflugfelder GO. Defective pigment granule biogenesis and aberrant behavior caused by mutations in the Drosophila AP-3beta adaptin gene ruby. Genetics. 2000 May;155(1):213-23.

18 Mullins C, Hartnell LM, Bonifacino JS. Distinct requirements for the AP-3 adaptor complex in pigment granule and synaptic vesicle biogenesis in Drosophila melanogaster. Mol Gen Genet. 2000 Jul;263(6):1003-14.

19 Syrzycka M, McEachern LA, Kinneard J, Prabhu K, Fitzpatrick K, Schulze S, Rawls JM, Lloyd VK, Sinclair DA, Honda BM. The pink gene encodes the Drosophila orthologue of the human Hermansky-Pudlak syndrome 5 (HPS5) gene. Genome. 2007 Jun;50(6):548-56.

20 Harris DA, Kim K, Nakahara K, Vásquez-Doorman C, Carthew RW. Cargo sorting to lysosome-related organelles regulates siRNA-mediated gene silencing. J Cell Biol. 2011 Jul 11;194(1):77-87.

21 Yang Q, He X, Yang L, Zhou Z, Cullinane AR, Wei A, Zhang Z, Hao Z, Zhang A, He M, Feng Y, Gao X, Gahl WA, Huizing M, Li W. The BLOS1-interacting protein KXD1 is involved in the biogenesis of lysosome-related organelles. Traffic. 2012 Aug;13(8):1160-9.

22 Gautam R, Novak EK, Tan J, Wakamatsu K, Ito S, Swank RT. Interaction of Hermansky-Pudlak Syndrome genes in the regulation of lysosome-related organelles. Traffic. 2006 Jul;7(7):779-92.

23 Giot L, Bader JS, Brouwer C, Chaudhuri A, Kuang B, Li Y, Hao YL, Ooi CE, Godwin B, Vitols E, Vijayadamodar G, Pochart P, Machineni H, Welsh M, Kong Y, Zerhusen B, Malcolm R, Varrone Z, Collis A, Minto M, Burgess S, McDaniel L, Stimpson E, Spriggs F, Williams J, Neurath K, Ioime N, Agee M, Voss E, Furtak K, Renzulli R, Aanensen N, Carrolla S, Bickelhaupt E, Lazovatsky Y, DaSilva A, Zhong J, Stanyon CA, Finley RL Jr, White KP, Braverman M, Jarvie T, Gold S, Leach M, Knight J, Shimkets RA, McKenna MP, Chant J, Rothberg JM. A protein interaction map of Drosophila melanogaster. Science. 2003 Dec 5;302(5651):1727-36.

24 Morgan NV, Pasha S, Johnson CA, Ainsworth JR, Eady RA, Dawood B, McKeown C, Trembath RC, Wilde J, Watson SP, Maher ER. A germline mutation in BLOC1S3/reduced pigmentation causes a novel variant of Hermansky-Pudlak syndrome (HPS8). Am J Hum Genet. 2006 Jan;78(1):160-6.

CHAPTER 5

Conclusions

The work presented here describes the generation and characterization of a group of *Drosophila* gene deletions of putative and established non-canoncial BLOC-1 subunits: *Vab2*, *Kxd1* and *Blos3*. *Vab2* and *Kxd1* are *Drosophila* homologs of yeast BLOC-1 subunits [this study and 1], and *Blos3* is the *Drosophila* homolog of a validated BLOC-1 subunit that elicits an atypical BLOC-1 phenotype in mice [2-4]. The purpose of this work was to determine if metazoan homologs of yeast BLOC-1 subunits might also play a role in the function of canonical BLOC-1. Because deletion of the *Drosophila blos1* gene had already been shown to elicit clear BLOC-1 phenotypes arising from the reduced accumulation of eye pigment granules (a class of lysosome related organelle [5]) and manifesting as reduced levels of red and brown eye pigments [2], targeting these genes for deletion in *Drosophila* provided an efficient means of quantitatively determining their effects in relation to a previously characterized canonical BLOC-1 gene. For *Vab2* and *Kxd1*, this promised to allow the direct and quantitative assessment, not only of whether or not these genes phenocopied canonical BLOC-1 gene deletions, but also of the degree to which these genes influenced the normal functions of BLOC-1. In the case of *Blos3*, the identification of *Blos3* as the genetic cause of the mouse 'reduced pigmentation' phenotype and the characterization of BLOS3 as a classical protein subunit of BLOC-1 (*i.e* BLOC3 biochemically purifies as a component of BLOC-1, and the absence of full length BLOS3 negatively affects the stability of other BLOC-1 subunits) had previously defined BLOS3 as a *bona fide* component of BLOC-1 [3, 4], but the attenuated coat, eye and skin color phenotypes of 'reduced pigmention' mice brought into question whether BLOS3 was functioning in a distinct manner from other BLOC-1 subunits or if the 'reduced pigmentation' phenonotype of *Blos3* was a species-specific effect. By deleting *Blos3* in a phylogenetically distant species and in a background isogenic to that of the previously characterized *blos1* mutation, I sought to answer quantitatively answer this question.

Deletion of Vab2

In Chapter 2, I described the deletion of the *Drosophila CG11802* gene. One of the main reasons for performing these sets of experiments is that using PSI-BLAST (Position-Specific Iterated - Basic Local Alignment Search Tool) iterative protein homology searches [6], Esteban Dell'Angelica recognized that *CG11802* was the *Drosophila* homolog of yeast *VAB2*. This discovery allowed us to consider deletion of two of the three non-canonical yeast BLOC-1 homologs in metazoans and obtaining firm understanding of the relation of these genes to the canonically recognized BLOC-1 subunits.

Since a line of flies was available that harbored a P element insertion in the 5' UTR of *Vab2*, I decided to use this line as a starting point for deletion of *Drosophila Vab2* by imprecise excision. Using standard P element imprecise excision strategies [7], I obtained and isolated two fly lines that harbored deletions of *Vab2* genomic sequences: $Vab2^{114}$ and $Vab2^{115}$. When characterized, it was determined that both alleles represented unidirectional deletions originating from P{EPg}CG11802^{HP10420} insertion site.

$Vab2^{114}$ showed deletion of sequences 5' of the P element insertion site, removing consensus upstream and downstream promoter elements, and $Vab2^{115}$ showed deletion of sequences downstream of the P element insertion site, removing the entirety of the *Vab2* ORF. By characterizing the mRNAs found in flies homozygous for either of these alleles, it was revealed that $Vab2^{114}$ produced reduced amounts of Vab2 mRNA making it a putative hypomorphic allele of *Vab2*, while $Vab2^{115}$ was a complete genetic null.

Technically, the P element imprecise excision efforts for *Vab2* proceeded in a 'textbook' manner [7]. Gene deletions were obtained at frequency of roughly 2.6% (1% representing deletions of interest), and the deletions that were obtained were unidirectional from the original site of P element insertion. As was also typical of textbook P element imprecise excision efforts, these deletions were made starting from a line of flies that was held in genetic isolation in order to

preserve the integrity and identity of the P element inserted in *Vab2*. Because I needed to isogenize the *Vab2* deletions that I isolated with wildtype Canton S flies and with the previously characterized *blos1* mutants [2] in order to properly characterize effects of *Vab2* deletion, this required several generation of outcrossing to Canton S flies.

Since *Vab2* is located on the X chromosome, it was possible that deletion of *Vab2* would cause a visible eye pigmentation phenotype, characteristic of BLOC-1 mutation, in hemizygous males. Such a phenotype would have been useful for following the deletion alleles as they were outcrossed and brought into a Canton S background. This was not observed and therefore the presence of the *Vab2* allele had to be followed in an *ex post facto* manner by PCR screening flies after they had been successfully mated. However, in all other manners, P element imprecise excision of *Vab2* was performed and realized as expected.

Deletion of Kxd1 and Blos3

As described in Chapter 3, I deleted both *Kxd1* and *Blos3* using a CRISPR/Cas9-based approach [8]. Although my initial efforts relied on monitoring the status of *Kxd1* by following the w^{+mC} marker carried by a piggyBac insertion in the 5' UTR of the gene [9], these efforts were frustrated by a duplication of *Kxd1* in the line of flies that harbored the PBac insertion. Nevertheless, these initial attempts revealed that gene deletion using this CRISPR-mediated approach was efficient enough that genes could be targeted without the assistance of a visibly scorable marker of gene retention, and that deletion alleles could be identified by unguided molecular screening. I therefore again targeted *Kxd1* using the same set of CRISPR/Cas9 reagents but did so directly in wildtype Canton S flies. This resulted in the generation and isolation of the anticipated *Kxd1* deletion in the desired genomic background.

As observed of the *Vab2* deletion alleles arrived at by imprecise excision, the *Kxd1* CRISPR deletion did not have a visible phenotype and was only recognizable by molecular

screening. However, since this allele was generated directly in a Canton S background, it did not require the same extensive backcrossing that each of the *Vab2* imprecise excision deletions required. This significantly reduced the time and reagents needed before being able to proceed to phenotypic characterization of this deletion.

In the case of *Blos3*, I utilized the strategies that I developed while deleting *Kxd1* and targeted *Blos3* with CRISPR reagents directly in wildtype Canton S flies. This resulted in the precise deletion of *Blos3* and the isolation of three independently generated *Blos3* deletion alleles. Notably, whereas I first decided to use a CRISPR-based approach to delete *Kxd1* because of the lack of P element insertions in *Kxd1*, there was an available P element insertion in the region upstream of *Blos3*. However, *Blos3* is in a complex genomic locus, and this P element, P{EP}Rad9^{G20120} [10], is actually located in the 3' UTR of *Rad9* and is positionally closer to the upstream *CG6852* gene than to *Blos3*. Using a CRISPR-based approach allowed me to precisely delete a region of *Blos3* while causing minimal deletion of the overlapping *Rad9* gene (only a portion of the *Rad9* 3' UTR was removed). This would not have been possible by transposon-mediated imprecise excision with any of the available transposon insertion in *Rad9*/*Blos3*.

Generation of Drosophila gene deletions in Canton S flies

I set out to make CRISPR-generated *Kxd1* and *Blos3* deletion flies using the tools and protocols first described by Gratz *et al.* [8]. This approach relies on the injection of plasmid DNA templates to express the Cas9 endonuclease and the chiRNA(s) that direct Cas9 activity to specific genomic locations. Subsequent to the Gratz *et al.* paper, other groups published additional approaches to generating CRISPR-mediated heritable gene deletions in *Drosophila* [11, 12]. Notable differences between these approaches include the injection of *in vitro* transcribed Cas9 mRNA and sgRNAs (single guide RNAs) rather than plasmid templates for these transcripts [13 14], or the use of transgenic promoters, both somatic and germline-specific,

to express either Cas9 or both Cas9 and the desired sgRNA molecules [15-17]. Other improvements consist of introducing alternative visual indications of gene deletion, such as incorporation of fluorescent markers [16, 18, 19], or developing approaches for high-throughput screening such as restriction fragment polymorphism screening [20, 21] or high resolution melt analysis [13, 17] for identifying effectively modified individuals. Emphasis has also been placed on gene modification strategies using ssODN approaches such as insertion of stop codons, FRT sequences or attP docking sites [18, 19, 22]. Finally, off-target effects have been addressed by using engineered Cas9 molecules that, rather than making double-stranded DNA breaks, perform single-stranded DNA nicking, in order to increase CRISPR specificity by requiring proximal Cas9 target sites in order for dsDNA breaks to be generated [22, 23].

The approach that I described here utilized the first generation of Gratz *et al*. CRISPR reagents, but it improved upon the protocols and approaches described so far by eschewing the dependence on visible screening to identify putative gene deletion or gene replacement animals. Although my protocol was not aimed at adapting CRISPR reagents to high-throughput work, the approaches that I used did significantly improve upon the ease of using CRISPR reagents to carryout classical reverse genetics studies by targeting genes for deletion in the final genetic background of interest, rather than using genetically specialized starting lines such as transposon insertions in the genetic targets or specialized lines harboring transgenic sources of Cas9 or sgRNAs/chiRNAs. I found that it was neither necessary to use lines that visibly mark the targeted locus, nor was it required to use lines that transgenically express CRISPR/Cas9 components. Rather, my approach directly targeted specific genes in the final desired genetic background, and I found that the isolation of multiple alleles of a gene deletion adequately served to phenotypically distinguish gene-specific effects from off-target effects.

Phenotypic characterization of Vab2 and *Kxd1*

In Chapter 4, I described the phenotypic characterization of the *Vab2* and *Kxd1* gene deletion lines relative to wildtype Canton S flies and *blos1* deletion flies. I found that deletion of *Vab2* had no discernable effect on the accumulation of either red or brown eye pigments (drosopterins and ommochromes, respectively) in *Drosophila*. Since the accumulation of these pigments is dependent on biogenesis of pigment granules and deletion of BLOC-1 subunits causes a marked decrease in both pigments [2, 5], these results indicated that deletion of *Vab2* does not phenocopy loss of *blos1*. In addition, deletion of *Vab2* did not modify either loss of BLOC-1 (blos1) or loss of BLOC-2 (pink), reinforcing the interpretation that *Vab2* does not influence BLOC-1 or BLOC-2 function.

In contrast, deletion of *Kxd1* resulted in the increased accumulation of red and brown eye pigments. Flies lacking *Kxd1* accumulated 14% more red pigments and 18% more brown pigments than wildtype Canton S flies. Because the biosynthesis of red and brown eye pigments occurs via distinct and unrelated biosynthetic pathways but both pigments are synthesized and accumulate in pigment granules [2, 5, 24], the coordinated increase of red and brown pigments points toward a pigment granule effect. However, these results contrasted with the interpretation of the effects of *Kxd1* deletion in mice [25]. The authors of that report concluded that loss of *Kxd1* caused a mild BLOC-1-like phenotype. I observed that loss of *Kxd1* had a phenotype that stood in contrast to those conclusions. Instead of phenocopying loss of BLOC-1 in *Drosophila* and causing a reduction of eye pigment accumulation [2], deletion of *Drosophila Kxd1* resulted in the increased accumulation of *Drosophila* eye pigments. Thus, rather than supporting the interpretation that *Kxd1* positively regulates BLOC-1 function, as was concluded from the mouse study [25], the results obtained here argue that *Kxd1* may have a negative regulatory effect on BLOC-1 – elimination of *Kxd1* lifting a *Kxd1*-imposed repression of BLOC-1 activity.

Phenotypic characterization of Blos3

Chapter 4 also describes the phenotypic characterization of *Blos3* mutant flies. Here I show that, as was found for mutation of *Blos3* in mice [3, 4], deletion of *Drosophila Blos3* causes attenuated BLOC-1 phenotypes. Unlike *blos1*, which causes a loss of 60-70% of wildtype quantities of red and brown eye pigments [2], deletion of *Blos3* caused a loss of roughly half as much red and brown eye pigments (approximately 30-35% reduction in pigment accumulation relative to wildtype Canton S flies). These results are consistent with the interpretation that Blos3 is unique among the BLOC-1 subunits, in that, when *Blos3* is mutated, it does not elicit phenotypes as intense as mutation of other BLOC-1 subunit genes [3, 4]. In other words, Blos3 acts in an intrinsically distinct manner in terms of its role in BLOC-1 function.

Yeast BLOC-1 versus metazoan BLOC-1 and BORC

As I was completing these studies, a paper was published describing an octameric BLOC-one related complex (BORC) in human cells that contains three of the canonical metazoan BLOC-1 subunits: BLOS1, BLOS2 and snapin, and two of the yeast-specific BLOC-1 subunits: LOH12CR1 (Vab2/myrlysin) and KXD1 [26]; however, the authors of this report did not realize that myrlysin is the metazoan homolog of yeast Vab2p. CRISPR-mediated deletion of the myrlysin gene in HeLa cells results in a lysosome positioning defect where lysosomes are no longer efficiently trafficked centrifugally toward the positive end of microtubules. The authors found that BORC normally recruits the Arl8 GTPase to lysosomal membranes and initiates a cascade of Kinesin-1 dependent lysosomal transport [26]. Furthermore, when HeLa cells are fractionated and lysosomal fractions are probed for the presence or absence of BLOC-1 subunits, the BLOC-1 subunits that are also associated with BORC are detected (BLOS1, BLOS2 and

Snapin) but those associated only with BLOC-1 are not found (pallidin, cappuccino, muted, dysbindin and BLOS3) [26].

The findings presented in the report describing mammalian BORC [26], along with the results described here indicating that *Vab2* and *Kxd1* did not phenocopy BLOC-1 deficiency, make a compelling argument that *Vab2* and *Kxd1* are not components of *Drosophila* BLOC-1. In addition, these findings make it more likely that yeast BLOC-1 is an analog of metazoan BORC. Whereas yeast BLOC-1 contains two, possibly three, homologs of the eight canonical metazoan BLOC-1 subunits (Bls1p, Snn1p and Cnl1p), the authors of the original paper describing yeast BLOC-1 explicitly stated that Cnl1p is a DUF2365 homolog, and thus a cappuccino-like protein that coexists along side the *bona fide* cappuccino homolog in nematodes, humans and flies [1, 3]. In contrast, yeast BLOC-1 contains homologs of four of the eight metazoan BORC subunits (Bls1p, Snn1p, Vab2p and Kxd1p) [1, 26]. Yeast have a lysosome-like organelle, the vacuole, that shares much of the same metabolic processes and protein effectors with the classical metazoan lysosome [27], but they do not have organelles that have been characterized to be LRO-like [28]. Defects in yeast BLOC-1 result in changes in protein flux to the yeast vacuole [28], and defects in metazoan BORC are associated with changes in protein recruitment to classical metazoan lysosomes that result in a collapse of peripheral lysosome positioning and pericentriolar accumulation [26].

Possible roles for Vab2 and Kxd1 in BLOC-1 and BORC assembly

Although my findings do not directly support further conclusions for the role of *Vab2* and *Kxd1* in relation to metazoan BLOC-1 function, it is tempting to hypothesize how these proteins might interact with and regulate *Drosophila* BLOC-1.

Among the constituents of yeast BLOC-1, only Vab2p shows distinct vacuolar localization when expression of other BLOC-1 subunits is disrupted [28]. The remaining yeast

BLOC-1 proteins exhibit a diffuse cytosolic localization when expression of any of the other BLOC-1 subunits is compromised. Furthermore, Vab2p was shown to strongly associate with Kxd1p [1].

In *Drosophila*, deletion of *Vab2* had no effect on BLOC-1 function. In contrast, deletion of *Kxd1* increased the accumulation of BLOC-1-dependent products, while deletion of *Blos3* caused a sub-stoichiometric reduction in BLOC-1-dependent products. BLOS3 is also unique among BLOC-1 subunits in that, in mice, the association of BLOS3 with BLOC-1 appears to occur in a phosphorylation dependent manner [4], but disruption of *Blos3* negatively affects the cellular accumulation of other BLOC-1 subunits in a manner analogous to loss of other BLOC-1 subunits [3, 4].

The findings presented here would be consistent with a model in which Blos3 might compete with Kxd1 to recruit common BLOC-1 and BORC subunits to assemble into the respective complexes in metazoans, and Vab2, a predicted myristolated protein [26], might serve as the lysosomal membrane anchor for the assembling BORC complex once common BLOC-1/BORC subunits have been sequestered by Kxd1 to form BORC. In this manner, deletion of *Vab2* would not directly affect BLOC-1 activity because Vab2 might only associate with other subunits in the context of a BORC or BORC-like protein complex. In contrast, deletion of *Kxd1* would eliminate the factor that competes against Blos3 to recruit common BLOC-1/BORC subunits for complex assembly. Accordingly, deletion of *Kxd1*, therefore, would allow shared subunits to more readily assemble into functional BLOC-1, which would allow the increased production and accumulation of BLOC-1-dependent products such as *Drosophila* eye pigments. If this model was correct and accurately described the relationship between *Vab2*, *Kxd1*, *Blos3*, BLOC-1 and BORC, one could predict that additional *Blos3* phenotypes would include more efficient formation of BORC and increased BORC activity in a manner analogous to the way that deletion of *Kxd1* resulted in increased accumulation of BLOC-1-dependent products.

As an avenue of further investigation, it would be interesting to determine the phenotypes of *Blos3* and *Kxd1* double mutants, and to determine the epistatic relationships between *Blos3* and *blos1* and between *Kxd1* and *blos1*. If my model of *Vab2*, *Kxd1* and *Blos3* function is correct, I predict that *Blos3* would show complete epistatsis to *blos1* since loss of *blos1* would eliminate all BLOC-1 activity whereas deletion of *Blos3* appears to preserve a substantial amount of residual BLOC-1 activity for reasons not yet understood. For similar reasons I predict that loss of *Kxd1* would be entirely epistatic to loss of *blos1* since Blos1 functions downstream of Kxd1.

Lastly, although loss of *Vab2* clearly failed to phenocopy deletion of *blos1*, it would be desirable to validate the phenotypes observed from the $Kxd1^{76i}$ allele either by generating additional deletion alleles of *Kxd1* using the alternative *Kxd1*-targeting CRISPR reagents described in Chapter 3 or by complimenting loss of *Kxd1* with a CaSpeR genomic rescue construct [29].

REFERENCES

1 Hayes MJ, Bryon K, Satkurunathan J, Levine TP. Yeast homologues of three BLOC-1 subunits highlight KxDL proteins as conserved interactors of BLOC-1. Traffic. 2011 Mar;12(3):260-8.

2 Cheli VT, Daniels RW, Godoy R, Hoyle DJ, Kandachar V, Starcevic M, Martinez-Agosto JA, Poole S, DiAntonio A, Lloyd VK, Chang HC, Krantz DE, Dell'Angelica EC. Genetic modifiers of abnormal organelle biogenesis in a Drosophila model of BLOC-1 deficiency. Hum Mol Genet. 2010 Mar 1;19(5):861-78.

3 Starcevic M, Dell'Angelica EC. Identification of snapin and three novel proteins (BLOS1, BLOS2, and BLOS3/reduced pigmentation) as subunits of biogenesis of lysosome-related organelles complex-1 (BLOC-1). J Biol Chem. 2004 Jul 2;279(27):28393-401.

4 Gwynn B, Martina JA, Bonifacino JS, Sviderskaya EV, Lamoreux ML, Bennett DC, Moriyama K, Huizing M, Helip-Wooley A, Gahl WA, Webb LS, Lambert AJ, Peters LL. Reduced pigmentation (rp), a mouse model of Hermansky-Pudlak syndrome, encodes a novel component of the BLOC-1 complex. Blood. 2004 Nov 15;104(10):3181-9.

5 Lloyd V, Ramaswami M, Krämer H. Not just pretty eyes: Drosophila eye-colour mutations and lysosomal delivery. Trends Cell Biol. 1998 Jul;8(7):257-9.

6 Altschul SF, Madden TL, Schäffer AA, Zhang J, Zhang Z, Miller W, Lipman DJ. Gapped BLAST and PSI-BLAST: a new generation of protein database search programs. Nucleic Acids Res. 1997 Sep 1;25(17):3389-402.

7 Ryder E, Russell S. Transposable elements as tools for genomics and genetics in Drosophila. Brief Funct Genomic Proteomic. 2003 Apr;2(1):57-71.

8 Gratz SJ, Cummings AM, Nguyen JN, Hamm DC, Donohue LK, Harrison MM, Wildonger J, O'Connor-Giles KM. Genome engineering of Drosophila with the CRISPR RNA-guided Cas9 nuclease. Genetics. 2013 Aug;194(4):1029-35.

9 Thibault ST, Singer MA, Miyazaki WY, Milash B, Dompe NA, Singh CM, Buchholz R, Demsky M, Fawcett R, Francis-Lang HL, Ryner L, Cheung LM, Chong A, Erickson C, Fisher WW, Greer K, Hartouni SR, Howie E, Jakkula L, Joo D, Killpack K, Laufer A, Mazzotta J, Smith RD, Stevens LM, Stuber C, Tan LR, Ventura R, Woo A, Zakrajsek I, Zhao L, Chen F, Swimmer C, Kopczynski C, Duyk G, Winberg ML, Margolis J. A complementary transposon tool kit for Drosophila melanogaster using P and piggyBac. Nat Genet. 2004 Mar;36(3):283-7.

10 Bellen HJ, Levis RW, He Y, Carlson JW, Evans-Holm M, Bae E, Kim J, Metaxakis A, Savakis C, Schulze KL, Hoskins RA, Spradling AC. The Drosophila gene disruption project: progress using transposons with distinctive site specificities. Genetics. 2011 Jul;188(3):731-43.

11 Bassett AR, Liu JL. CRISPR/Cas9 and genome editing in Drosophila. J Genet Genomics. 2014 Jan 20;41(1):7-19.

12 Xu J, Ren X, Sun J, Wang X, Qiao HH, Xu BW, Liu LP, Ni JQ. A Toolkit of CRISPR-Based Genome Editing Systems in Drosophila. J Genet Genomics. 2015 Apr 20;42(4):141-9.

13 Bassett AR, Tibbit C, Ponting CP, Liu JL. Highly efficient targeted mutagenesis of Drosophila with the CRISPR/Cas9 system. Cell Rep. 2013 Jul 11;4(1):220-8.

14 Yu Z, Ren M, Wang Z, Zhang B, Rong YS, Jiao R, Gao G. Highly efficient genome modifications mediated by CRISPR/Cas9 in Drosophila. Genetics. 2013 Sep;195(1):289-91.

15 Kondo S, Ueda R. Highly improved gene targeting by germline-specific Cas9 expression in Drosophila. Genetics. 2013 Nov;195(3):715-21.

16 Sebo ZL, Lee HB, Peng Y, Guo Y. A simplified and efficient germline-specific CRISPR/Cas9 system for Drosophila genomic engineering. Fly (Austin). 2014;8(1):52-7.

17 Ren X, Sun J, Housden BE, Hu Y, Roesel C, Lin S, Liu LP, Yang Z, Mao D, Sun L, Wu Q, Ji JY, Xi J, Mohr SE, Xu J, Perrimon N, Ni JQ. Optimized gene editing technology for Drosophila melanogaster using germ line-specific Cas9. Proc Natl Acad Sci U S A. 2013 Nov 19;110(47):19012-7.

18 Gratz SJ, Ukken FP, Rubinstein CD, Thiede G, Donohue LK, Cummings AM, O'Connor-Giles KM. Highly specific and efficient CRISPR/Cas9-catalyzed homology-directed repair in Drosophila. Genetics. 2014 Apr;196(4):961-71.

19 Gratz SJ, Rubinstein CD, Harrison MM, Wildonger J, O'Connor-Giles KM. CRISPR-Cas9 Genome Editing in Drosophila. Curr Protoc Mol Biol. 2015 Jul 1;111:31.2.1-31.2.20.

20 Ran FA, Hsu PD, Wright J, Agarwala V, Scott DA, Zhang F. Genome engineering using the CRISPR-Cas9 system. Nat Protoc. 2013 Nov;8(11):2281-308.

21 Lee HB, Sebo ZL, Peng Y, Guo Y. An optimized TALEN application for mutagenesis and screening in Drosophila melanogaster. Cell Logist. 2015 Feb 27;5(1):e1023423.

22 Port F, Chen HM, Lee T, Bullock SL. Optimized CRISPR/Cas tools for efficient germline and somatic genome engineering in Drosophila. Proc Natl Acad Sci U S A. 2014 Jul 22;111(29):E2967-76.

23 Ren X, Yang Z, Mao D, Chang Z, Qiao HH, Wang X, Sun J, Hu Q, Cui Y, Liu LP, Ji JY, Xu J, Ni JQ. Performance of the Cas9 nickase system in Drosophila melanogaster. G3 (Bethesda). 2014 Aug 15;4(10):1955-62.

24 Kim H, Kim K, Yim J. Biosynthesis of drosopterins, the red eye pigments of Drosophila melanogaster. IUBMB Life. 2013 Apr;65(4):334-40.

25 Yang Q, He X, Yang L, Zhou Z, Cullinane AR, Wei A, Zhang Z, Hao Z, Zhang A, He M, Feng Y, Gao X, Gahl WA, Huizing M, Li W. The BLOS1-interacting protein KXD1 is involved in the biogenesis of lysosome-related organelles. Traffic. 2012 Aug;13(8):1160-9.

26 Pu J, Schindler C, Jia R, Jarnik M, Backlund P, Bonifacino JS. BORC, a multisubunit complex that regulates lysosome positioning. Dev Cell. 2015 Apr 20;33(2):176-88.

27 Li SC, Kane PM. The yeast lysosome-like vacuole: endpoint and crossroads. Biochim Biophys Acta. 2009 Apr;1793(4):650-63. doi: 10.1016/j.bbamcr.2008.08.003. Epub 2008 Aug 13.

28 John Peter AT, Lachmann J, Rana M, Bunge M, Cabrera M, Ungermann C. The BLOC-1 complex promotes endosomal maturation by recruiting the Rab5 GTPase-activating protein Msb3. J Cell Biol. 2013 Apr 1;201(1):97-111.

29 Pirrotta V. Vectors for P-mediated transformation in Drosophila. Biotechnology. 1988;10:437-56.